UNIVERSITY OF OKLAHOMA

GRADUATE COLLEGE

COALBED METHANE COMPREHENSIVE CHARACTERIZATION AND MODELING – BIG GEORGE COAL, POWDER RIVER BASIN, WYOMING

A THESIS

SUBMITTED TO THE GRADUATE FACULTY

in partial fulfillment of the requirements for the

Degree of

MASTER OF SCIENCE

By

TAREK MOHAMED
Norman, Oklahoma
2019

COALBED METHANE COMPREHENSIVE CHARACTERIZATION AND MODELING – BIG GEORGE COAL, POWDER RIVER BASIN, WYOMING

A THESIS APPROVED FOR THE
MEWBOURNE SCHOOL OF PETROLEUM AND GEOLOGICAL ENGINEERING

BY

Dr. Zulfiquar Reza, Chair

Dr. Mashhad Fahes

Dr. Hamidreza Karami

I dedicate this thesis to my mom, Aisha Mohamed, to whom I owe every success I have achieved, who has been my lifelong teacher and advisor and has made me everything I am; to my dad, Sabry Sultan; to my brother, Sameh Sabry; and to my sister, Marwa Sabry.

Acknowledgments

First and foremost, I thank Allah for the countless blessings he has bestowed on me, for my health, persistence, and ability to pursue every dream I have.

I am immensely grateful for the Fulbright Association for funding my master's program and granting me the honor of being a Fulbright Scholar. It has been an amazing experience being a part of the Fulbright network of extremely impressive scholars and leaders from all over the world. Thank you to my Fulbright advisors, Shannon Conheady and Dianne Price, for helping me navigate through my program and life in the United States.

To my advisor, Dr. Zulfiquar Reza, thank you for all your guidance, help, time, and patience throughout my program. Thanks to my committee members, Dr. Mashhad Fahes and Dr. Hamidreza Karami, for taking part in supervising my thesis.

I am also very thankful for my friends and Fulbright fellows, for their great company and constant support. Special thanks to M. Mansi, M. Mehana, Y. Ashour, M. Omar, M. Ragab, M. El-Masry, A. El-Naggar, S. El-Shereef, M. Awad, A. Aboulnaga. S. El-Fouly, H. Kobea, and A. Sharma.

Many thanks to my research teammates, Tien Phan, Any Ordonez, and Yuliana Zapata, for always being very helpful and friendly. Special thanks to Tien Phan for helping me with my Big George Coal numerical model and for being a wonderful friend.

Finally, I would like to express my deepest gratitude to my amazing family. Thank you for your prayers, and unconditional love and support that you always give me even when I am thousands of miles away from home.

Table of Contents

List of Tables

List of Figures

Abstract

Over the past two decades, coalbed methane (CBM) has become one of the major unconventional gas resources in the US, Canada, Australia, and other countries. Despite substantial advances in CBM exploitation technologies, there is still a need for an accurate characterization/quantification and implementation of the gas-diffusion behavior, gas contents, moisture content and influence, and methane banking. Unlike what once was widely assumed, the value of the gas-diffusion coefficient is not constant over the life of a CBM reservoir. In low-rank coal reservoirs, the free and soluble gas contents cannot be considered negligible compared to the adsorbed gas content and they need to be quantified. Coal moisture impact on the sorption isotherms and processes needs to be identified.

Through a comprehensive characterization, modeling, and integrated simulation study of the coalbed methane of the Big George Coal, Wyoming, this study investigates implications of variable diffusion coefficients; quantifies the free, soluble, and adsorbed gas contents to examine their contributions to the total gas production; and examines the impact of the moisture content on CH_4 and CO_2 sorption isotherms and CBM recovery processes. This study incorporates the impact of the pressure and temperature on coal adsorption capacity variation. Additionally, the effects of coalbed water properties - salinity, density, and methane solubility - were explored.

There is a negative correlation between diffusion coefficient and pressure at low pressures. Since the pressure in Big George Coal is relatively low, this study investigates the impact of having a varying diffusion coefficient on gas production. For low permeabilities, the assumption that methane production is permeability-controlled may be accurate, but for high permeabilities, variable diffusion coefficients can have a significant impact on methane production. Amongst many aspects, this study explored an accurate estimation of the free, soluble, and adsorbed gas

contents, and diligently accounted for methane and CO_2 solubilities in water. In the case of undersaturated coal and during ECBM, the injection of CO_2-rich gas leads to methane banking. Furthermore, the impact of anisotropy and heterogeneity on gas flow was analyzed in terms of diffusion, adsorption, and permeability.

A moderate increase in the diffusion coefficients significantly impacts the gas production rates. This should, particularly, be considered for CBM reservoirs with high permeabilities or when considering enhancing low-permeability CBM reservoirs through hydraulic fracturing. The free and soluble gas contents in low-rank coal should not be ignored, and an estimation of their values is provided. The coal moisture content has a significant impact on the sorption isotherms and gas production rates. Future work should include monitoring methane banking and using this consideration in the planning of optimum well spacings.

Chapter 1. Introduction

1.1 Motivation

Over the past two decades, coalbed methane (CBM) has become one of the major unconventional gas resources in the US, Canada, Australia, and other countries. Coalbed formations have unique characteristics which make them very different and difficult to characterize, model, and simulate. It is also challenging to predict the fluids behaviors in the coalbed formations since the nature of the fluid movement in the coal formation is quite different than in all other oil and gas conventional and unconventional reservoirs. The gas existence in the coal formations differs from the gas existence in the conventional and other unconventional oil and gas reservoirs. That is, it does not exist as a continuous gas phase that overlays the oil or water. In coal formations, most of the gas exists as an adsorbed phase on the surfaces of the coal matrices. The adsorbed gas has a liquid-like density while adsorbed.

For the gas to be produced, there are a lot of physical processes that are involved. Coal formations are composed of matrix and natural fractures. While most of the gas in medium and high-rank CBM reservoirs is adsorbed on the surfaces of the matrices, the fractures are the main medium through which the gas needs to flow to be produced. These natural fractures are referred to as cleats and they are different than other natural fractures that they consist of two types of fractures which are butt and face cleats. Butt and face cleats are perpendicular to each other while the main fractures that have higher permeabilities and porosities are the face cleats which are almost horizontal in this study.

The fractures are originally fully saturated with water- which might have soluble gas as well. The adsorbed gas must desorb off the matrix surface first, then diffuse through the matrix until entering the fractures. For that to happen, the water in the fractures needs to be extracted first-

the process that is called dewatering. Then the pressure slightly goes down and the gas starts to desorb. The adsorption and desorption processes are governed and characterized by many adsorption isotherms among them Langmuir Isotherms are the most commonly used and approved. The transmissibility of gas to the fractures is a complex process that is represented and governed by the matrix-fracture coupling and gas diffusion, which is different than the case in most of the conventional gas reservoirs.

In addition to pressure and temperature, the coal adsorption capacity is affected by many factors that need to closely be studied and understood such as the ash content and moisture content. Meaning that by varying the ash and moisture contents on the coal surfaces, the amount of gas like methane and carbon dioxide that could be adsorbed on their faces also vary.

The coal matrix and fracture permeabilities and porosities vary with changing pressure and temperature. That is, it is not safe to assume that when the pressure depletes, the permeability decreases due to the reduction of the pore pressure. That is, because the matrix itself interacts with the process of adsorption and desorption by shrinkage and swelling, which contributes to permeability changes and makes it vital to find a way to understand, characterize, and predict the resultant impact on the absolute permeability and whether there is a possibility that the permeability rebounds or exceeds the initial permeability.

Gas diffusion is hard to characterize as well because studies showed that it should not be treated as constant and it is always changing during the production process and there is a need for a modeling technique and software that takes that change behavior into account. Gas contents need to be studied in more accountability for the soluble and free gas contents as well instead of assuming that all the existed methane is adsorbed gas. While such an assumption might be acceptable in case of high-rank coal formations, it is important to find a way to predict the soluble

and free gas contents in low-rank coals. Several issues appear during the methane production that calls for accurate prediction and handling such as the methane banking that might occur during enhanced coal bed methane (ECBM) when one injects carbon dioxide into the CBM Reservoir.

Coal formations have challenging characteristics that still need accurate characterization and understanding of the many aspects that vary from the geologic nature to the interaction and flow of the water and methane. For the aforementioned reasons, particular interest was expended in providing and understanding a comprehensive way of modeling the coalbed methane formations. One needs to better characterize and deal with the coal formations for many reasons. This thesis highlights two of these reasons. First, methane is the cleanest fossil fuel. Second, coal formations are excellent prospects for carbon dioxide sequestration where one can sequester huge amounts of carbon dioxide in the coal formations through enhanced coal bed methane process. This would reduce the greenhouse emissions in the atmosphere and the CO_2 injection cost would be offset by the excess profit resulting from the increasing methane production due to the carbon dioxide injection.

1.2 Statement of Problem

Coalbed formations have a lot of challenging aspects that need more accurate modeling and characterization. This study used the commercial numerical modeling and simulation software PETREL and ECLIPSE, respectively, to model 22 wells of the Big George Coal Unit in the Powder River Basin in Wyoming, USA (ECLIPSE Industry-Reference, Version 2018.1). A major focus was on providing ways of modeling the varying gas-diffusion coefficient, the adsorbed, free, and soluble gas contents, and the moisture content impact on sorption processes.

1.3 Study Objectives

The main study objectives of the thesis are as follows:

- To provide comprehensive characterization and modeling approach of CBM of the Big George Coal of Powder River Basin, Wyoming.
- To characterize the impact of the moisture content on the gas adsorption/storage capacities of CBM reservoirs.
- To highlight the importance of accounting for free and soluble gas contents in low-rank CBM reservoirs.
- To address the importance of variable gas diffusion coefficient for high-permeability CBM reservoirs.
- To test different models to characterize CBM permeability changes with stresses.

1.4 Thesis Organization

Chapter 2 provides a background on the main physics of coalbed methane reservoirs with a focus on low-rank CBM reservoirs since the studied Big George Coal is mainly low-rank coal. The main aspects of CBM physics covered are the gas adsorption in CBM reservoirs and the considerations associated with its characterization, gas diffusion in CBM reservoirs, and the permeability changes in CBM reservoirs. This chapter also addresses the different models and approaches to characterize and calculate free, soluble and adsorbed gas contents in low-rank CBM reservoirs. It also discusses the importance of accounting for free and soluble gas contents in low-rank CBM reservoirs.

Chapter 3 describes the methodology and processes that were followed to characterize and model Big George Coal. This chapter also provides a brief description of the geology of Powder River Basin and Big George Coal.

Chapter 4 presents CBM reservoir simulation and history-matching processes and the sensitivity analysis performed in the study and finally the results.

Chapter 5 covers discussions and limitations of the CBM characterization and modeling using numerical modeling software.

Chapter 6 summarizes the conclusions of the study.

Chapter 7 discusses the future work and recommendations building upon this study of the Big George Coal.

Chapter 2. Coalbed Methane Physics and Gas Contents

2.1 CBM Physics

Coal bed methane reservoirs have unique geometrical, geological, and geomechanical characteristics. such characteristics result in unique physics associated with CBM reservoirs. Coalbed methane formations are naturally fractured formations. That is, coal formations are composed of matrices and fracture systems. Fracture system is called cleats system and it has two types of fractures/ cleats: Face cleats and butt cleats. Face and butt cleats are perpendicular to each other. The major cleats that have higher permeability and that are more continuous are the face cleats. Thus, CBM reservoirs are considered dual-porosity dual-permeability formations where matrices have very low permeability and the cleats have higher permeability and porosity. Thus, the cleats provide the primary medium for the fluids- water or gas- flow.

Most of the methane in high and medium-rank CBM reservoirs is stored as an adsorbed phase on the surface of the coal matrices while the free and soluble gas contents are negligible. However, in low rank-coal CBM Free and soluble gas contents are significant and should not be ignored. In most virgin CBM reservoirs, cleats are fully saturated with water that provides the pressure for the adsorbed gas to stay in place as an adsorbate. Thus, at the first stage of CBM production, water is depleted and the reservoir pressure decreases enough for the adsorbed gas to desorb meaning to leave the matrix surface, diffuse through the matrix according to diffusion laws, and then flow through the cleats alongside water according to Darcy laws of fluid flow in porous media. Finally, after all the water has been produced, the gas flows through the cleats as a single phase. Water extraction phase is named de-watering.

Throughout the entire process of methane production from a CBM reservoir, many physical processes are involved such as sorption processes, gas diffusion, and matrix shrinkage/swelling.

Sorption processes govern how much gas could be adsorbed. They also need to be characterized using adsorption isotherms to determine the conditions that are needed for the adsorbed gas to desorb. Gas diffusion laws describe the gas movement behavior inside the coal matrix after desorption until it reaches to the cleats. Coalbed methane reservoirs are highly stress-sensitive formations meaning that during the whole process of depleting the reservoir from the water (i.e. de-watering) and then gas desorption, the matrix and cleat systems react in a very complex way to the pressure and stress changes. Also, adsorption and desorption processes affect the matrix and cause it to swell and shrink, respectively. Stress sensitivity and matrix shrinkage/ swelling play an important role in changing the coal permeability throughout production time.

Clearly, such physics that are associated with CBM reservoirs must be first to address and understand when one deals with CBM reservoirs. This chapter covers all such different physics and physical processes that take place in a CBM reservoir. Since Big George coal is a low-rank coal unit, this study emphasizes more on low-rank coal seams physics.

2.1.1 Gas Adsorption in CBM Reservoirs

Most of the gas in CBM reservoirs presents as an adsorbed gas on the surfaces of the coal matrices, especially for higher-rank coal formations. Understanding the adsorption phenomenon and the factors affecting the adsorption and desorption processes of the gas is vital to model and predict the gas amounts and flow rates in CBM reservoirs.

Adsorption capacity depends on several factors that are related to both the adsorbate and the adsorbent. These factors will be reviewed and tested through modeling, simulation and sensitivity study. These factors include temperature, pressure, moisture content, ash content and specific surface area of the coal matrix which is the surface area of the coal matrix available for adsorption per gram of the coal. It is favorable for the coal matrix to have a larger specific surface

area so more gas molecules could be adsorbed on its surface and more gas could be stored in a CBM reservoir. A good adsorbent is an adsorbent that has a large specific surface area.

2.1.1.1 Adsorption Equilibrium

The adsorption equilibrium occurs when the amount of the adsorbed gas on the surface of the adsorbent equals the maximum adsorption capacity for that gas. There are different ways to study the adsorption equilibrium depending on which variable is kept constant as follows.

2.1.1.1.1 Adsorption Isotherm

When the temperature is kept unchanged, an adsorption isotherm for a combination of gas, adsorbate, and solid, adsorbent, represents the amount of the gas adsorbed at equilibrium as a function of the pressure. That is, an adsorption isotherm is a way of characterizing the adsorption process and the adsorption capacity of an adsorbent to specific gases. Thus, it is the relationship, at a specific temperature, between the equilibrium amount of the adsorbed gas and the gas pressure corresponding to that amount. **Figure 2.1** represents the simplest illustration of an adsorption isotherm where *a* is the gas adsorption capacity, *P* is the pressure, and *T* is the temperature.

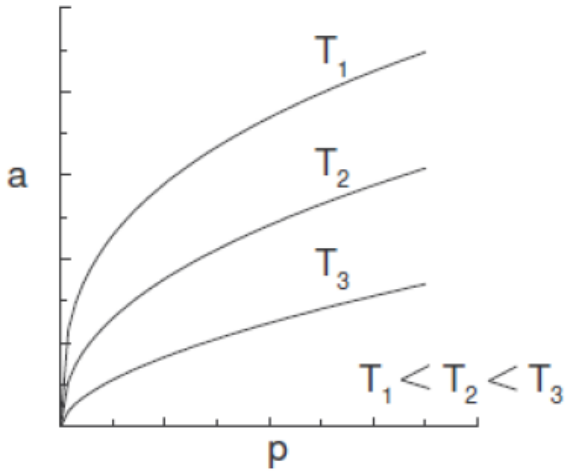

Figure 2.1 The simplest representation of an adsorption isotherm. It also illustrates that adsorption capacity increases with decreasing temperature.

2.1.1.1.2 Adsorption Isobar

An adsorption isobar for a combination of gas, adsorbate, and solid, adsorbent, represents the amount of the gas adsorbed at equilibrium as a function of the temperature when the pressure is kept constant. **Figure 2.2** represents the simplest illustration of an adsorption isobar where *a* is the gas adsorption capacity, *P* is the pressure, and *T* is the temperature.

2.1.1.1.3 Adsorption Isostere

An adsorption isostere for a combination of gas, adsorbate, and a solid, adsorbent, represents the equilibrium pressure as a function of the temperature for a given amount of adsorbed gas. **Figure 2.3** represents the simplest illustration of an adsorption isostere where *a* is the gas adsorption capacity, *P* is the pressure, and *T* is the temperature.

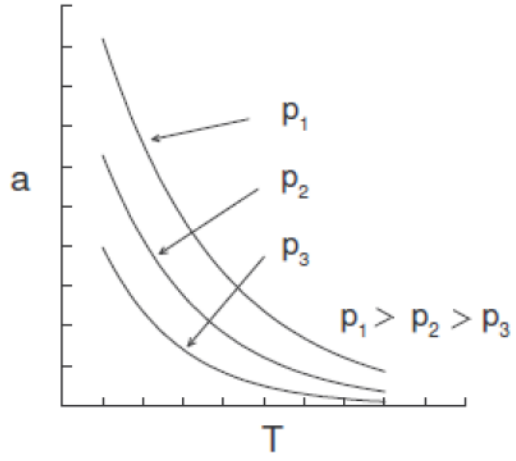

Figure 2.2 The simplest representation of an adsorption isobar. It also illustrates that adsorption capacity increases with increasing pressure.

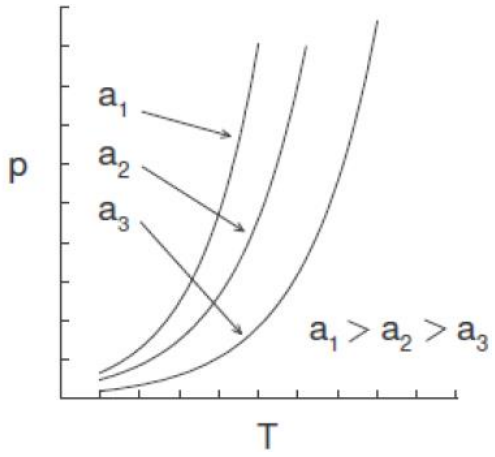

Figure 2.3 The simplest representation of an adsorption isostere. It also illustrates that adsorption capacity increases with increasing pressure.

2.1.1.2 Adsorption Isotherms/ Models

2.1.1.2.1 Freundlich Adsorption Isotherm

An adsorption isotherm that was introduced in 1895 by Boedecker and it is based on **Equation 2.1** which is known as Freundlich adsorption equation.

$$a = kp^{1/n} \tag{2.1}$$

where k, and n are constants that depend on the adsorbent and adsorbate at a specific temperature.

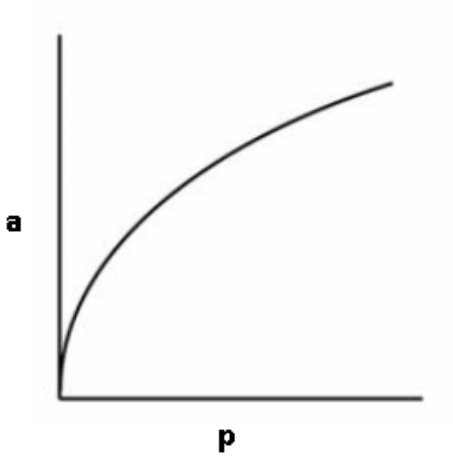

Figure 2.4 Freundlich Adsorption Isotherm.

Taking both log sides of the Freundlich equation, one gets **Equation 2.2**.

$$log\ a = log\ k\ +\ {}^{1}/_{n}\ log\ p \qquad (2.2)$$

Plotting graph between log a and log p gives a linear relation with a slope of ${}^{1}/_{n}$. $log\ k$ is the y-axis intercept.

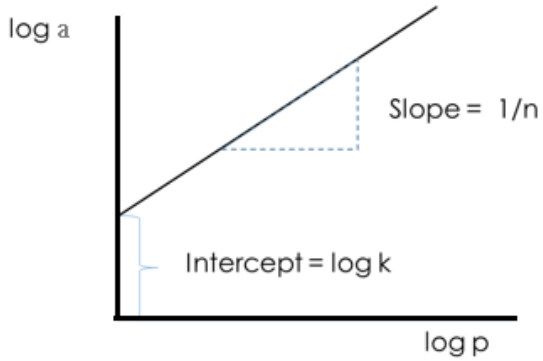

Figure 2.5 Determination of the constants from the logarithmic form of Freundlich Isotherm.

The value *n* changes from 0.2 to 0.9 and increases with temperature increase up to 1 while the value *k* changes within a wide range depending on the kind of adsorbent and adsorbed substance.

2.1.1.2.1.1 Limitation of the Freundlich Adsorption Isotherm

- It is applicable within certain limits of pressure. At higher pressure, it shows deviations.
- The values of constants *k* and *n* change with the temperature.
- The Freundlich isotherm is an empirical one and it does not have any theoretical basis.

2.1.1.2.2 Langmuir Theory and Adsorption Isotherm

Irving Langmuir 1916 introduced his adsorption isotherm/ model which describes the gases adsorption on the surface of solids. Langmuir Isotherm is the most widely used isotherm that

quantifies the maximum amount of the gas that could be adsorbed at equilibrium on the surface of solids as a function of partial pressure at a specific temperature. Langmuir Isotherm is represented by **Equation 2.3** and **Figure 2.6** and its linear form is represented by **Equation 2.4** and **Figure 2.7**.

$$a = \frac{a_m kp}{1+kp} \tag{2.3}$$

Where a_m is the number of moles of the gas or adsorbate that cover the surface area of one gram of the adsorbent by forming a monolayer and it is also referred to as the adsorption capacity or the monolayer capacity.

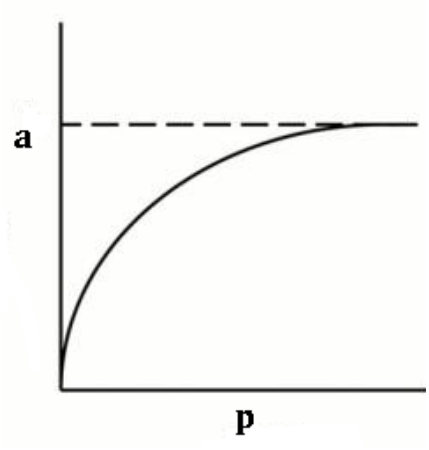

Figure 2.6 Langmuir Adsorption Isotherm.

Langmuir Isotherm linear form is expressed through **Equation 2.4.**

$$\frac{p}{a} = \frac{1}{a_m}p + \frac{1}{a_m K} \tag{2.4}$$

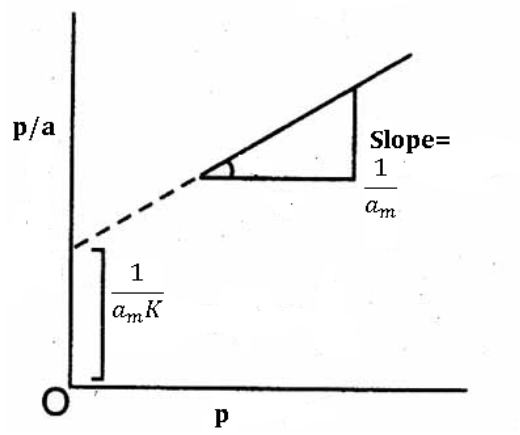

Figure 2.7 The linear form of the Langmuir Isotherm and determination of the constants a_m and K.

If given $\omega_m$which is the surface area that each molecule of the adsorbate occupies of the adsorbent, one can calculate the specific surface area of the adsorbent using **Equation 2.5** where N is the Avogadro's number.

$$S = a_m \, N \, \omega_m \tag{2.5}$$

Langmuir Isotherm is proven to be accurate in describing the experimental data in many cases. The only case that is not anticipated by Langmuir Isotherm is when the multilayer adsorption occurs while Langmuir Isotherm assumes monolayer adsorption. Multilayer adsorption is most likely to happen in the case of low temperatures and high heterogeneity of the adsorbent surface. Langmuir Isotherm is used to model the adsorption in coalbed methane reservoirs and with CBM reservoirs conditions of temperature and heterogeneity, it has been proven to be efficient in describing the adsorption and the monolayer adsorption assumption has been proven to be reasonable. Many factors affect the adsorption capacity such as pressure, temperature, moisture content, and gas itself and these factors will be addressed later. However, it is important to be aware of the adsorption difference between different gases. That is, if a gas component in a mixture has higher partial pressure than other components, its adsorption also will be higher than the other

components. For a system that has a gas mixture as the adsorbate, the Langmuir Isotherm is represented by **Equation 2.6.**

$$\theta_i = \frac{k_i p_i}{1+\Sigma k_i p_i} \tag{2.6}$$

2.1.1.2.2.1 Langmuir Isotherm Assumptions

1. Only one molecule could be adsorbed per active site of the adsorbent surface which is composed of a specific number of such sites and that number depends on the adsorbent surface area.

2. The heat of adsorption is independent of coverage and it has a constant value since it is assumed that there are no lateral interactions between the adsorbed molecules.

3. The adsorption is localized meaning that the adsorbed molecule stays on the same active site until it desorbs.

4. Langmuir assumes monolayer adsorption meaning that at the maximum adsorption capacity only one molecule per active site could be adsorbed and it is not possible for the gas molecules to be adsorbed on each other forming multi-layer. That is, the adsorbate molecules could only become adsorbed on the available free sites that do not already have adsorbed molecules on them.

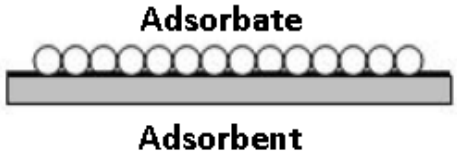

Figure 2.8 Monolayer model of Langmuir Adsorption.

The formulation of the Langmuir Isotherm assumes a dynamic equilibrium between the adsorbed phase of the adsorbate and the vapor phase of the adsorbate. Equilibrium state occurs

when the rate of adsorption of molecules onto the surface equals the rate of desorption of the adsorbed molecules back into the vapor phase. Thus, dynamic equilibrium occurs when the adsorption rate equals the desorption rate.

The rate of adsorption depends on:

1. Surface coverage change because of the adsorption process and this change is proportional to the pressure *P*.

2. Probability of collision with an available free active site that is described as follows.

$$1 - \frac{a^s}{a_m^s}$$

Where,

a^s: The gas concentration on the surface of the adsorbent, and

a_m^s: The gas concentration where the surface is covered by the monolayer of the gas.

3. The adsorption activation energy.

The rate of desorption depends on:

1. Surface fractional coverage that is described as follows.

$$\frac{a^s}{a_m^s}$$

2. The desorption activation energy.

2.1.1.2.3 Comparison Between Langmuir and Freundlich Isotherms

Comparing the two popular isotherms, the Freundlich Isotherm lacks the linear relationship between the adsorption capacity *a* and the pressure *P* when dealing with low pressures. Additionally, Freundlich Isotherm is an empirical model, unlike the Langmuir Isotherm which is theoretically justified. Moreover, Freundlich Isotherm has a limited application range compared to

the Langmuir Isotherm. That is, Freundlich Isotherm is not reliable when dealing with low pressures where the linear relationship is not obtained unless the value of *n* was 1. Also, at high pressures, the Freundlich Isotherm curve increases unreasonably while the adsorbent has a finite surface area and it gets to a point where it is fully saturated and cannot adsorb more gas. To conclude, Freundlich Isotherm is easy to deal with, yet it is not very reliable unless one deals with a limited pressure range. It can be used mostly to qualitatively describe the adsorption process.

2.1.1.3 Modeling the Adsorption of Gas Mixtures Using Extended Langmuir Model

Adsorbed gas in CBM reservoirs is most likely to be a mixture of more than one component. In this study, the gas of Big George Coal of Powder River Basin, Wyoming, US, is composed of 87% to 94% CH_4, 4% to 12 % CO_2, and trace amounts of other hydrocarbons (Boreck and Weaver, 1984). An Extended Langmuir Isotherm was needed to efficiently model and predict the adsorption of the gas mixture by accounting for the gas different components. Kapoor et al. (1989) proposed the Extended Langmuir model. Their model was introduced to model and calculate the adsorption of a gas mixture on adsorbents that have heterogeneous surfaces (Kapoor et al., 1989). The extended model assumes that the adsorption energies are uniformly distributed over the adsorbent surface. The Extended Langmuir Model is utilized to predict the adsorption of a gas mixture on each patch of a surface that has uniform energy distribution.

To model the process of the adsorption of a gas mixture, one must understand that each gas component does not sorb independently. In case of a gas mixture of methane and carbon dioxide in a CBM reservoir, both gases compete for the available free active sorption sites. Many factors contribute to giving one gas a better chance at sorption than the other. In this case, CO_2 has a higher adsorption capacity. Current common reservoir simulators like ECLIPSE use the Extended Langmuir (EL) model to predict the equilibrium state between the adsorbed and free gas in CBM

reservoirs (Arri et al., 1992). The Extended model is also vital when considering the enhanced coal bed methane (ECBM) process by injecting carbon dioxide into the coal formations. In this case, the EL model is needed to model the sorption of CO_2 and CH_4 mixture even if the CBM reservoir had only CH_4 before the CO_2 injection.

Arri et al. (1992) conducted a study that investigated the binary sorption of methane mixtures whether it is a methane-nitrogen or a methane- carbon dioxide mixture. They carried out a binary sorption experiment and then correlated the data using the Extended Langmuir model which was found efficient in providing a decent reasonable correlation of the data.

They ran the test first for single components and established a good match with the original Langmuir model. In general, Methane has an intermediate sorption capacity while the nitrogen has the least capacity and carbon dioxide has the highest sorption capacity. That is, the carbon dioxide sorption at a specific pressure is 182% of the methane sorption at the same pressure. **Table.2.1** and **Figure 2.9** Indicate the sorption capacities for single components (Arri et al., 1992).

Table 2.1 Sorption results for the pure gases (Arri et al., 1992).

Methane Adsorption 115.1°F & 10.84% Moisture			Nitrogen Adsorption 114.8°F & 4.88% Moisture			Carbon Dioxide Adsorption 115.3°F & 10.23% Moisture		
P psia	V SCF/ton Gibbs	V SCF/ton Absolute	P psia	V SCF/ton Gibbs	V SCF/ton Absolute	P psia	V SCF/ton Gibbs	V SCF/ton Absolute
165.5	245.3	249.4	151.5	60.1	61.0	126.0	436.2	441.8
384.5	370.9	386.1	248.5	91.8	93.9	244.5	592.1	607.6
555.5	428.6	454.9	505.5	150.9	158.1	425.5	716.8	752.3
742.5	464.6	504.2	766.5	193.9	208.3	612.5	782.4	844.2
992.5	494.9	554.3	1013.5	227.3	250.0	822.5	812.9	912.4
1245.5	509.3	590.1	1549.5	276.1	320.0			
1494.5	514.2	617.2						

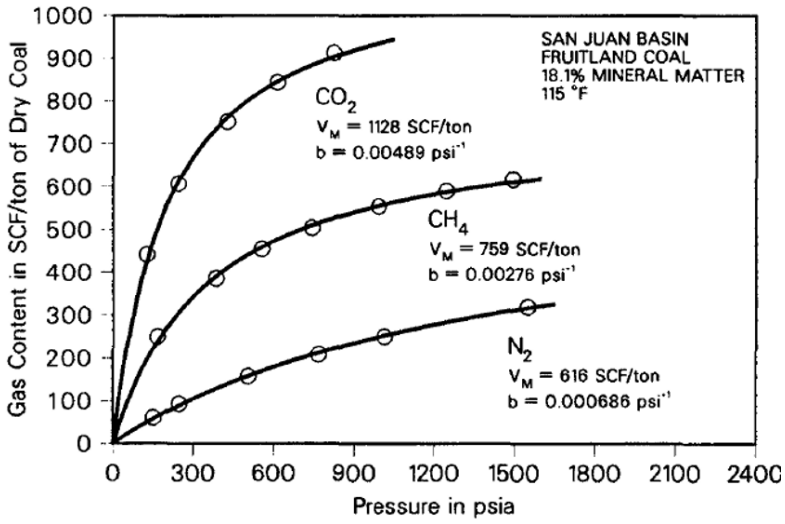

Figure 2.9 Sorption data for pure gases (Arri et al., 1992).

The binary adsorption processes were then conducted on the methane-nitrogen and methane-carbon dioxide mixtures at pressures of 500, 1000, and 1500 psia. The sorption results for the methane-nitrogen mixture alongside the Extended Langmuir Isotherm predictions are illustrated in **Table 2.2**. and **Figures 2.10, 2.11**., and **2.12**.

Looking at the total sorption, one can see that the total sorption minimum value corresponds to pure nitrogen while the maximum value corresponds to pure methane. This result is consistent with the conclusion that the sorption capacity for methane is higher than the sorption capacity for nitrogen. This also confirms that both gases do not sorb independently and they compete for the active sites.

Table 2.2 Methane-nitrogen binary sorption results (Arri et al., 1992).

Free Gas				Absolute Adsorption					Gibbs Adsorption		
P psia	T°F	y_{CH_4}	y_{N_2}	V_{CH_4} SCF/ton	V_{N_2} SCF/ton	V_{total} SCF/ton	x_{CH_4}	x_{N_2}	V_{CH_4} SCF/ton	V_{N_2} SCF/ton	V_{total} SCF/ton
576.5	114.9	0.7582	0.2418	401.9	25.5	427.4	0.9403	0.0597	382.7	19.4	402.1
1053.5	114.9	0.7709	0.2291	524.2	34.2	558.4	0.9388	0.0612	476.4	19.9	496.3
1545.5	114.9	0.7779	0.2221	610.6	43.9	654.5	0.9329	0.0671	526.1	19.8	545.9
553.0	115.1	0.1560	0.8440	114.9	142.8	257.7	0.4459	0.5541	112.8	131.4	244.2
1051.5	115.0	0.1644	0.8356	174.4	208.3	382.7	0.4557	0.5443	168.1	176.5	344.6
1540.5	115.0	0.1718	0.8282	209.2	266.4	475.6	0.4399	0.5601	197.4	209.3	406.7
566.5	115.5	0.1475	0.8525	110.2	128.3	238.5	0.4621	0.5379	108.3	117.4	225.7
1063.5	115.5	0.1570	0.8430	161.2	184.9	346.1	0.4657	0.5343	155.7	155.5	311.2
1556.5	115.5	0.1630	0.8370	196.2	232.0	428.2	0.4583	0.5417	186.0	179.5	365.5
553.5	116.0	0.1073	0.8927	82.0	154.6	236.6	0.3466	0.6534	80.7	143.7	224.4
1064.5	116.0	0.1144	0.8856	123.0	225.8	348.8	0.3527	0.6473	119.1	195.1	314.2
1549.5	116.0	0.1185	0.8815	151.9	286.5	438.4	0.3465	0.6535	144.5	231.1	375.6
557.5	116.5	0.0877	0.9123	67.2	136.6	203.8	0.3298	0.6702	66.3	127.0	193.3
1059.5	116.4	0.0937	0.9063	100.4	200.9	301.8	0.3333	0.6667	97.7	174.0	271.7
1569.5	116.4	0.0980	0.9020	123.4	260.9	384.3	0.3211	0.6789	118.0	210.8	328.8

Generally, Extended Langmuir model provided a reasonable match with the binary sorption results. However, it is more accurate at 500 psia pressure and its accuracy begins to decrease with increasing pressures to 1000 psia and 1500 psia (Arri et al., 1992).

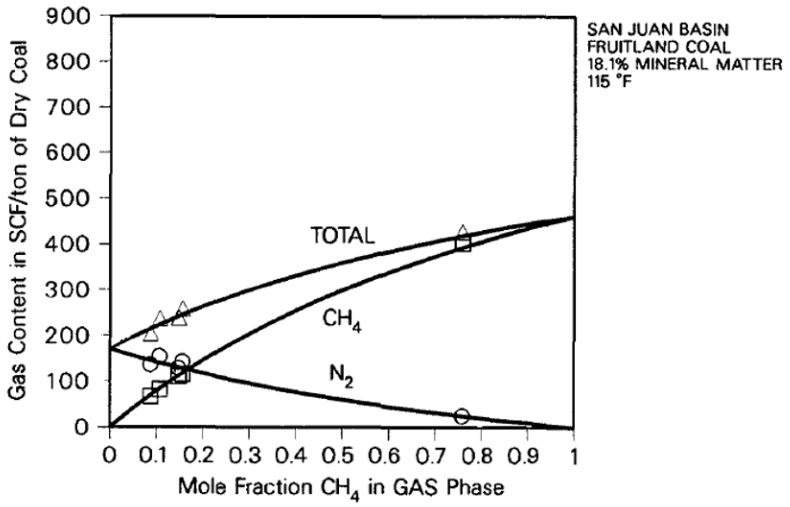

Figure 2.10 Methane- nitrogen sorption data at 500 psia (Arri et al., 1992).

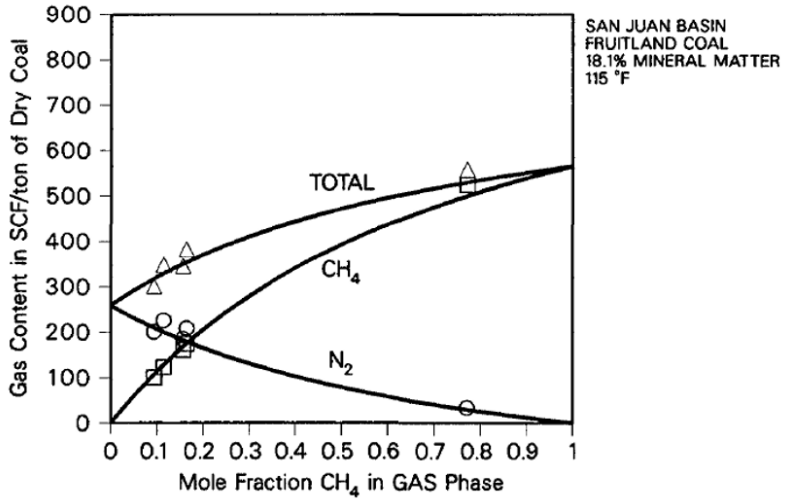

Figure 2.11 Methane- nitrogen sorption data at 1000 psia (Arri et al., 1992).

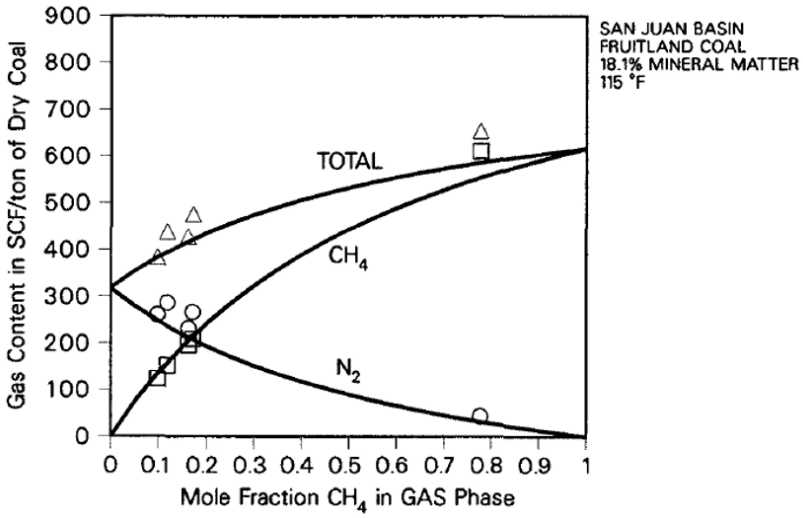

Figure 2.12 Methane-nitrogen sorption data at 1500 psia (Arri et al., 1992).

Similar sorption results were obtained for methane-carbon dioxide mixture and illustrated in **Figures 2.13, 2.14**, and **2.15.**

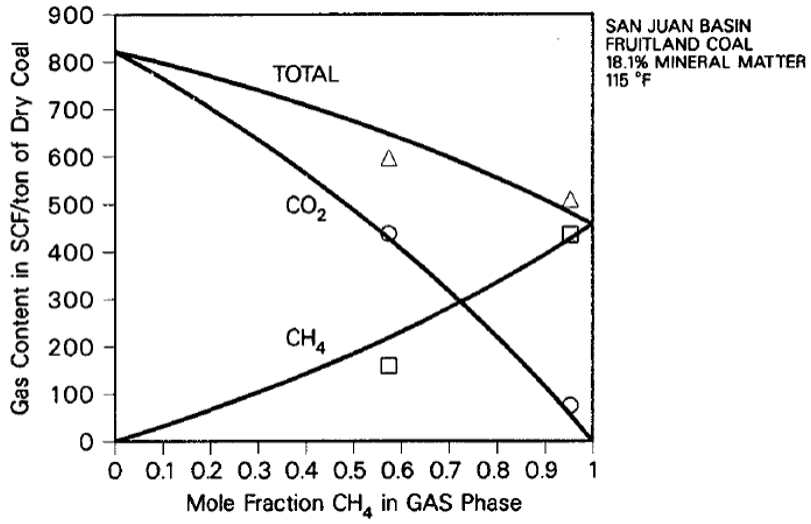

Figure 2.13 Methane-carbon dioxide sorption data at 500 psia (Arri et al., 1992).

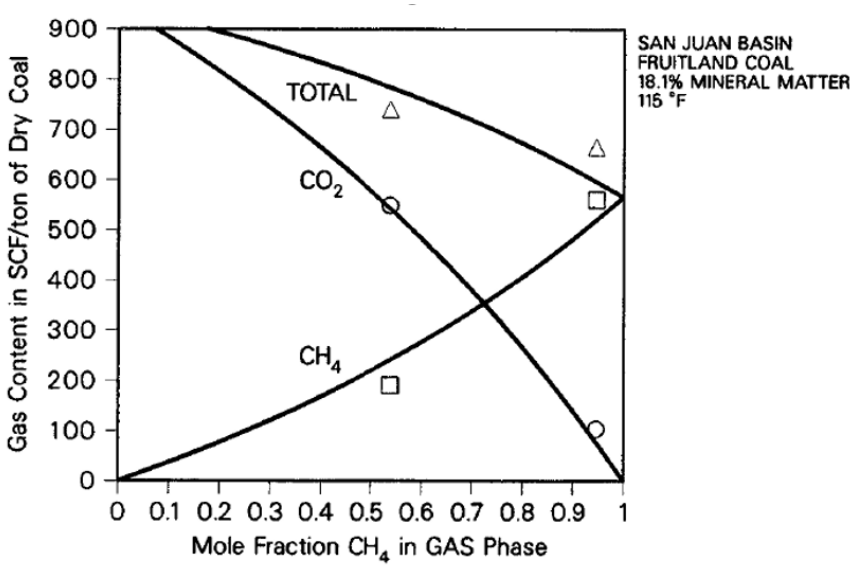

Figure 2.14 Methane-carbon dioxide sorption data at 1000 psia (Arri et al., 1992).

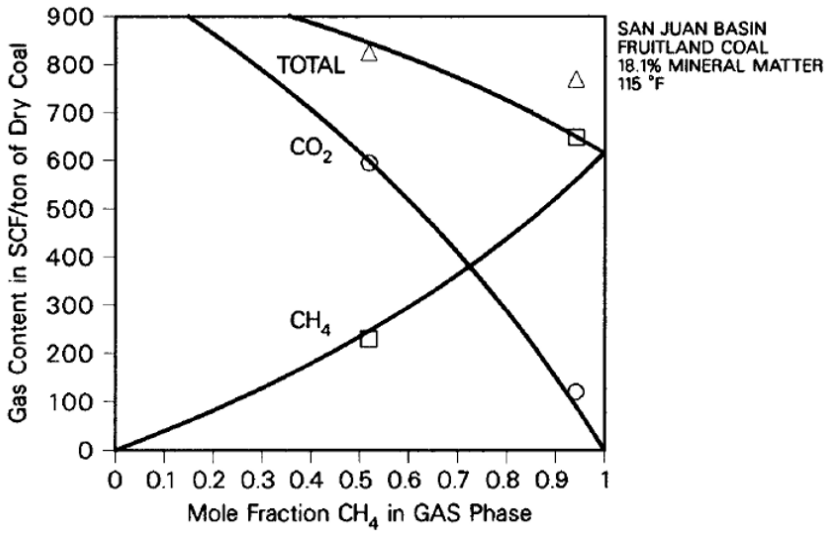

Figure 2.15 Methane-carbon dioxide sorption data at 1500 psia (Arri et al., 1992).

2.1.2 Gas Diffusion in CBM Reservoirs

2.1.2.1 Gas Flow in CBM Reservoirs

Cleats in coalbed formations in the US are usually fully saturated with water. The pressure of that water is what holds the adsorbed methane in place and prevents its desorption. When the first phase of the production occurs by dewatering, the pore pressure decreases, and the gas starts to diffuse within the matrices and then flow into the cleats. That is, the gas flows to the depressurized zone. In order to understand the gas flow, it is divided into two stages as follows:

A- Concentration gradient-driven flow: Where the gas flows through the matrix due to the gas diffusion which is commonly modeled using Fick's Second Law of Diffusion (Harpalani and Chen, 1997).

B- Pressure-driven flow: Where gas flows through the cleats after it desorbs and diffuses through the matrix. This flow is a gas flow through porous media and could be described using Darcy's law (Pillalamarry et al., 2011). The two kinds of gas flow are illustrated in **Figure 2.16.**

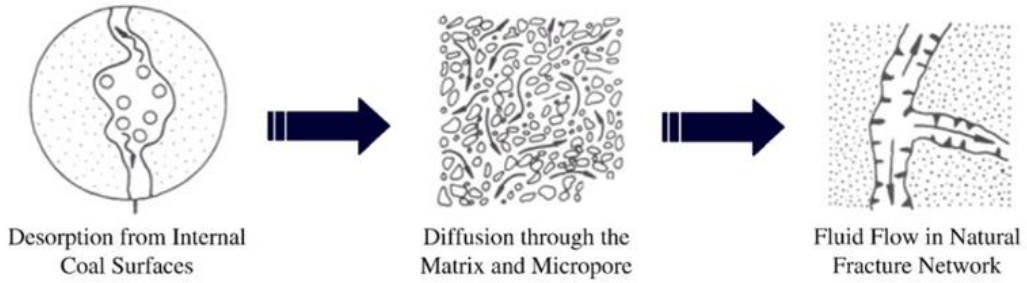

Figure 2.16 Gas transport mechanisms in CBM reservoirs (King, 1985).

The first phase of gas flow, diffusion flow, needs to be more investigated and understood because it has a vital impact on the methane flow and production in CBM reservoirs.

2.1.2.1.1 Gas Diffusion Mechanisms in CBM Reservoirs

The coal matrices have pores of microscale. Gas diffusion through micropores is composed of three diffusion mechanisms:

A- Knudsen diffusion: Gas molecules flow from higher to lower concentration place when the pressure is very low or when the mean free path of the gas molecules is greater than the molecular diameter (Collins, 1991; Zhao, 1991). It is dominated by the molecule- wall collisions since molecules collide more with the flow path walls than with each other (Shi and Durucan, 2003; Thorstenson and Pollock, 1989). Thus, the resistance to gas flow is primarily caused by the collisions of the molecules with the pore walls rather than with each other (intermolecular collisions) (Pillalamarry et al., 2011).

B- Surface diffusion: Gas flows through physically adsorbed layer (Shi and Durucan, 2003). It happens when the adsorbed gas molecules move along the adsorbent surface as liquid (Collins, 1991). It could be negligible compared to Knudsen diffusion at room temperature and it is normally ignored for CBM production (Pillalamarry et al., 2011).

C- Bulk diffusion: Molecule-molecule collisions dominate (Shi and Durucan, 2003). Unlike Knudsen diffusion, it happens at higher pressures (Collins, 1991). That is, it happens when the mean free path of the gas molecules is smaller than the molecule diameter. Therefore, the resistance to flow is primarily caused by intermolecular collisions, not the molecule- wall collisions.

The gas diffusion in CBM reservoirs is a complex parameter that may include one or more types of diffusion. Many studies investigated characterizing and quantifying gas-diffusion coefficient in CBM reservoirs, and yet more studies are needed. Gas exists in CBM reservoirs as adsorbed, free, and soluble phase, but the greater part of the gas in place especially for coals of medium and high rank is composed of the adsorbed gas which gives more importance to gas diffusion phenomenon when one deals with high or medium rank coal formations.

2.1.2.2 Gas Diffusion Models in CBM Reservoirs

2.1.2.2.1 Unipore Model

This is the conventional model which uses Fick's law to describe gas diffusion in coal. It assumes that the coal particles are uniform spheres and that the matrix pore structure is homogenous. The fractional uptake under isothermal conditions of the gas mass follows **Equation 2.7** (Crank 1975).

$$\frac{M_t}{M_\infty} = 1 - \frac{6}{\pi^2}\sum_{n=1}^{\infty}\frac{1}{n^2}exp\left(-\frac{n\pi^2 Dt}{R^2}\right) \quad (2.7)$$

Where,

M_t : The total mass of gas desorbed at time t, g;

M_∞: The total desorbed mass after an infinite time, g;

t : The diffusion time, s;

R : The radius of the sphere, mm; and

D : The diffusion coefficient, mm^2/s.

(Clarkson and Bustin 1999) presented **Equation 2.8** for the gas desorption off coal particles as follows:

$$\frac{V_t}{V_\infty} = 1 - \frac{6}{\pi^2}\sum_{n=1}^{\infty}\frac{1}{n^2}exp\left(-\frac{n\pi^2 Dt}{R^2}\right) \quad (2.8)$$

Where,

V_t : The volume of gas desorbed at time *t, ml*; and

V_∞ : The final desorbed volume, *ml*.

2.1.2.2.2 Bidisperse Model

Ruckenstein et al. (1971) presented the first bidisperse model and they made the following assumptions:

1- The adsorbent (coal surface in CBM) is microsphere that is composed of uniform microspheres.

2- The gas sorption isotherm is linear.

3- Gas concentration changes suddenly off the coal particle (Cheng-Wu et al., 2018).

Clarkson and Bustin (1999) improved their model to include the nonlinear adsorption isotherm. Shi and Durucan (2003) introduced another bidisperse model considering isothermal and isobaric conditions for methane desorption caused by CO_2 injection. A simplified bidisperse model describes a slow micropore diffusion stage and a fast macropore diffusion stage was introduced by (Pan et al., 2010). The uptake can be expressed by **Equation 2.9** for the micropore diffusion (Wang et al., 2014b).

$$\frac{V_{it}}{V_{i\infty}} = 1 - \frac{6}{\pi^2}\sum_{n=1}^{\infty}\frac{1}{n^2}exp\left(-\frac{n\pi^2 D_i t}{{R_i}^2}\right) \quad (2.9)$$

Where,

V_{it} : Total volume of the adsorbed/desorbed gas in the micropores,

t : Time,

R_i : Microsphere radius,

$V_{i\infty}$: Final adsorbed/desorbed gas volume, and

D_i : Micropore diffusivity.

The uptake can be expressed by **Equation 2.10** for the macropore diffusion stage (Wang et al., 2014b).

$$\frac{V_{at}}{V_{a\infty}} = 1 - \frac{6}{\pi^2}\sum_{n=1}^{\infty}\frac{1}{n^2}exp\left(-\frac{n\pi^2 D_a t}{{R_a}^2}\right) \quad (2.10)$$

Where,

V_{at} : Total volume of the adsorbed/desorbed gas in the macropores,

t : Time,

R_a : Macrosphere radius,

$V_{a\infty}$: Final adsorbed/desorbed gas volume, and

D_a : Macropore diffusivity.

Thus, the total uptake could be calculated by **Equation 2.11.**

$$\frac{V_t}{V_\infty} = \eta\frac{V_{at}}{V_{a\infty}} + (1-\eta)\frac{V_{it}}{V_{i\infty}} \quad (2.11)$$

2.1.2.3 Gas-diffusion Coefficient

Gas diffusion is usually characterized and quantified through the gas-diffusion coefficient. There is a lot of speculation around modeling the gas-diffusion coefficient. One needs to know the factors that affect the gas-diffusion coefficient to be able to predict and model it. Among those factors, the kinetics of adsorption depends on the nature of gas, moisture content, and temperature

(Clarkson and Bustin, 1999b). Gas in CBM reservoirs is usually composed of combinations of methane with nitrogen or carbon dioxide or both. For that, one needs to investigate how each different gas diffuses. Due to the physicochemical properties, CO_2 diffuses in higher amounts than methane in CBM reservoirs (Pillalamarry et al., 2011). Reservoir pressure impact on gas diffusion coefficient should also be considered. Cui et al. (2004) found that there is a negative correlation between reservoir pressure and gas diffusion coefficient. This was found by using the bi-square diffusion model for different coal systems at different pressures. Furthermore, it was found that besides the bi-square model, the unipore model is also practical for modeling the methane diffusion in coal.

Pillalamarry et al. (2011) conducted a study using the unipore model to investigate the gas diffusion coefficient variation with gas depletion and they found that for pressure below 3.5 MPa, there is a negative correlation between pressure and diffusion coefficient making it easier for the gas to flow in the CBM formations with continued gas production. There is also an impact of the increasing adsorption on the gas diffusion coefficient as Cui et al. (2004) observed that increasing the adsorption caused the reduction of the diffusion coefficient and this might be attributed to the fact that increasing the adsorbed molecules causes an increase in the coal matrix swelling making the pore size smaller and increasing the resistance to the flow of the gas (Cui et al., 2004). This relationship could also be the result of the increasing repulsive forces between the molecules on the adsorbent surface due to the increase in the surface coverage (Chen and Yang, 1991).

2.1.2.3.1 Varying Diffusion Coefficient

Gas flow in coal is impacted by both permeability and diffusion, but it used to be assumed to be controlled only by permeability with a fixed gas-diffusion coefficient. However, Pillalamarry et al. (2011) carried out a simulation study to investigate the impact of the varying diffusion

coefficient on gas production throughout 10 years. They treated both permeability and diffusion as variables instead of considering a constant diffusion coefficient. They found that for high-permeability reservoirs (25 mD), increasing the diffusion coefficient from 2.4×10−10 cm^2/s to 38.2×10−10 cm^2/s had a significant impact on increasing the production, while for low-permeability reservoirs (14 mD), the increase in gas production due to increasing the diffusion coefficient was not significant meaning that for low-permeability reservoirs the gas diffusion coefficient is not a controlling parameter in gas production. They also pointed out that the simulators need to consider a varying diffusion coefficient value instead of considering it as a constant (Pillalamarry et al., 2011). Gas production in CBM reservoirs used to be considered permeability-controlled which might not be the case, especially for high-permeability reservoirs. **Figure 2.17** Illustrates the impact of increasing the diffusion coefficient for high permeability reservoir and for low-permeability reservoir where one can see that for low-permeability reservoirs, there is no much impact of increasing the diffusion coefficient on the gas production while increasing the diffusion coefficient in case of high-permeability reservoirs has a significant impact on gas production suggesting that diffusion could be a controlling parameter and should be considered as a variable alongside the permeability while for low-permeability reservoir, gas production could still be considered permeability- controlled (Pillalamarry et al., 2011).

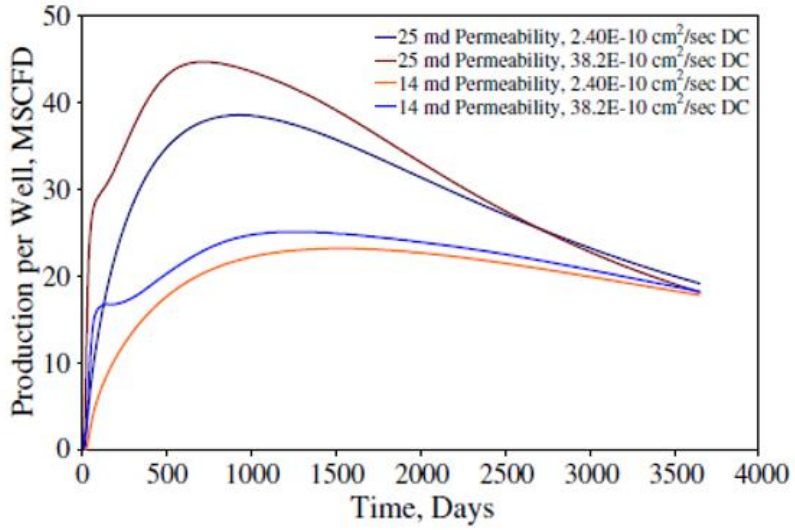

Figure 2.17 Impact of varying the gas diffusion coefficient with different permeability levels on gas production (Pillalamarry et al., 2011).

Building on the study conducted by Pillalamarry et al. (2011) and based on the finding that the gas-diffusion coefficient varies with time, Cheng-Wu et al. (2018) presented a time-dependent gas-diffusion coefficient that is named dynamic diffusion coefficient (DDC). They were able to describe experimental data using both DDC and bidisperse model. However, the fit of the data to the DDC model was slightly better (Cheng-Wu et al., 2018). Unlike the findings made by Pillalamarry et al. (2011) that the diffusion increases with time due to the reduction in pore pressure, Cheng-Wu et al. (2018) concluded that the diffusion coefficient decreases with time due to the gas diffusion through the interconnected pores that interact with each other.

2.1.2.3.2 Factors Affecting Gas-diffusion Coefficient in CBM Reservoirs

2.1.2.3.2.1 Effect of Pore Size Distribution on Gas Diffusion

Coal has a wide range of pore sizes from subnanometer to millimeters. However, the common models that were previously mentioned, unipore and bidisperse, only consider one, two or three pore sizes and deal with their impact independently. Unipore model assumes that

micropores in coal have just one size while bidisperse assumes two sizes: micropore and macropore. Since coal formations contain a wide range of pores sizes, diffusion models that consider and take the pore size distributions into account are more realistic (Staib et al., 2014). Fractual pore size distributions are a way of modeling gas diffusion in porous media and it correlates the methane sorption capacity for different coals, but it still needs more investigation to be accepted to model gas diffusion in coal (Zheng et al., 2012; Lesne and Lagües, 2011; Chen et al., 2011). More studies are needed to accurately characterize the impact of pore size distribution on the gas diffusion in coal. However, if the rate of the gas flowing out of a pore in a coal formation is related to the size of that pore, then the pore size distribution could be an indicator of gas diffusion rates distribution (Staib et al., 2014).

2.1.2.3.2.2 Effect of Coal Rank and Maceral Composition on Gas Diffusion

Through the investigation of 18 bituminous and sub-bituminous Australian coal Keshavarz et al. (2017) investigated the effect of maceral composition and coal rank on CO_2 and CH_4 diffusion and they found that the diffusion times and rates vary significantly over 6 orders of magnitudes with varying the coal rank and maceral composition. With the lower and medium-rank coal, the diffusion rates increased significantly with the inertinite content of the coal while they were independent of the pressure, 1-5 bar. While for higher rank coal, the diffusion rates were not very responsive to the changes in the maceral composition (Keshavarz et al., 2017).

The impact of maceral composition on the gas diffusion is not agreed upon by investigators, but some studies conducted on Australian basin, Bowen Basin suggested that the gas diffusion changes with the coal type and rank (Hunt and Botz, 1986; Beamish and Crosdale, 1995; Crosdale and Beamish, 1993; Laxminarayana and Crosdale, 1999). However, other studies showed a weak relationship between gas diffusion and coal rank and type (Faiz and Cook, 1991; Faiz et al., 1992;

Crosdale and Beamish, 1994). Using crushed coal samples from Bowen Basin Australia, Laxminarayana and Crosdale (1999) Concluded upon examining the impact of the coal rank and maceral composition on gas diffusion rate that the coals that are inertinite-rich have faster diffusion rates. However, they disagreed on the impact of the maceral composition on the gas sorption and diffusion.

Based on a new laboratory method Xu et al. (2015) found that the adsorption capacity increases when the metamorphic degree of coal increases. With increasing the coal rank, the gas diffusion in coal first decreases and then increases (Xu et al., 2015). Different coal ranks have different gas adsorption capacity because of the difference in their pore structure (Gan et al., 1972). The influence of the coal rank on the gas diffusion coefficients is related to the different adsorption capacities of different coal ranks. The higher the coal rank, the higher the adsorption capacity, that is, more gas could be adsorbed (Xu et al., 2015).

2.1.2.3.2.3 Effect of Gas Pressure on Gas Diffusion

For constant temperature, increasing gas pressure results in increasing methane diffusion coefficient. This is correct with any values of water saturation and with different coal ranks (Xu et al., 2015). This could be explained by the fact that the methane uptake nonlinearly increases with pressure increase. However, at a certain pressure, the methane uptake does not increase with increasing the pressure meaning that the coal becomes fully gas saturated (Smith and Williams, 1984).

2.1.2.3.2.4 Effect of Moisture Content on Gas Diffusion

Increasing the moisture content results in reducing the surface area of the coal matrix that is available for adsorption. Thus, the matrix adsorption capacity decreases. As a result, it becomes harder to have a higher gas concentration gradient. Thus, the gas diffusion coefficient is higher in

less water-saturated coal samples than in fully water saturated samples. Additionally, the existence of water on the coal surface results in a significant reduction in the desorption of the methane in the coal micropores due to the high capillary pressure (Van Bergen et al., 2009).

2.1.3 Stress-sensitive Permeability in CBM Reservoirs

In coal and other naturally fractured formations, permeability is sensitive to changes in the pore pressure meaning that it is sensitive to changes in effective stress (Palmer and Mansoori, 1994). Pore pressure reduction results in decreasing the coal permeability due to the compression of the cleats and the reduction of the pore volume. However, Coal permeability is sensitive to another factor which is the matrix shrinkage/swelling due to the gas desorption/adsorption. The matrix shrinkage results in increasing coal permeability. Thus, matrix shrinkage impact on the coal permeability is opposite to the impact of the pore pressure reduction on permeability. There is a very interesting and unique interplay between these factors. These opposite impacts make it hard to characterize or predict the permeability variations.

Many researchers tried to effectively model the coal absolute permeability changes. Palmer and Mansoori (1998) presented the most common and widely accepted model to calculate pore volume compressibility and permeability in coals as a function of matrix shrinkage and effective stress. They assumed uniaxial strain conditions which are most likely to present in a CBM reservoir. That is, the model predicts the permeability changes as the reservoir pressure decreases. Pore volume compressibility is also considered as a variable that changes with pressure. Pore volume compressibility tends to be high in coal where the porosity is very small. It is of great interest to predict if the permeability could keep increasing until it becomes higher than the original permeability as a result of the two opposite influences of the pore pressure reduction and matrix shrinkage. With gas production, pore pressure decreases, which increases the effective stress and

compresses the cleats resulting in permeability reduction. Meanwhile, the methane desorbs off the coal matrix surface making the matrix shrink and permeability increase. While the matrix shrinkage is a function of coal pore pressure, the permeability depends on porosity elasticity, adsorption capacity, and pore pressure. Palmer and Mansoori expected that if the matrix shrinkage is high enough, the permeability increase due to the matrix shrinkage may result in a permeability rebound at very low pressures (Palmer and Mansoori, 1998).

2.1.4 Effect of Coal Anisotropy and Heterogeneity on CBM Physics

Coal formations are highly heterogeneous and anisotropic. Many geological factors result in coal high heterogeneity such as depositional environments, tectonic settings, temperature, and hydrology (Fu et al., 2016). Even the coal samples that are taken from the same coal reservoir might have different mineral compositions (Tan et al., 2018). Busch et al. (2004) analyzed the grain size fractions data of coal sample from Silesia coal and they found that the vitrinite, and inertinite contents, and maceral composition varied with the grain size fraction. One should also note that there are other factors that contribute to the anisotropy of the coal formations such as the directional cleat system, and the bedding structure (Tan et al., 2018). The interbedded rocks in coal formations that result from geochemical interaction between waste rocks and coal boundaries also contribute to the coal heterogeneity (Heriawan and Koike, 2008). Coal composition in the vertical direction is highly heterogeneous and the cleat system is highly heterogeneous in the horizontal direction (Tan et al., 2018). From investigating the cleat delineation, Cai et al. (2015) concluded that coal is highly heterogeneous regarding the cleat density.

2.1.4.1 Effect of Coal Anisotropy and Heterogeneity on Gas Adsorption and Diffusion in CBM Reservoirs

The effect of coal heterogeneity and anisotropy on the gas adsorption capacity and gas diffusion behaviors needs more research to achieve a better understanding of that effect (Tan et al., 2018). One could assume that the different pore sizes would have different adsorption capacities. Anisotropy impacts gas diffusion and makes it heterogeneous. Also, gas diffusion is heterogeneous due to the impact of the variant composition and fabric (Tan et al., 2018). Even the diffusion mechanisms differ with different mineral components. Additionally, diffusion mechanisms and diffusivity change for different pore sizes (Tan et al., 2018).

Accounting for the impact of the anisotropy and heterogeneity of coal on gas diffusion is important for accurate modeling of the gas diffusion in CBM reservoirs (Tan et al., 2018).

2.1.4.2 Effect of Coal Anisotropy and Heterogeneity on CBM Reservoirs Permeability

Besides gas diffusion, it is also critical to understand and account for the impact of coal anisotropy and heterogeneity on the coal permeability in CBM reservoirs. It was found that the permeability in CBM reservoirs is also highly anisotropic and heterogeneous (Tan et al., 2018). The ratio of the permeability anisotropy of the perpendicular to parallel to bedding planes might reach to 1:17 (Koenig and Stubbs, 1986). Permeability changes affect every single aspect of gas flow behavior. Permeability in the matrix could be ignored compared to the values of the cleats permeabilities whereas cleats represent the main flow medium for the gas.

Coal permeability anisotropy has been studied through experimental work and modeling, yet a better understanding is still needed regarding the permeability anisotropy and the heterogeneity effect on the permeability in CBM reservoirs (Tan et al., 2018).

2.2 Adsorbed, Free, and Soluble Gas Contents Characterization and Calculation in Low-rank CBM Reservoirs

In medium and high-rank coalbed reservoirs, most of the gas in place is stored as adsorbed gas while the free and soluble gas contents are negligible. However, in low-rank coalbed reservoirs, free and soluble gas contents are significant and should not be ignored. Neglecting free and soluble gas contents in low-rank CBM reservoirs would result in an underestimation of the gas in place and an inaccurate gas production rates prediction. Accurate characterization and calculation of adsorbed, free, and soluble gas contents are important for CBM modeling and simulation. One needs a reliable characterization of gas contents as input for the reservoir model. Additionally, one needs accurate gas contents that could be used for future gas production rates forecasting through reservoir simulation. In this study of the Big George coalbed in Powder River Basin, Wyoming, I focused on having a good understanding of gas contents estimation mechanisms since BGC seams are low-rank coal. In this section, I address the detailed characterization and calculation of free, soluble, and adsorbed gas contents in low-rank coalbed methane reservoirs.

2.2.1 Adsorbed Gas Content

Adsorbed gas content in CBM reservoirs is usually characterized and quantified using Langmuir Isotherm for single component gases and Extended Langmuir model for binary/multi-component gas mixtures. Using Langmuir Isotherms, one can calculate the adsorbed gas concentration per unit area of the coal matrix surface at specific pressure and temperature. That amount is then used by the modeling and simulation software to calculate the adsorbed gas content of the entire reservoir at each different pressure while the reservoir temperature is constant.

Liu et al. (2013) introduced a mathematical model to calculate the adsorbed gas content, **Equation 2.12**. Their model also accounts for moisture and ash contents impacts on the adsorbed

gas content. Increasing the moisture content and/or ash content results in reducing the adsorption capacity of the coal and then the adsorbed gas content.

$$V_{ad} = [V_{T,daf} - \Delta V' \times (T_R - T_T)] \times \frac{100 - M_{ad} - A_{ad}}{100} \quad (2.12)$$

Where,

$V_{T,daf}$: Adsorbed gas content of the dry coal that has no ash at reservoir temperature, m^3/t;

T_R : Reservoir temperature, c °;

T_T : Experimental temperature, c °;

$\Delta V'$: Adsorption decrement ratio;

M_{ad} : Moisture content, *wt.%*; and

A_{ad} : Ash content on the air-dried basis, *wt.%* (Liu et al., 2013).

The common practice when evaluating a CBM reservoir potential of methane is ignoring free and soluble gas contents. This is not a very inaccurate approximation for middle or high-rank coal seams as they normally do not contain a significant amount of methane that is stored as free or soluble (Zhang et al., 2001; Fu et al., 2008; Alexeev et al., 2007; Cui et al., 2005; Mares et al., 2009) . However, It is critical for low- rank coal reservoirs to characterize the free and soluble gas contents because studies found that they are not negligible amounts and that the free and soluble gas contents make up a percentage that ranges from 8% to 34 % of the total in-situ gas content (Liu et al., 2013). Thus, free and soluble gas contents must be accounted for when evaluating a low-rank coalbed methane reservoir.

2.2.2 Free Gas Content

Since low-rank coal formations usually have higher permeability and lower absorbability, they are more capable to store free gas than medium and high-rank coal formations (Zhang et al.,

2006; Zhang et al., 2004). Thus, the assumption that the free gas content is negligible in low-rank coal would cause an underestimation of the gas reserves and production rates.

2.2.2.1 Free Gas Content Calculation

Liu et al. (2013) used Mariotte's law to model free gas content. The pore space in coal reservoir is occupied by the moisture, adsorbed gas, and free gas molecules. Methane molecule diameter is very limited compared to the coal pore diameter. Additionally, adsorbed gas is mainly stored in the micropores which have small volume in low- rank coal compared to mesopores and macropores (Cui et al., 2005; CR and Bustin, 1996; Levy et al., 1997). Thus, one can ignore the volume occupied by the adsorbed methane and then consider that the free gas takes up all the pores except for the ones that are occupied by moisture. Then, Mariotte's law could be used to predict the free gas content (Liu et al., 2013), **Equation 2.13**.

$$V_g = \frac{\Phi_r p T_0}{p_0 T Z} \tag{2.13}$$

Where,

V_g : Free gas content volume, m^3/t;

Φ_r : Subscript that refers to residual pore volume, m^3/t;

p : Gas pressure, *MPa*;

p_o : Standard pressure, *MPa*;

T_o : Standard temperature, *c* °;

T : Reservoir temperature, *c* °; and

Z : Gas compressibility factor (Liu et al., 2013).

Residual pore volume could be calculated using **Equation 2.14**.

$$\Phi_r = (\Phi - \Phi_w) \times (1 - \Phi_p)/\rho_{ca} \tag{2.14}$$

Where,

Φ : Measured total porosity, *%*;

Φ_w : Water volume percentage of the porosity, *%*;

Φ_p : Accumulative volume strain, *%*; and

ρ_{ca} : Coal apparent density, t/m^3 (Liu et al., 2013).

2.2.2.2 Factors Affecting the Free Gas Content

Free gas content changes with moisture content, in-situ porosity, initial water saturation, and gas pressure.

2.2.2.2.1 Effect of Moisture Content

As the moisture content and the pressure increase, the free gas content decreases as the volume of the pores that the free gas occupies becomes less (Liu et al., 2013).

2.2.2.2.2 Effect of Porosity/ Pore Volume

Free gas content increases with porosity and since the macro-pores have the greater impact on the total porosity and since macro-pores are the majority in low-rank coal (Alexeev et al., 2007; Levy et al., 1997), free gas content in low-rank coal is significant. With higher coal ranks, the macro-pores volume decreases and the total porosity and free gas content decrease. The pore volume also changes when the coal is subjected to confining pressure (Liu et al., 2013). **Figure 2.18** shows how the porosity changes with coal rank and one can see that the lower the rank is, the higher the porosity and the free gas content become.

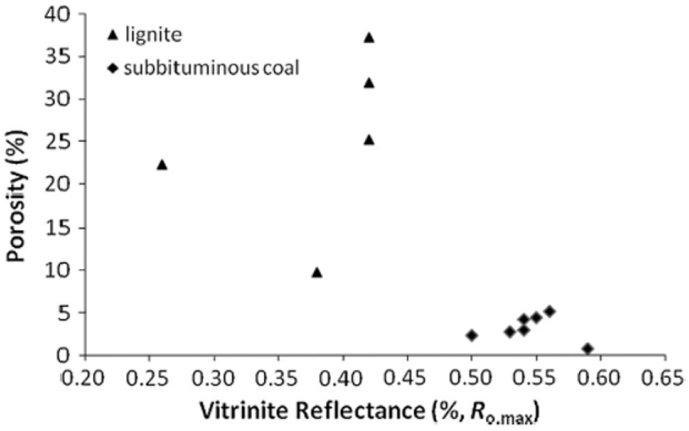

Figure 2.18 The change of coal porosity with the vitrinite reflectance (Liu et al., 2013).

The relationship between porosity and confining pressure could be described by **Equation 2.15** and illustrated in **Figure 2.19** of four different samples tested by (Liu et al., 2013).

$$\Phi_p = aLn(\sigma_{hv}) + b \tag{2.15}$$

Where,

a and b: Constants

Initially, it is easier to compress the pore volume, and then with increasing confining pressure, it becomes harder to compress the pore volume and the porosity changes slow down (Liu et al., 2013).

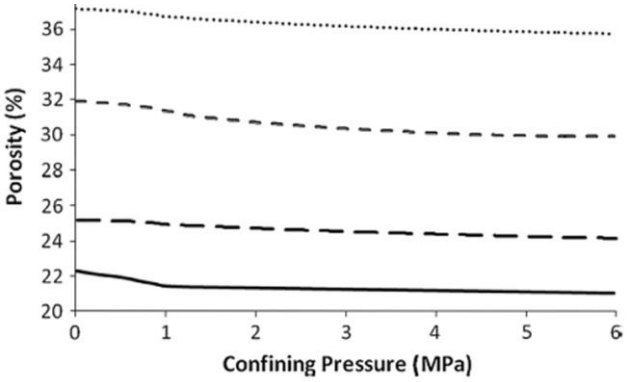

Figure 2.19 Effect of confining pressure on porosity (Liu et al., 2013).

2.2.2.2.3 Effect of Pressure and Temperature

Free gas content increases with residual pore volume under specific pressure and temperature (Liu et al., 2013). Residual pore volume is a volume under stress without considering the moisture volume. Residual pore volume is also changing with pressure and stress at a constant temperature. With increasing confining pressure, pore volume shrinks, and free gas content decreases (Liu et al., 2013).

2.2.2.2.4 Effect of Burial Depth

Liu et al. (2013) found that free gas content increases with increasing depth of the CBM reservoir. **Figure 2.20** illustrates the results.

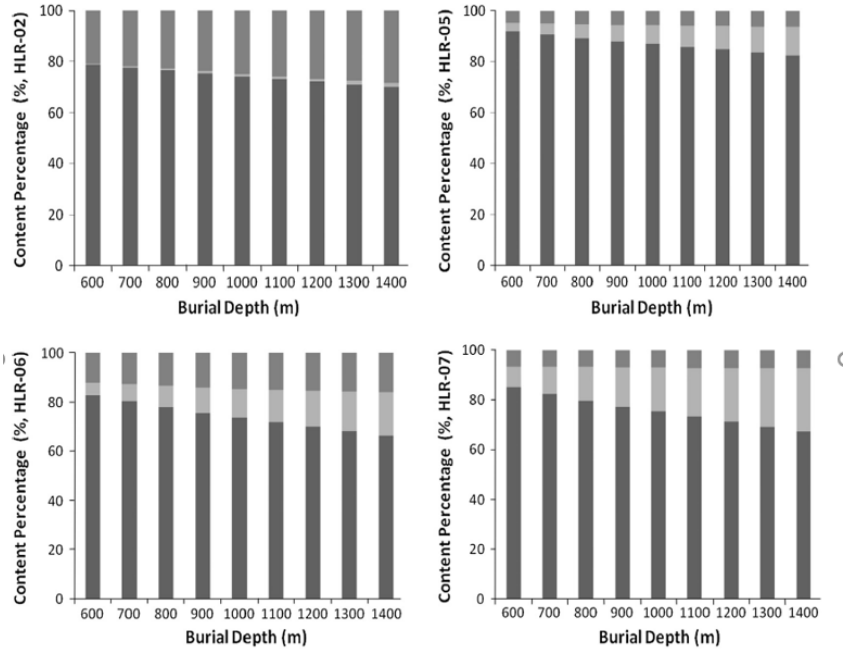

Figure 2.20 Free gas content increases with increasing burial depth (Liu et al., 2013).

2.2.3 Soluble Gas Content

Through studying the methane solubility in coalbeds formation water, the soluble gas content could be quantified (Liu et al., 2013).

2.2.3.1 Soluble Gas content Calculation

Soluble gas content in CBM reservoirs is the volume of methane dissolved in the formation water. Thus, one needs to determine the methane solubility in the formation water of the studied CBM reservoir under the reservoir conditions to determine the volume of soluble gas (i.e. Soluble gas content) (Liu et al., 2013). Methane solubility could be calculated using **Equation 2.16.**

$$b_m = c \times n \times \rho_w \quad (2.16)$$

Where,

c : Methane concentration, *mol/kg*; and

n : Methane molar volume, *L/mol* (Liu et al., 2013).

Water content could be determined according to the equilibrium water content at the reservoir conditions (Liu et al., 2013). Soluble gas content could be calculated using **Equation 2.17**.

$$V_m = \frac{b_m}{\rho_w} \times M_e \quad (2.17)$$

Where,

V_m : Soluble gas content;

b_m : Methane solubility, m^3/m^3;

ρ_w : CBM reservoir water density, *g/mL*; and

M_e : CBM reservoir moisture content, *%* (Liu et al., 2013).

2.2.3.2 Factors Affecting the Soluble Gas Content

It was found that the solubility of methane in CBM formation water depends mainly on pressure, temperature, and water salinity (Chen, 2001; Berbesi et al., 2009; Clarkson and Bustin, 1996).

2.2.3.3 Factors Affecting the Soluble Gas Content

2.2.3.3.1 Effect of Pressure and Temperature

Liu et al. (2013) found that pressure and temperature are the main factors that impact the methane solubility in formation water. As pressure and temperature increase, methane solubility also increases. However, the pressure has a more significant impact on the methane solubility in comparison to the temperature. Temperature effect becomes clearer as temperature and pressure become high.

Methane solubility is low under standard temperature and pressure, but at specific temperatures and pressures, it increases. That is, at some pressures and temperatures, soluble methane might make up a large portion of the total gas content in a CBM reservoir (Cui et al., 2005; Fu et al., 2005; Zhang et al., 2006).

It is noted that the temperature effect on methane solubility is complicated while the methane solubility increases with increasing pressure (Fu et al., 1996). Methane solubility decreases with increasing temperature until 80c° temperature where the trend is reversed for temperatures above 80 *c*° (Yang et al., 1997). Additionally, the temperature has a higher impact on methane solubility at higher pressures than at lower pressures (Chapoy et al., 2004; Folas et al., 2007; Sachs, 1998).

2.2.3.3.2 Effect of Water Salinity

Even though the relationship between methane solubility in CBM formation water and the salinity of that water was found to be complex, it was concluded that the water salinity has an impact on methane solubility. However, the impact of water salinity on methane solubility is limited compared to the impact of pressure and temperature (Fu et al., 2004; Wang et al., 2006).

2.2.4 Total Gas Content

Liu et al. (2013) introduced a mathematical model that could be used to calculate the total in-situ gas content in low-rank CBM reservoirs, including adsorbed, free, and soluble gas contents. After calculating adsorbed, free, and soluble gas contents using **Equations 2.12**, **2.13**, and **2.17**, one can calculate the total in-situ gas content in low-rank coal by calculating the summation of the three gas contents according to **Equation 2.18.**

$$V_{in\_situ} = [V_{T,daf} - \Delta V' \times (T_R - T_T)] \times \frac{100 - M_{ad} - A_{ad}}{100} + \frac{\left\{(\Phi - \Phi_w) \times \left\{1 - \left\{aLn\left[\frac{\nu}{1-\nu}(\sigma_\nu - \alpha p)\right] + b\right\}\right\} / \rho_c\right\} \times P \times T_o}{P_o T Z} + \frac{b_m}{\rho_w} \times M_e \quad (2.18)$$

It was found that the total gas content increases with increasing depth of the CBM reservoir. **Figure 2.21** illustrates the measured results that back this conclusion (Liu et al., 2013).

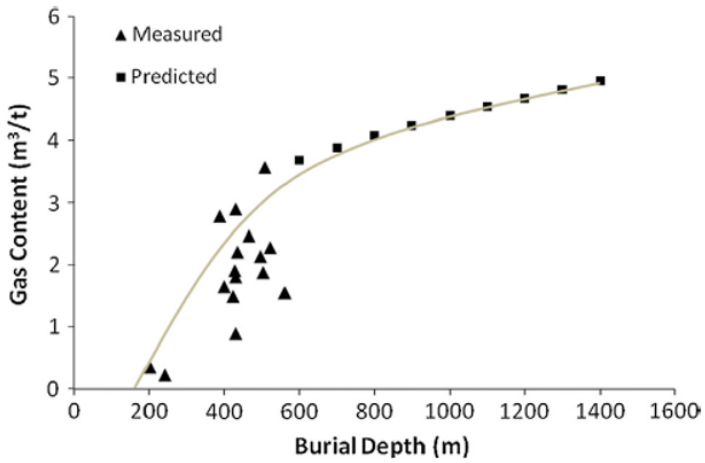

Figure 2.21 Total gas content in CBM reservoirs increases with increasing burial depth. Both measured and predicted values back this conclusion (Liu et al., 2013).

Chapter 3. Powder River Basin Geology and Reservoir Characterization

3.1 Introduction

This chapter covers the detailed characterization and modeling methodology. This includes the 3d model construction and considerations, structural framework, fluid simulation parameters, gas adsorption characterization, and permeability changes characterization.

3.2 Geology of Powder River Basin

3.2.1 PRB Location and Surroundings

Powder River Basin is an asymmetrical syncline located in northeast Wyoming and southeast Montana. It is surrounded by the Black Hills in the east, the Bighorn Mountains in the west, the Hartville Uplift in the southeast, the Miles City Arch in the northeast, and the Casper-Arch-Laramie Range in the southwest (Ross et al., 2009) **Figure 3.1**.

The eastern flank of the basin has a gentle dipping to the west with a dipping angle of 2-5 degrees while the western flank has a dipping to the east with a dipping angle of 20- 25 degrees and the basin axis is close to its western side (NW-SE) (Flores and Bader,1999) **Figure 3.2**.

3.2.2 PRB Stratigraphy

The stratigraphy of PRB is composed of Upper Cretaceous and Tertiary fluvial and marine deposits and underlying Upper Cretaceous barrier shoreface marine shales and sandstones (Flores, 2004). The coal seams exist in Fort Union and Wasatch formations which are part of the Tertiary units and belong to the Paleocene and Eocene ages, respectively. These formations were connected to fluvial systems that resulted from the feed coming from highland plateaus. The Tertiary units contain the coal-bearing Fort Union (Flores, 2004).

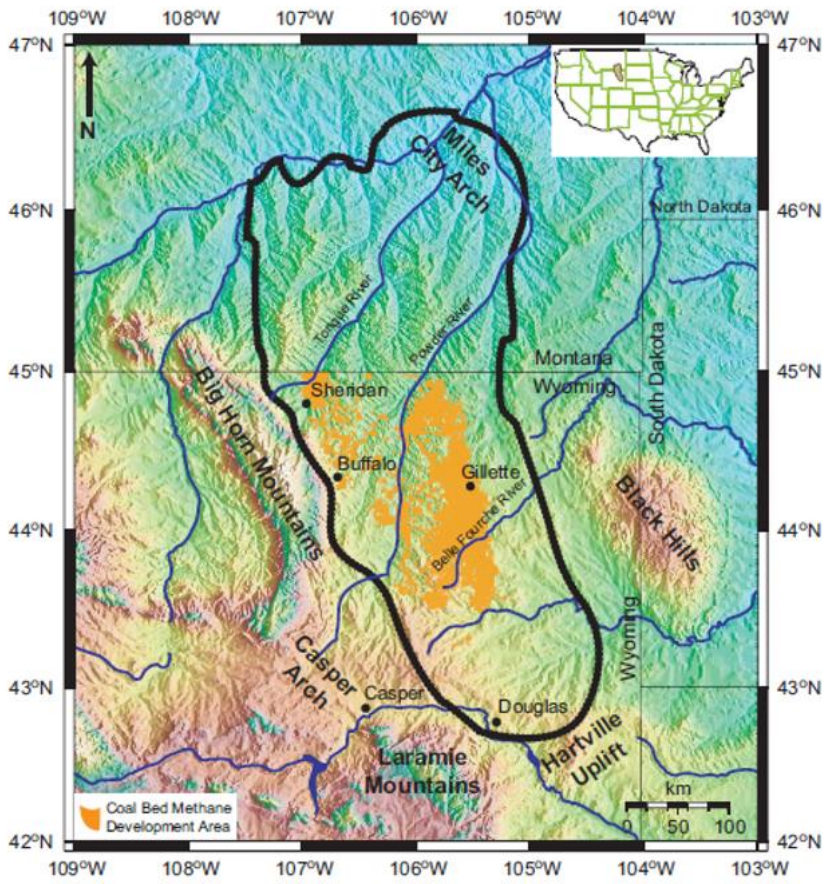

Figure 3.1 Map of Powder River Basin and its surroundings (Colmenares and Zoback, 2007).

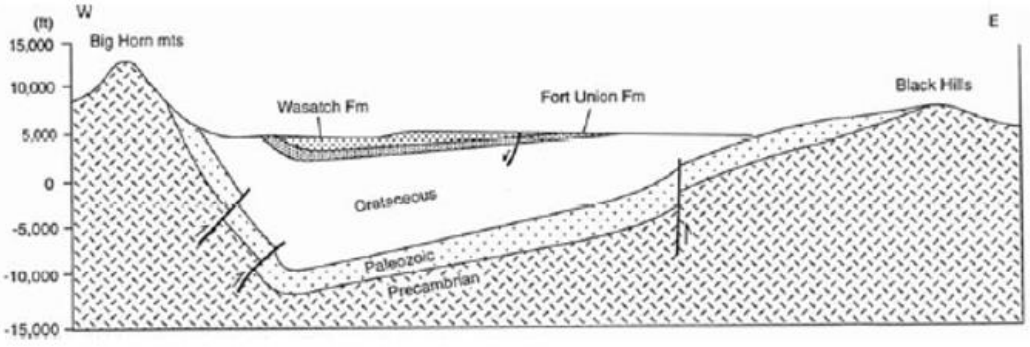

Figure 3.2 Cross section (Advanced Resources International, Inc., 2002).

Coal in PRB exists primarily in the Fort Union Formation especially in the Tongue River Member of the Fort Union Formation. The Tongue River Member contains interbedded sandstone, limestone, siltstone, coal, and conglomerate (**Figure 3.3)** (Advanced Resources International, Inc., 2002; Flores and Bader, 1999). The shapes of the coalbeds are elongate to lenticular and their thickness range from a few inches to about 200 ft (Flores and Bader, 1999; Flores, 2004).

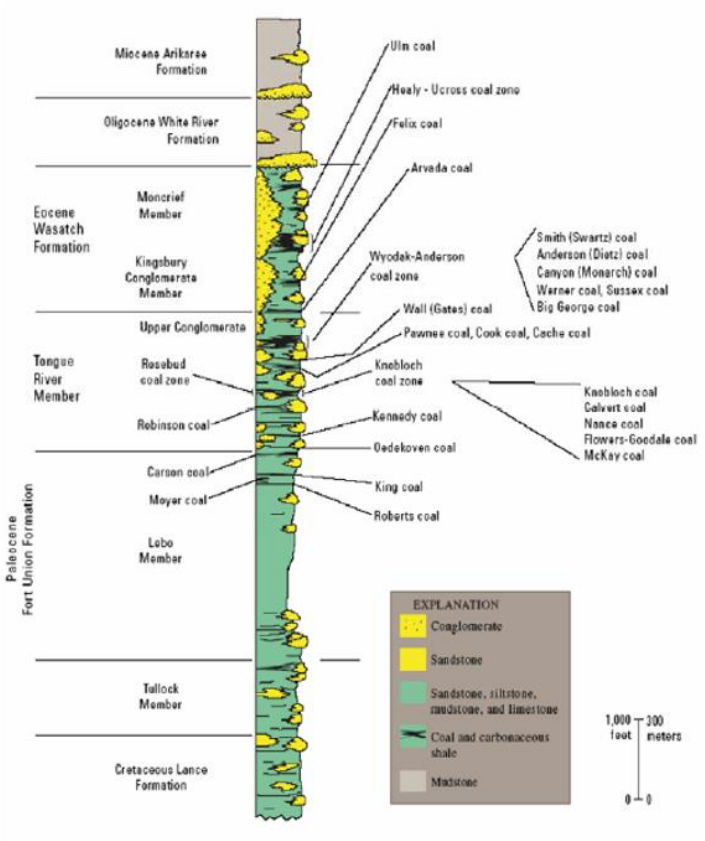

Figure 3.3 PRB general stratigraphic column (Flores, 2004).

3.2.3 Big George Coal Unit (BGC)

I chose to characterize and model the Big George Coal Unit (BGU) which bears low-rank sub-bituminous coal. BGU is in the central part of PRB (**Figure 3.4)** and is part of the Wyodak-Anderson zone which is a part of the Tongue River Member (Flores and Bader, 1999). The average

depth of the Big George Coal is 1100 ft while its thickness ranges from 46 to 203 ft (Ross et al., 2009). The gas in place in Big George Coal is biogenic in origin and composed mainly of methane and carbon dioxide with about 87-94% methane and 4-12% carbon dioxide, respectively. There are also traces amounts of other heavier hydrocarbons (Flores, 2004). Cleat spacing for Big George Coal has a wide range where it varies from 0.4 to 4.7 in. The face cleats in Big George Coal are parallel to NW and NE directions where these orientations might be caused by tectonic stresses (Flores, 2004).

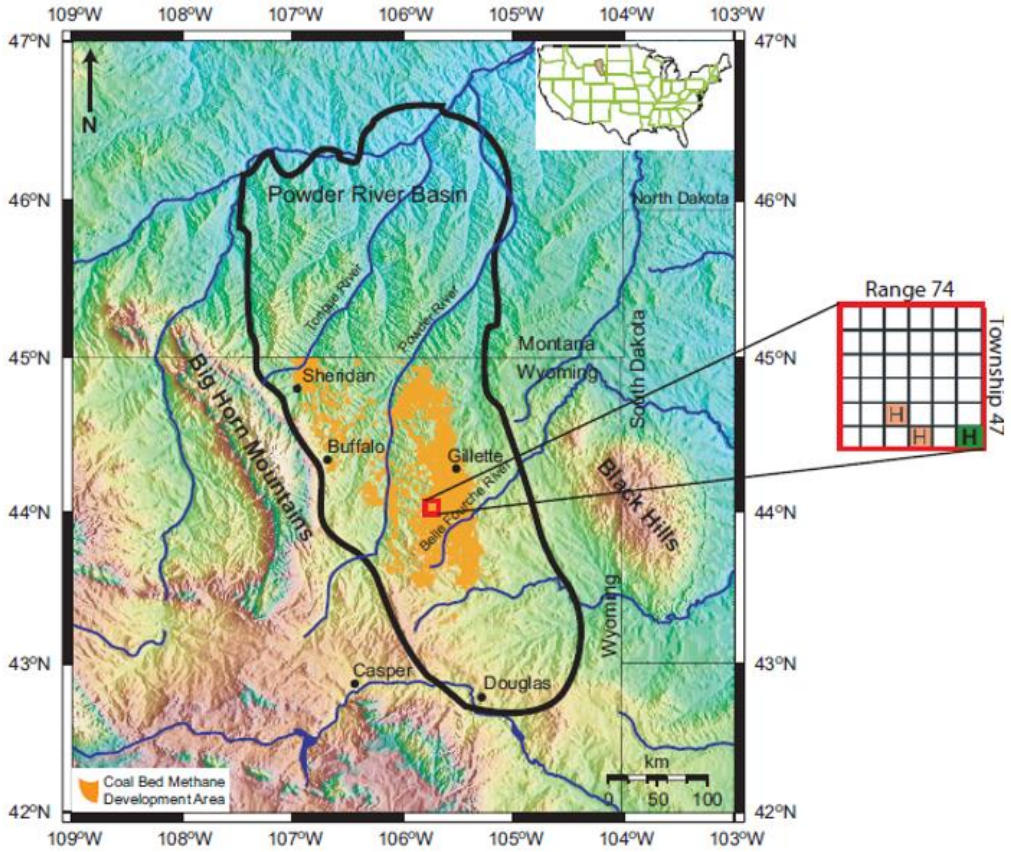

Figure 3.4 Big George Unit location with respect to Powder River Basin (Ross et al., 2009).

3.3 Reservoir Characterization

3.3.1 3D Static Model Dimensions and Description

My model of Big George Coal included 4 main layers: Top, Over Burden Shale, Big George Coal, and Under Burden Shale. These layers included different lithology units, but they were named according to the dominant lithology. The Big George Coal includes mainly coal with some amounts of shaly coal and sandy coal. Regarding the dimensions of my 3D static model, it extended for 25000 ft in the x-direction and 13000 ft in the y-direction and had a thickness of 225 ft (**Figure 3.5**). The average depth of the static model was 1400 ft. The number of cells was 254 in the x-direction, 137 in the y-direction, and 50 in the z-direction and the total number of grid cells was 1,739,900 cells (**Table 3.1**). The grid spacing aims to optimize the simulation running times and to avoid any numerical instability or significant loss of detail (Ross, 2007).

The number of cells is clearly huge which was handled by dividing the model into several models. This dividing was useful not only for reducing the computational time when running the simulation but also for comparing the petrophysical properties resulting from different models to ensure that such properties were within the same ranges which helped me validate my characterization and modeling approach.

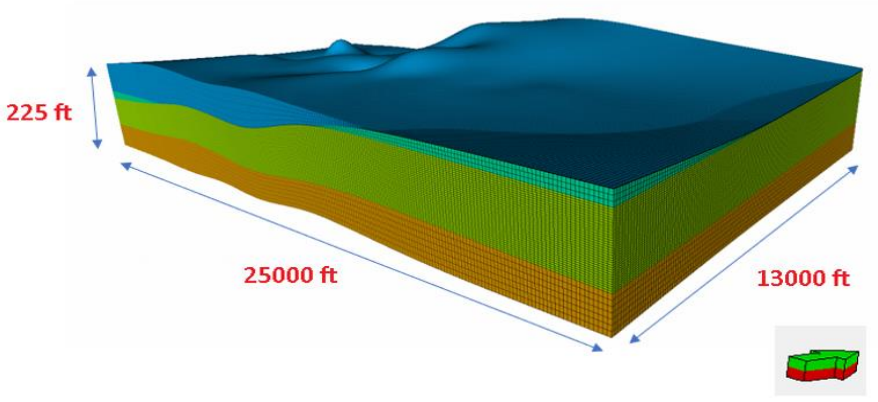

Figure 3.5 The 3D static model used for this study with the dimension in X, Y, and Z-directions.

Table 3.1 The number of grid cells in X, Y, and Z-directions and the total number of cells.

nx	254
ny	137
nz	50
Total number of grid cells	1,739,900

3.3.2 3D Static Model Structural Framework

3.3.2.1 Coal and Non-coal Facies Delineation and Characterization

Gamma-ray logs were used to initially characterize the Big George Unit since the coal is known to have a distinguishing very low gamma-ray log signal. I looked at the GR logs of several wells and matched the same coal signal at almost the same depth for all the wells. Gamma-ray logs were used to determine the depth and thickness of the Big George Coal formation. **Figure 3.6** shows the gamma-ray logs for seven of the wells where the signal of the coal formation is highlighted.

Cross-plotting techniques of the well logs were then used to characterize and model the other facies. Gamma-ray and density logs for 10 wells were used to characterize 7 different facies using the approach introduced by (Chatterjee and Paul, 2012). The values used to distinguish the different facies are illustrated in **Table 3.2**. Among these values, one can see that coal has the lowest gamma-ray and density values compared to the other facies. The resulted 7 facies were coal, shale, sandstone, sandy coal, shaly coal, shaly sand, and igneous intrusions. **Figure 3.7** illustrates the cross plot of the 7 facies that were characterized.

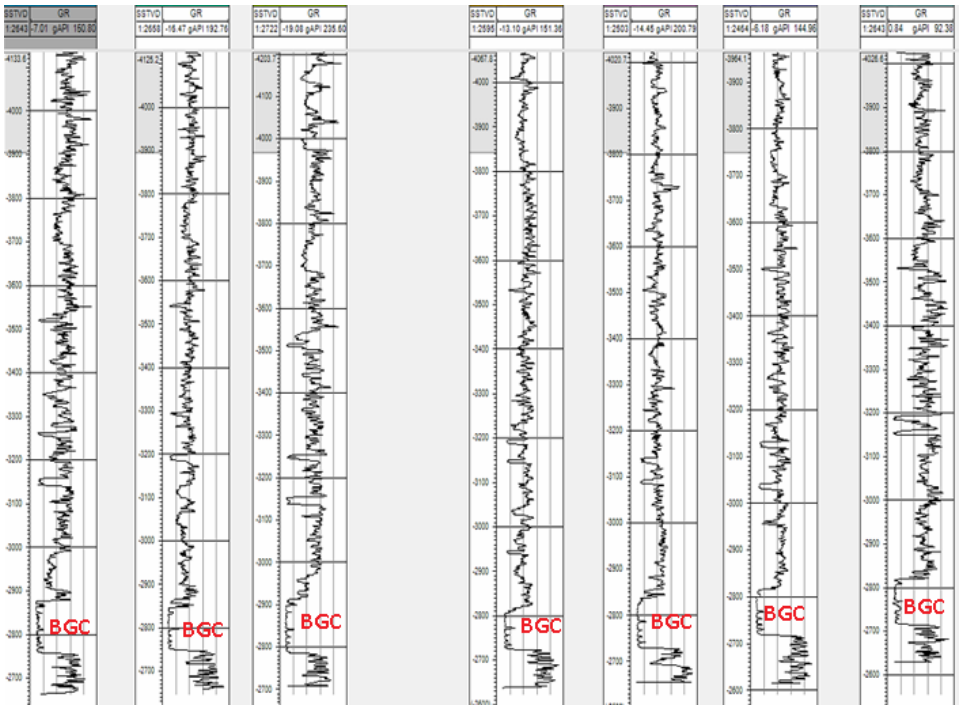

Figure 3.6 Gamma-ray logs for seven of the wells where the signal of the BGC is highlighted. (WOGCC, 2018).

Table 3.2 GR and density well-logs cut-off values that were used to characterize the 7 facies.

	Gamma ray log, (API)	Density log, (g/cc)
Shale	>90	>1.55
Sandstone	<30	>2.1
Coal	<30	<1.55
Shaly sandstone	30 - 90	>1.55
Shaly coal	>30	<1.55
Sandy coal	<30	1.55 - 2.1
Igneous intrusions	-	>2.85

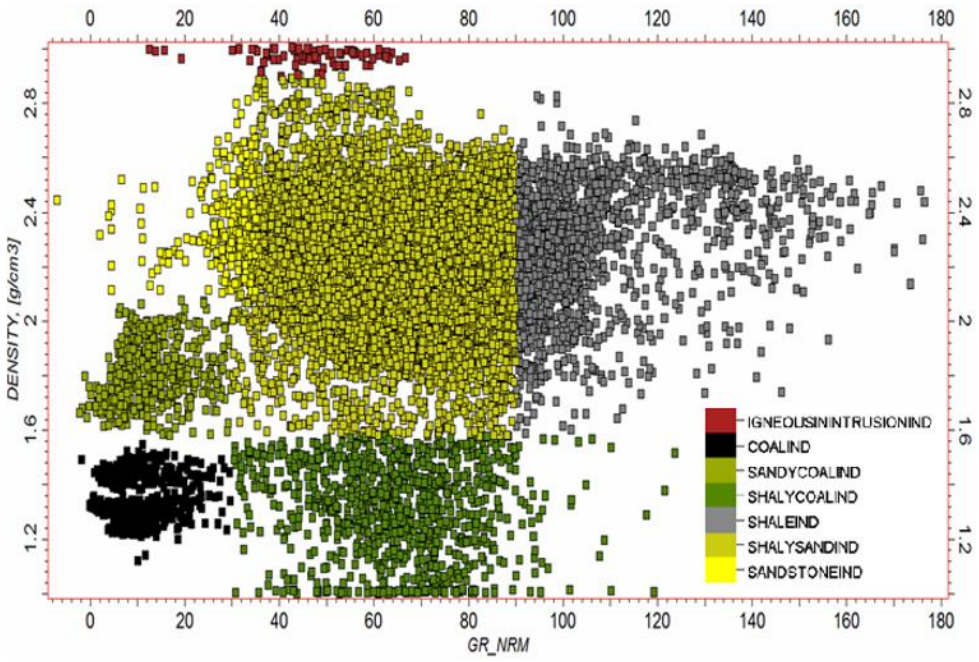

Figure 3.7 Cross-plot of the 7 facies that were characterized.

Looking into the resulted facies within the static model context, **Figure 3.8** is a fence diagram that provides a good illustration of the different facies and their distribution over the 3D static model. It also illustrates the locations of the 22 wells. **Figure 3.9** illustrates the final facies model for three of the wells where the facies are represented with their corresponding gamma-ray log values and their depths.

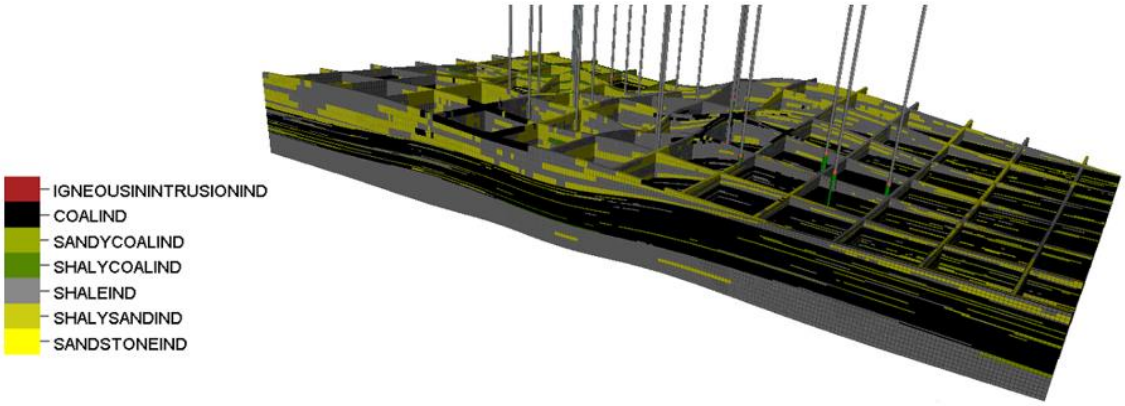

Figure 3.8 Fence diagram that provides a good illustration of the different facies and their distribution over the 3D static model.

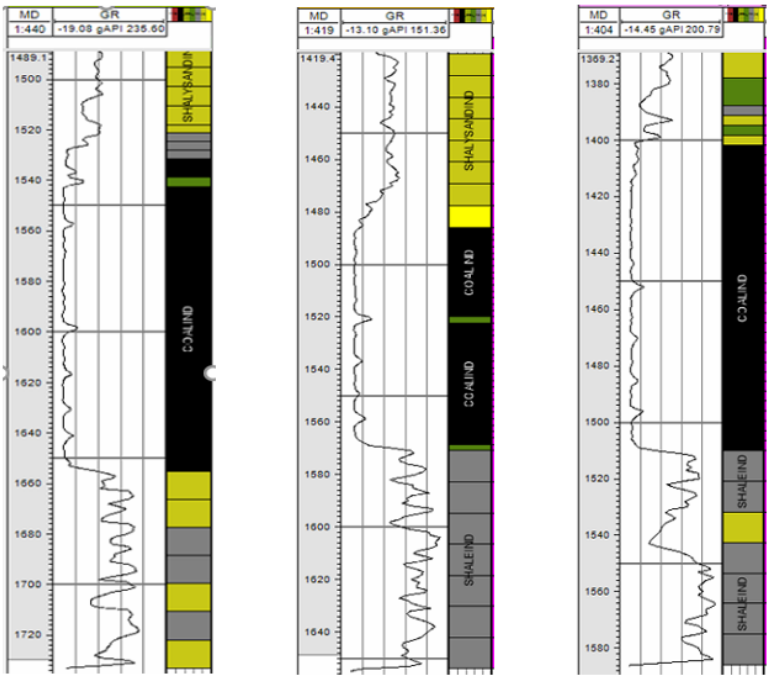

Figure 3.9 The final facies model for three of the wells where the facies are represented with their corresponding gamma-ray log values and their depths.

3.3.2.2 Petrophysical Modeling

The 3D model should honor all the available data and provide the ability to measure the properties uncertainty (Journel, 1994; Deutsch, 2002). Both field and well logs data (hard data) and calibrated data (soft data) are honored by having different realizations in the model through stochastic reservoir modeling (Journel, 1994). The uncertainty with these data that is implemented in the 3d model and would be transferred to the reservoir performance predictions resulting from reservoir simulations which provide different scenarios each of which is equally probable (Journel, 1994). Geostatistical techniques are utilized to populate the petrophysical properties in the 3D model (Journel, 1994). Heterogeneity could be implemented in horizontal and vertical directions using geostatistics and stochastics modeling which honors the exact hard data and the soft data with some variation (Ross, 2007).

For the construction of the model that is used in this study, only gamma-ray logs and density logs were available where there was no available seismic data. Thus, the literature values of the permeabilities and porosities were used and populated in the model (Flores, 2004; Twombly et al., 2004; Mavor et al., 2003; Ayers, 2002; USGS, 1995). Simple Gaussian simulation was used to populate these properties and then through history-mating over 12.5 years of production, I constrained the values of such properties further. They were also in agreement with Ross (2007) values. **Table 3.3** indicates the initial distributions of cleat and matrix porosities and permeabilities that were used (Ross, 2007). (Laubach et al., 1998) concluded that the horizontal permeability of face cleats can be as much as ten times the vertical permeability or the butt permeability. This conclusion was reflected in the initial values. The history-matching was conducted using the actual water and gas production data of the several wells (WOGCC, 2018).

Table 3.3 The initial distributions of cleat and matrix porosities and permeabilities that were used (Ross, 2007).

Property	Direction	Range
Cleat permeability, mD	Face cleat horizontal permeability (K_x)	100 - 500
	Butt cleat horizontal permeability (K_y)	10 - 160
	Face cleat vertical permeability (K_z)	10 - 160
Matrix permeability, mD		0.04 - 0.7
Cleat porosity, fraction		0.017 - 0.63
Matrix porosity, fraction		0.011 - 0.1

3.3.3 Gas Adsorption Characterization

Methane and carbon dioxide adsorptions were modeled using Langmuir Isotherm introduced by Tang et al. (2005) who obtained it using dry and moist crushed coal samples from PRB (**Figure 3.10**). This isotherm accounts for the moisture content impact on the adsorption capacities of CBM. The moisture content in Powder River Basin is 30% (Ellis, 2002). However,

Kovscek and Orr (2004) observed that when the coal moisture becomes higher than 5%, the adsorption isotherm does not change. ECLIPSE simulator does not allow having any moisture inside the coal matrix. Thus, adsorption isotherm that accounts for the moisture should be provided or the Langmuir adsorption scaling keywords should be used to account for the reduction in the adsorption capacity due to the moisture content.

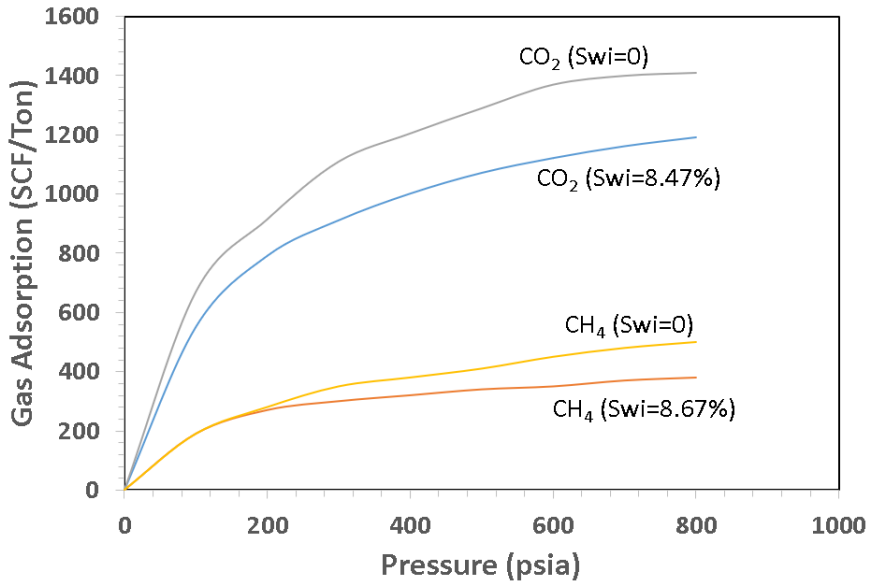

Figure 3.10 Methane and carbon dioxide adsorptions were modeled using Langmuir Isotherm introduced by (modified from Tang et al., 2005).

3.3.4 Permeability Changes Characterization

ECLIPSE uses either Palmer-Mansoori model or Extended Palmer-Mansoori model to model the permeability changes in CBM. In this study, I used Palmer-Mansoori model (**Equation 3.1**) (Palmer and Mansoori, 1998) (ECLIPSE Industry-Reference Simulator, Technical Description, Version 2018.1). This model accounts for pore volume changes with pressure and matrix shrinkage/swelling.

$$V(P) = V(P_0)\left\{1 + \frac{c_m}{\Phi_0}(P - P_0) + \frac{\varepsilon_l}{\Phi_0}\left(\frac{K}{M} - 1\right)\left(\frac{\beta P}{1+\beta P} - \frac{\beta P_0}{1+\beta P_0}\right)\right\} \quad (3.1)$$

Where,

Φ_0 : Initial porosity,

P_0 : Initial pressure,

$V(P_0)$: Pore volume at the initial pressure,

K : Bulk modulus,

M : Constrained axial modulus, and

β, ε_l : The parameters of the match between the change in a volumetric strain which results from matrix shrinkage, and the Langmuir Isotherm (Palmer and Mansoori, 1998).

C_m is expressed in **Equation 3.2**. as follows:

$$c_m = \frac{g}{M} - \left[\frac{K}{M} + f - 1\right]\gamma \tag{3.2}$$

Where,

g : Geometric factor that (0-1) and depends on the orientation of the cleats,

f : Fraction (0-1), and

γ : The grain compressibility (Clarkson et al., 2010).

The permeability variation as a function of porosity variation could be expressed in **Equation 3.3**.

$$\frac{k}{k_0} = \left(\frac{\Phi}{\Phi_0}\right)^n \tag{3.3}$$

Where n is an exponent with a typical value of 3. The transmissibility multiplier could be expressed as follows:

$$\left\{1 + \frac{c_m}{\Phi_0}(P - P_0) + \frac{\varepsilon_l}{\Phi_0}\left(\frac{K}{M} - 1\right)\left(\frac{\beta P}{1+\beta P} - \frac{\beta P_0}{1+\beta P_0}\right)\right\}^n$$

(ECLIPSE Industry-Reference Simulator, Technical Description, Version 2018.1).

3.3.5 Fluid Flow Simulation Parameters

Fluid flow Parameters listed in **Table 3.4** were used for the base case simulation case. For relative permeability curve, I followed the same approach of Mavor et al. (2003) who used San Juan Coal samples relative permeability curves during a simulation study of PRB CBM and obtained a good history-match with production data. This curve was developed by Gash (1991) **Figure 3.11**.

Table 3.4 Fluid flow parameters used for the base case.

Parameter/ property	Value	Reference
Initial temperature, f	100	(Tang et al., 2005)
Pressure gradient, psi/ft	0.315	(Advanced Resources International, Inc., 2002)
Coal gas composition	94% Methane, 6% Carbon dioxide	
Cleat water saturation, fraction	0.9	
Cleat gas saturation, fraction	0.1	
Cleat spacing, in	4	(Ayers, 2002), (Flores, 2004)
Matrix permeability, md	0.04 - 0.7	(Flores, 2004)
Matrix porosity, fraction	0.011 - 0.1	(Advanced Resources International, Inc., 2002)
Face cleat horizontal permeability, mD	100 - 500	(Flores 2004; Twombly et al.,2004; Mavor et al., 2003; Ayers, 2002; Laubach et al., 1998; USGS, 1995)
Butt cleat horizontal permeability, mD	10 - 160	(Flores 2004; Twombly et al., 2004; Mavor et al., 2003; Ayers, 2002; Laubach et al., 1998; USGS, 1995)
Face cleat vertical permeability, mD	10 - 160	(Flores 2004; Twombly et al., 2004; Mavor et al., 2003; Ayers, 2002; Laubach et al., 1998; USGS, 1995)
Cleat porosity, fraction	0.017 – 0.63	(Twombly et al., 2004; Mavor et al., 2003; Advanced Resources International, Inc., 2002; USGS, 1995)
Gas-diffusion coefficient, ft2/day	0.000093 for both gases (CH_4 and CO_2)	(Seto in Kovscek and Orr, 2004)

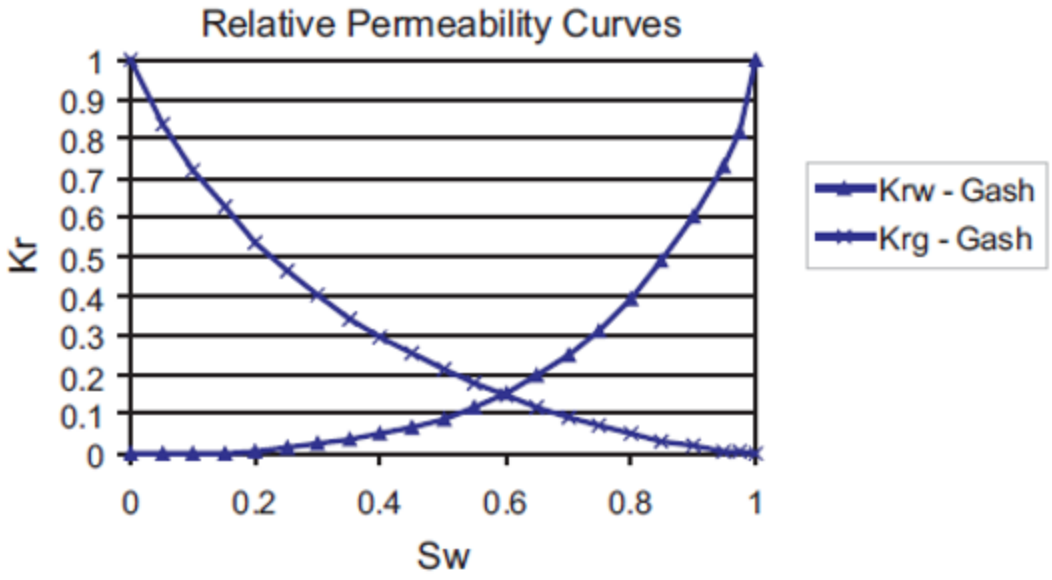

Figure 3.11 Relative permeability curve obtained from San Juan Coal samples by Gash (1991) where Kr is the relative permeability, Sw is the water saturation, Krw is the relative permeability for water, and krg is the relative permeability for gas (Gash 1991).

Chapter 4. Fluid Flow Simulation, History Matching, and Sensitivity Analysis of the Big George Coal of the Powder River Basin, Wyoming

4.1 History Matching

This chapter introduces the BGC model simulation and history matching. The impact of coal anisotropy and heterogeneity is briefly investigated. Also, sensitivity analyses were conducted for reservoir porosity, gas-diffusion coefficient, initial reservoir pressure, and temperature. The model was divided into 5 different single-well and multi-well models and the history-matching results obtained from the 5 models were in a reasonable agreement. The grid blocks and locations of the five models with respect to the entire Big George Coal model are illustrated through **Figures 4.1**, **4.2**, **4.4**, **4.5**, **4.7**, **4.8**, **4.10**, **4.11**, **4.13**, and **4.14** while the history-matching results of their modeled values with the observed data of gas production rates, cumulative gas productions, and cumulative water productions over 12.5 years of production starting from June 2006 until December 2018 are illustrated through **Figures 4.3**, **4.6**, **4.9**, **4.12**, and **4.15**. The number of wells enclosed by each model is as follows:

1. *Model 1*: 1 well
2. *Model 2*: 1 well
3. *Model 3*: 2 wells
4. *Model 4*: 3 wells
5. *Model 5*: 7 wells

History- matching of water and gas production over 12.5 years was conducted. I used the ECLIPSE simulator and ran a dual-porosity model. Dual-permeability model shall be used for future work with ECBM to consider the fluid movement from the cleats to the matrix due to the injection of carbon dioxide, nitrogen, or gas mixture. Water production rates that were predicted

by the simulator were systematically higher than observed data for some models. I assume this difference is attributed to ignoring the free gas content in the coal matrix. ECLIPSE does not allow accounting for free gas content in CBM matrices. History-matching was used to constraint the porosity and permeability values. During the characterization process, the cases of homogeneous-isotropic, heterogeneous-isotropic, homogeneous-anisotropic and heterogeneous- anisotropic models were tested until I obtained the average permeability and porosity values for homogeneous models and average ranges for heterogeneous models. **Table 4.1** indicates the petrophysical properties that resulted after the history matching. Overburden shale layer was assumed to be completely impermeable so I could ensure that there was no gas leakage to the upper layer.

Table 4.1 Petrophysical properties that resulted after the history matching.

Property	Homogeneous model	Heterogeneous model
Matrix permeability, mD	0.37	0.05 - 0.7
Matrix porosity, mD	0.05	0.011 - 0.1
Face cleat permeability, mD	24	10 - 50
Butt cleat permeability, mD	7	0.1 - 15
Cleat porosity, fraction	0.33	0.017 - 0.63
Initial Pressure, Psia	600	600
Cleat water saturation, fraction	0.7	0.7
Cleat gas saturation, fraction	0.3	0.3

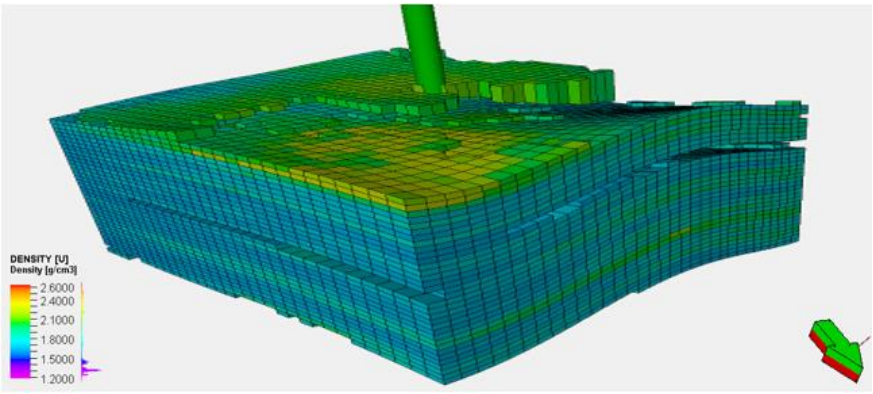

Figure 4.1 The grid block of Model 1 which includes a single well.

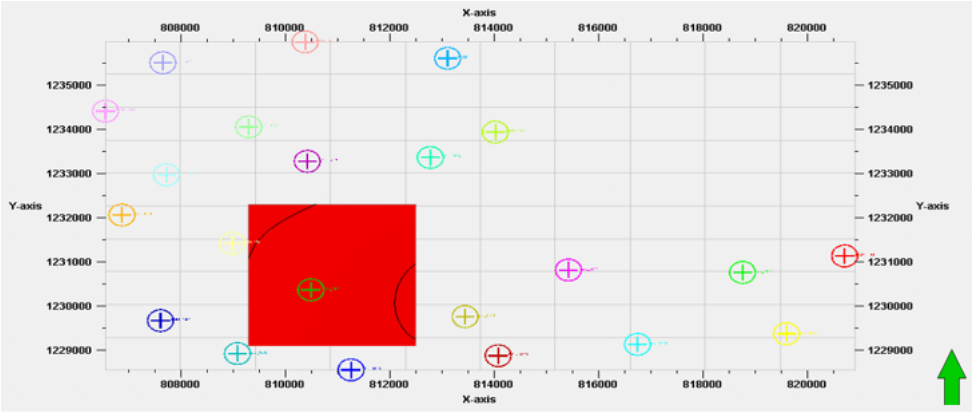

Figure 4.2 Top view location of Model 1 with respect to the entire BGC model.

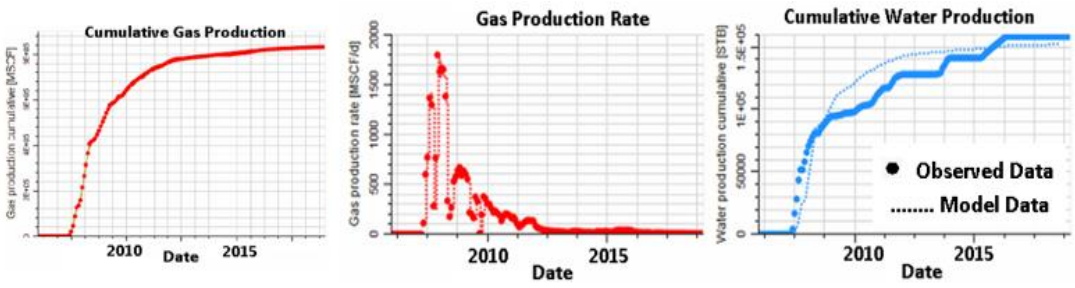

Figure 4.3 Model 1 history-matching of the production data.

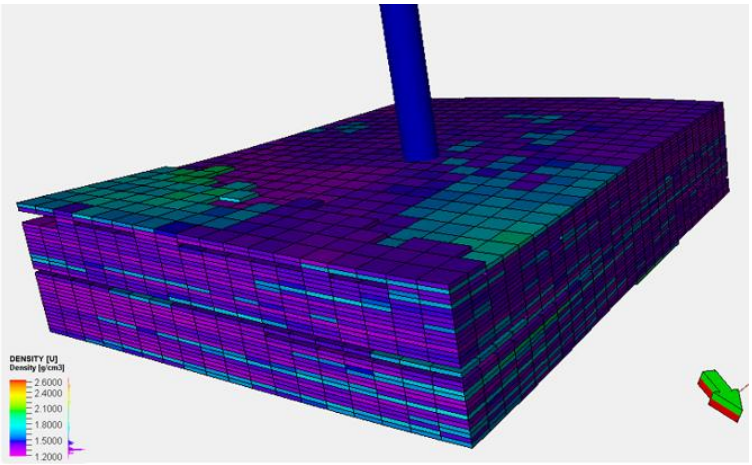

Figure 4.4 The grid block of Model 2 which includes a single well.

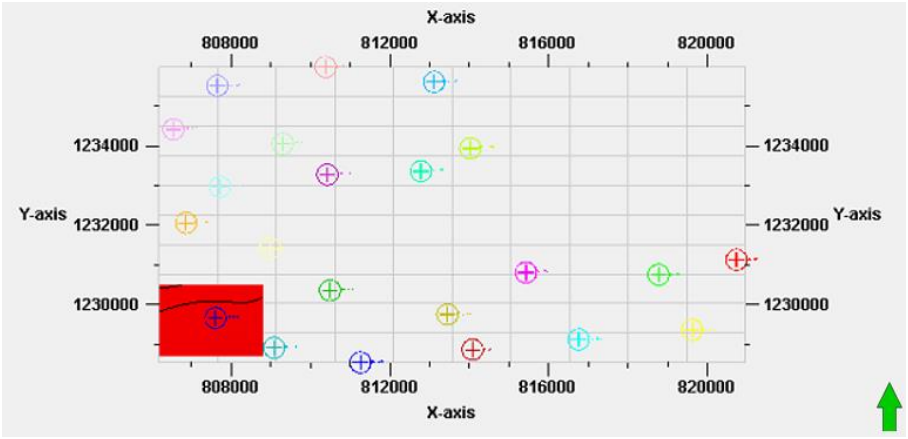

Figure 4.5 Top view location of Model 2 with respect to the entire BGC model.

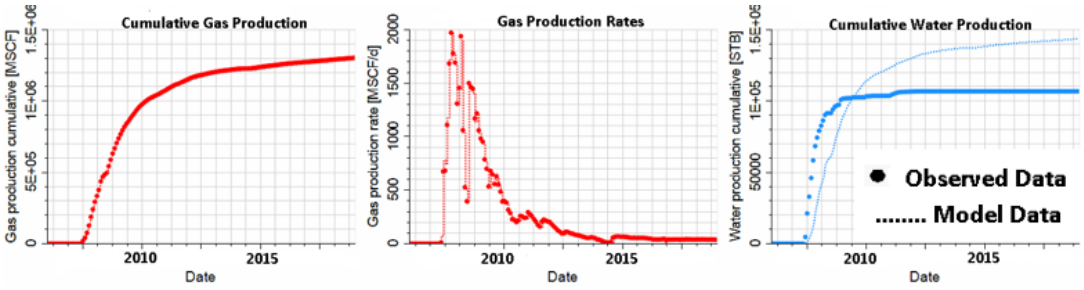

Figure 4.6 Model 2 history-matching of the production data.

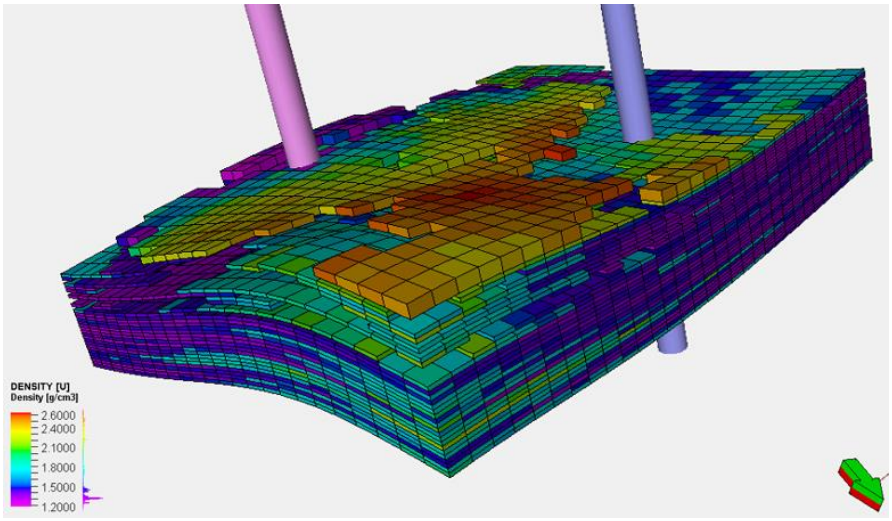

Figure 4.7 The grid block of Model 3 which includes 2 wells.

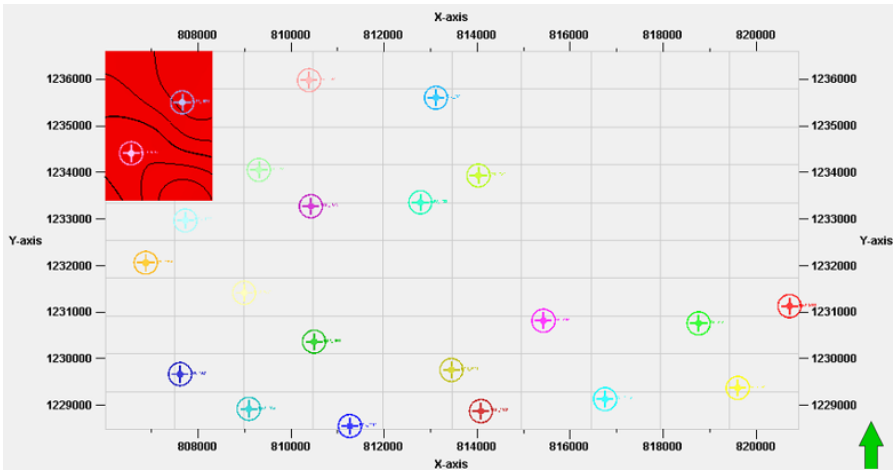

Figure 4.8 Top view location of Model 3 with respect to the entire BGC model.

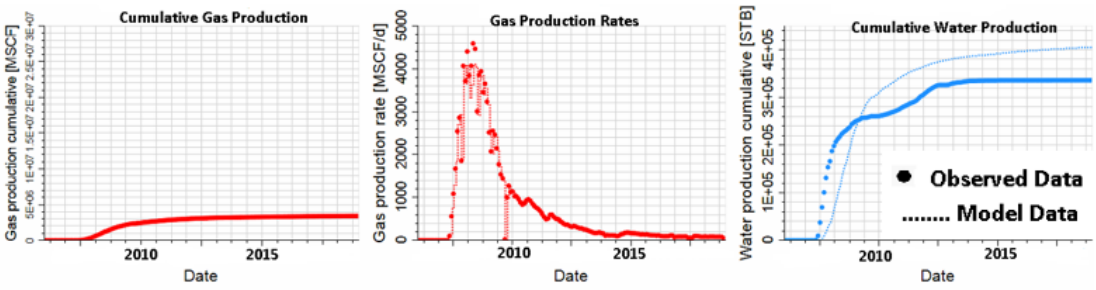

Figure 4.9 Model 3 history-matching of the production data.

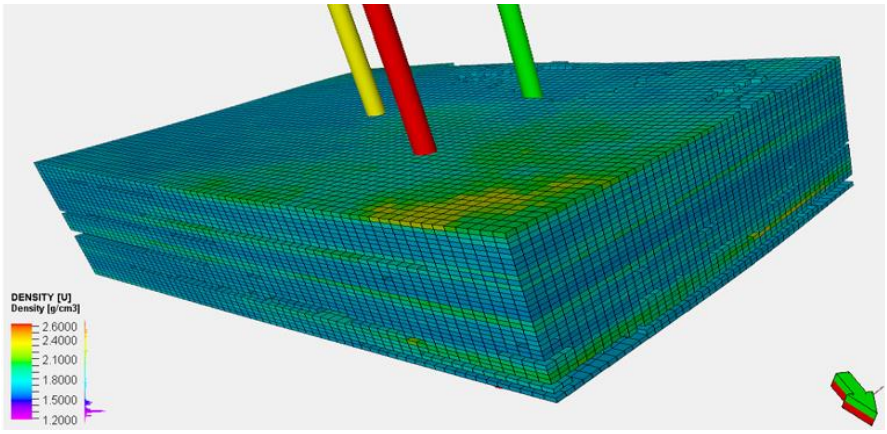

Figure 4.10 The grid block of Model 4 which includes 3 wells.

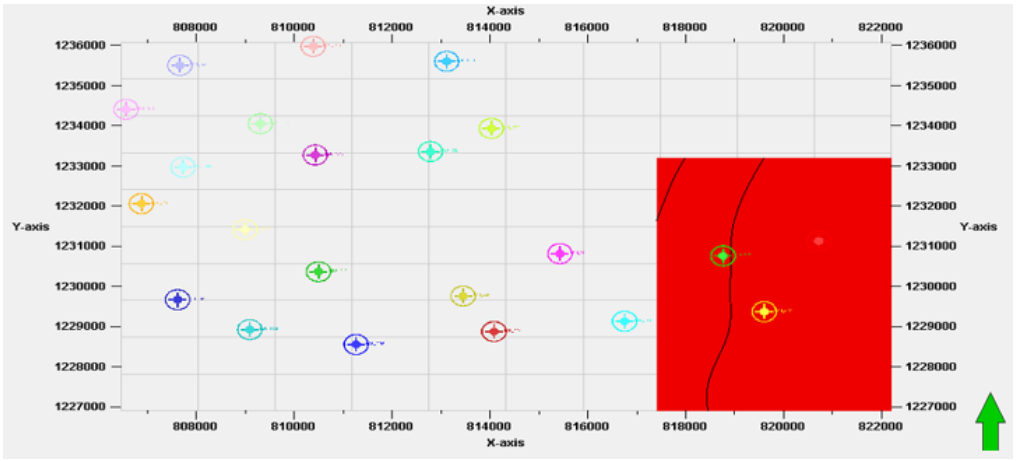

Figure 4.11 Top view location of Model 4 with respect to the entire BGC model.

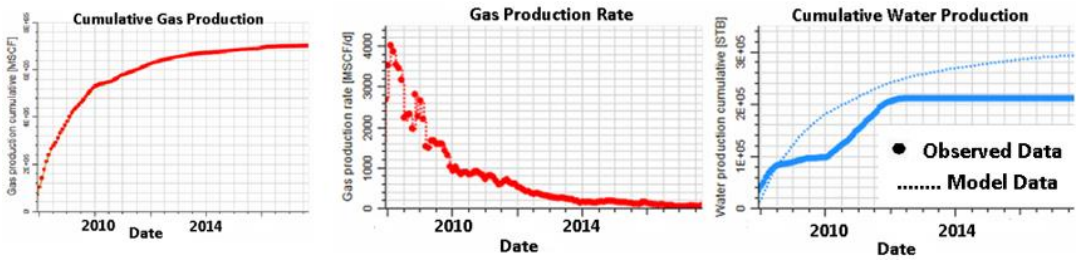

Figure 4.12 Model 4 history-matching of the production data.

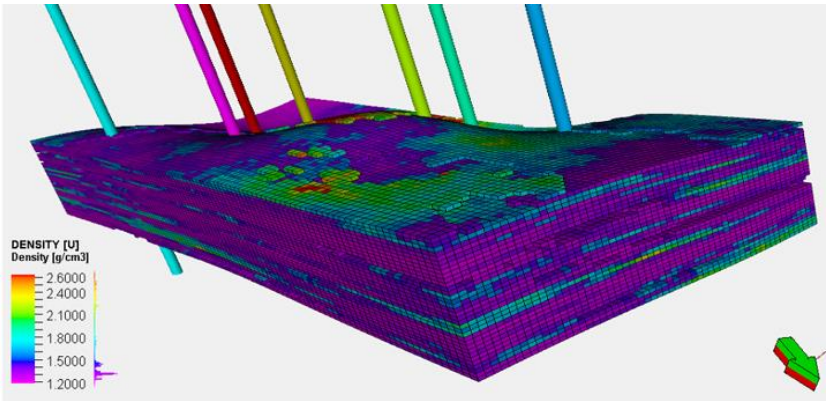

Figure 4.13 The grid block of Model 5 which includes 7 wells.

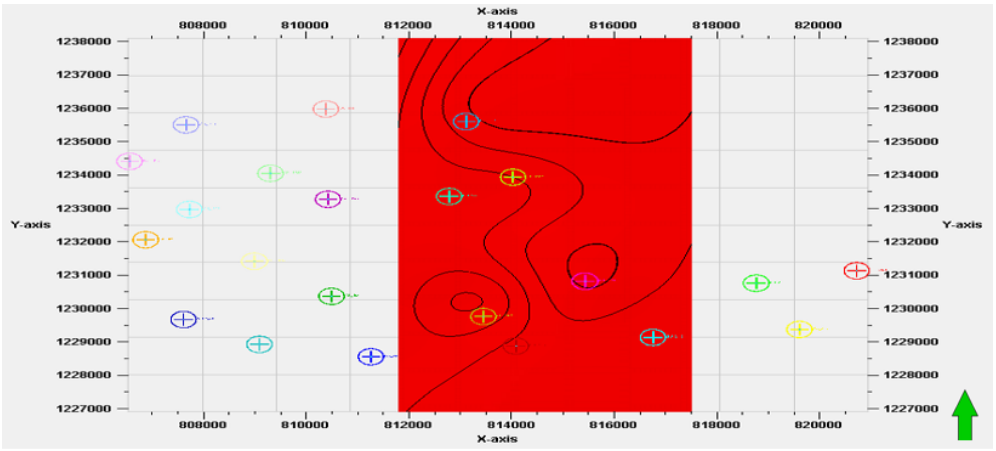

Figure 4.14 Top view location of Model 5 with respect to the entire BGC model.

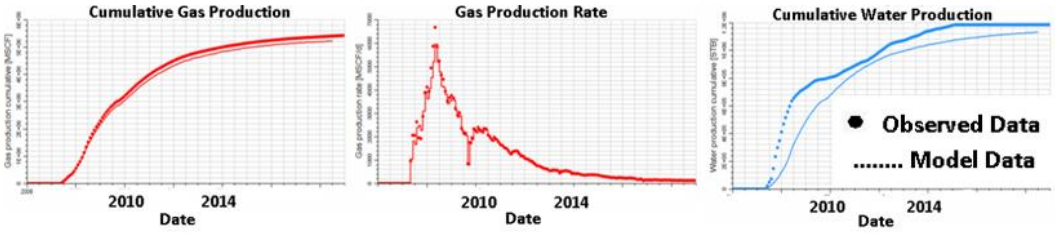

Figure 4.15 Model 5 history-matching of the production data.

4.2 Sensitivity Analysis

Sensitivity analysis study was conducted to investigate the impact of changing some parameters on the modeled gas and water production rates. The objectives of this sensitivity study were to compare the impact of different values and/or modeling approaches of some parameters on the production rates, and deciding which approaches are most accurate by investigating the accuracy of the history-match obtained from implementing such values/ approaches. During this sensitivity analysis study, cumulative production rates were mostly used for investigation rather than daily production rates because it was easier to notice the differences when they were accumulated. I also used smaller scales for the graphs to make the differences more visible. A

single-well model (Model 1) was used for this sensitivity analysis study to get more accurate insights by excluding other effects that could be involved in a bigger model.

4.2.1 Impact of Anisotropy and Heterogeneity

4.2.1.1 Impact of Anisotropy

To check the impact of anisotropy, I compared the history-matching results obtained from the isotropic models with the results obtained from the anisotropic models. The used values of the petrophysical properties are indicated in **Table 4.2**. Same matrix permeabilities in all three directions are used for isotropic and anisotropic models as the impact of changing matrix permeability on the production rates is insignificant since the cleat system provides the main fluid flow medium. That is, the impact of matrix permeabilities on the production rates is negligible compared to the impact of cleat permeabilities.

Table 4.2 Used values of the petrophysical properties.

Property	Isotropic-homogenous	Anisotropic-homogenous	Isotropic - heterogeneous	Anisotropic – heterogeneous
Face cleat horizontal permeability (K_x), md	24	24	10 – 50	10 – 50
face cleat vertical permeability (K_y), md	24	7	10 – 50	1 - 16
butt cleat permeability (K_z), md	24	7	10 – 50	1 - 16
Matrix permeability, md	0.37	0.37	0.04 – 0.7	0.04 – 0.7

Isotropic-homogeneous model vs Anisotropic-homogeneous model: **Figure 4.16** illustrates that there is a small difference in the modeled cumulative water and gas productions between the two cases. The difference may be considered insignificant, but one can see that the anisotropic-

homogenous model values are closer to the observed rates than the values of the isotropic-homogeneous model.

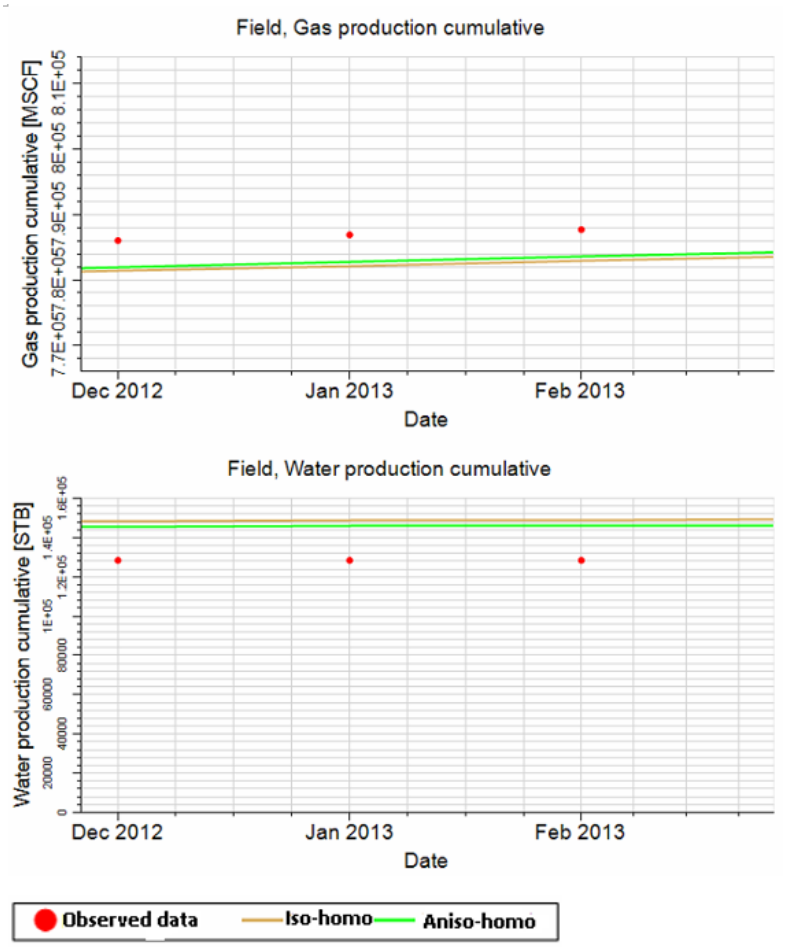

Figure 4.16 Anisotropic-homogenous model vs Isotropic homogenous model.

Isotropic-heterogeneous model vs Anisotropic-heterogeneous model: this comparison confirms the same observation and finding that was obtained from the previous comparison. That is, Anisotropic model gave more accurate values than the Isotropic **Figure 4.17**. This means that coal should be modeled as anisotropic not isotropic. This agrees with the fact that coal is highly anisotropic.

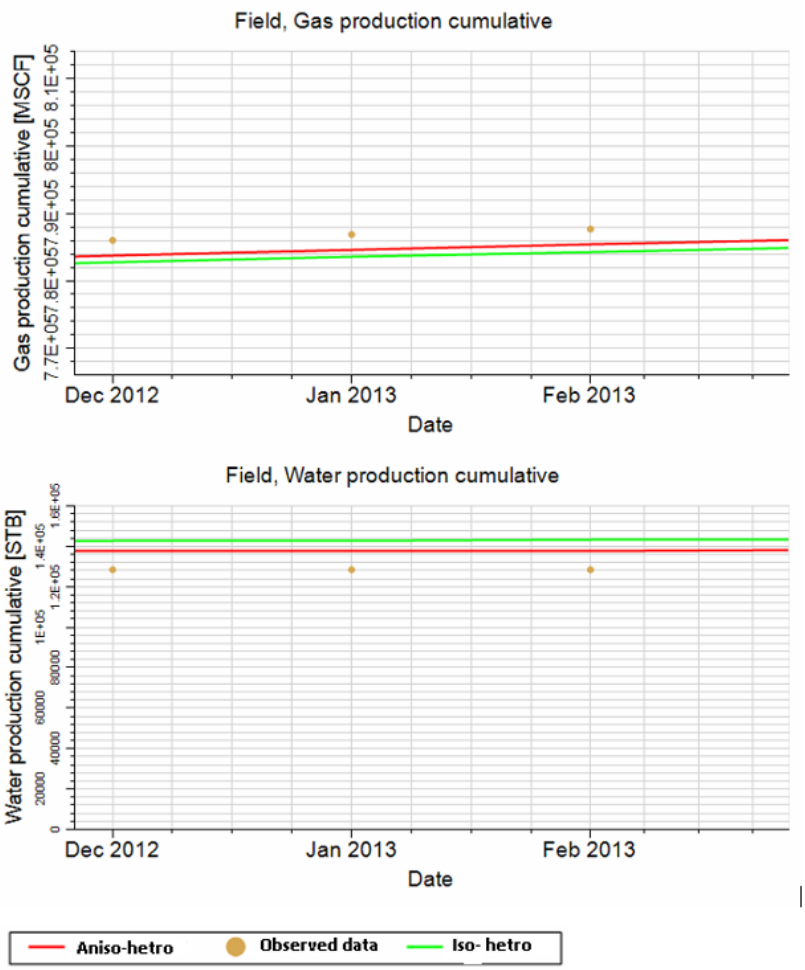

Figure 4.17 Anisotropic-heterogeneous model vs Isotropic-heterogenous model.

4.2.1.2 Impact of heterogeneity

Isotropic-homogeneous model vs Isotropic-heterogeneous model: **Figure 4.18** illustrates that the values obtained from the Isotropic-heterogeneous model are closer to the observed data than the value obtained from the Isotropic-homogeneous model.

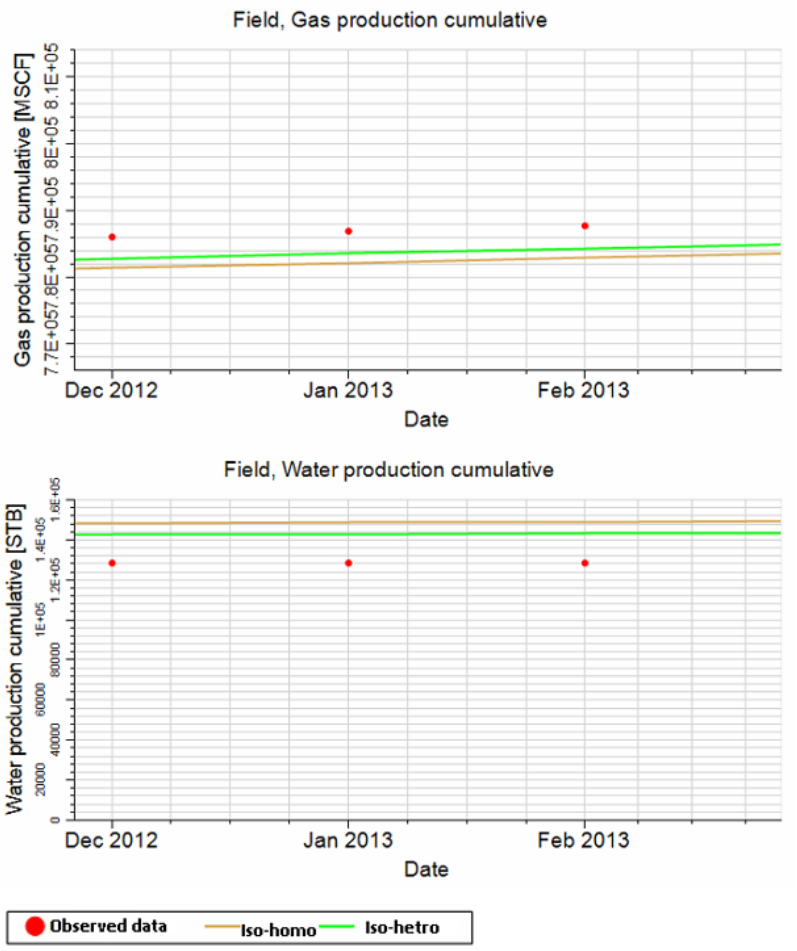

Figure 4.18 Isotropic-heterogeneous model vs Isotropic-homogenous model.

Anisotropic-homogeneous model vs Anisotropic-heterogeneous model: This comparison confirms the same previous observation that the Anisotropic-heterogeneous model is more accurate as its values are closer to the actual data (**Figure 4.19**). That is, assuming the heterogeneity when characterizing a CBM reservoir is more accurate than assuming that the model is homogenous. This agrees with the literature that CBM is highly heterogeneous.

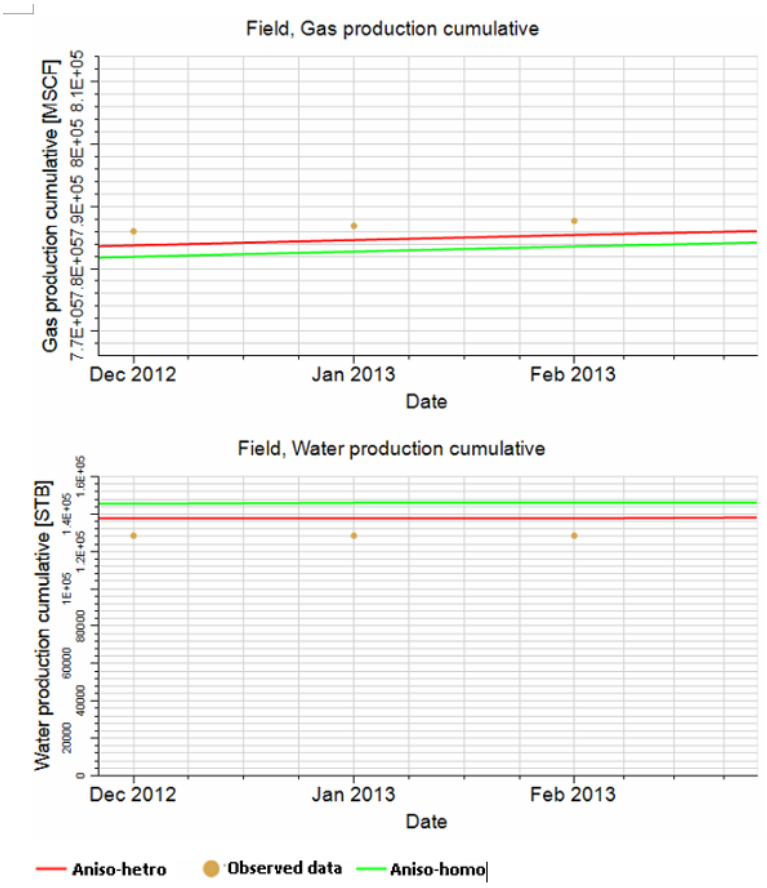

Figure 4.19 Anisotropic-heterogeneous model vs Anisotropic-homogenous model.

4.2.1.3 Combined Impact of Anisotropy and Heterogeneity

I also investigated the combined impact of isotropy and heterogeneity by comparing the production values obtained from the Isotropic-homogenous model with the values obtained from the Anisotropic-heterogeneous model. **Figure 4.20** illustrates that the production values obtained from the Anisotropic-heterogenous model were more accurate. This comparison confirms that the best way to model CBM reservoirs is to assume that the coal is anisotropic and heterogeneous. This finding agrees with the lab studies mentioned earlier that concluded that coal formations are highly anisotropic and heterogeneous.

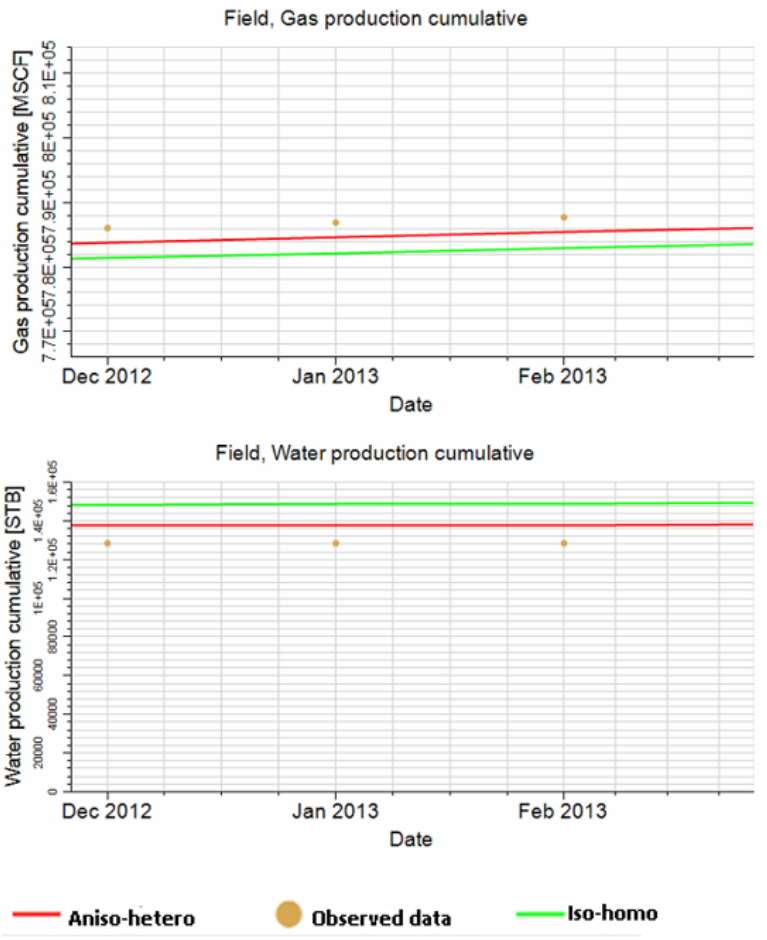

Figure 4.20 Anisotropic-heterogeneous model vs Isotropic-homogenous model.

Figure 4.21 indicates that the anisotropic-heterogenous model is the most accurate compared to the three other models and it is followed by the isotropic-heterogenous model, anisotropic-homogenous model, and isotropic-homogenous model, respectively. This order suggests that heterogeneity has a bigger impact than anisotropy on the production rates. It also confirms that the isotropic-homogenous model is the least accurate model.

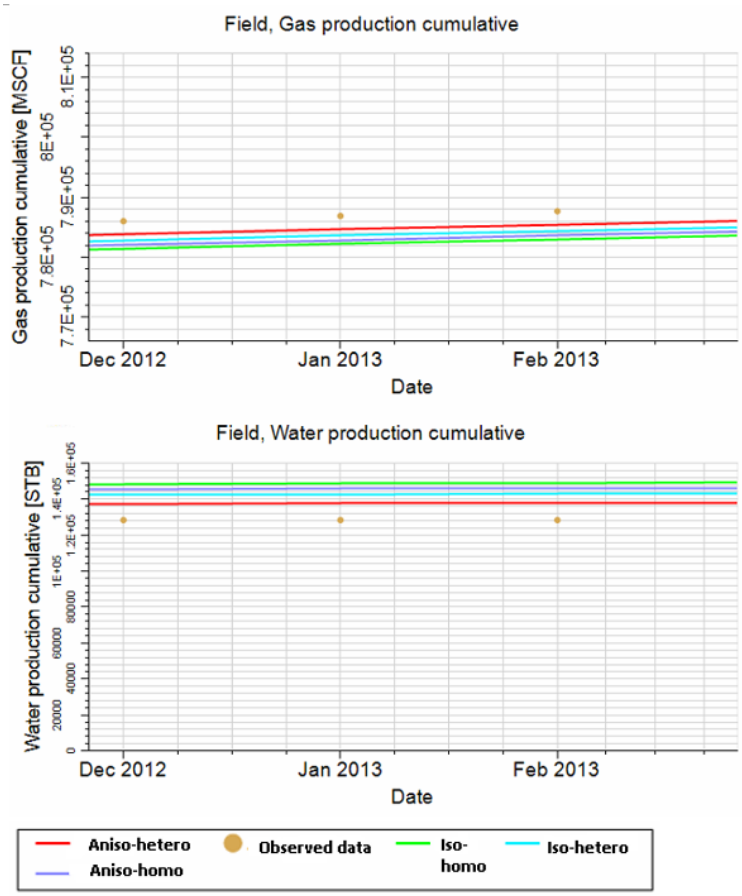

Figure 4.21 Comparison of the cumulative productions obtained from the four approaches of characterizing anisotropy and heterogeneity.

4.2.2 Porosity Sensitivity Analysis

Table 4.3 The values of the porosities that were used for this sensitivity analysis.

Property	Base value	High value	Low value
Cleat porosity	0.33	0.8	0.05
Matrix porosity	0.05	0.3	0.02

A porosity sensitivity analysis was carried out using the anisotropic-homogeneous approach of a single-well mode (Model 1). **Table 4.3** illustrates the values of the porosities that were used for this sensitivity analysis. It was found that by increasing porosities, water and gas production rates and cumulative production significantly increase. Thus, the differences are easily distinguished without having to investigate smaller scales (**Figure 4.22**). This is an expected result

because with higher porosities, the pore volume available for fluids storage increase. Hence, gas in place and production rates increase.

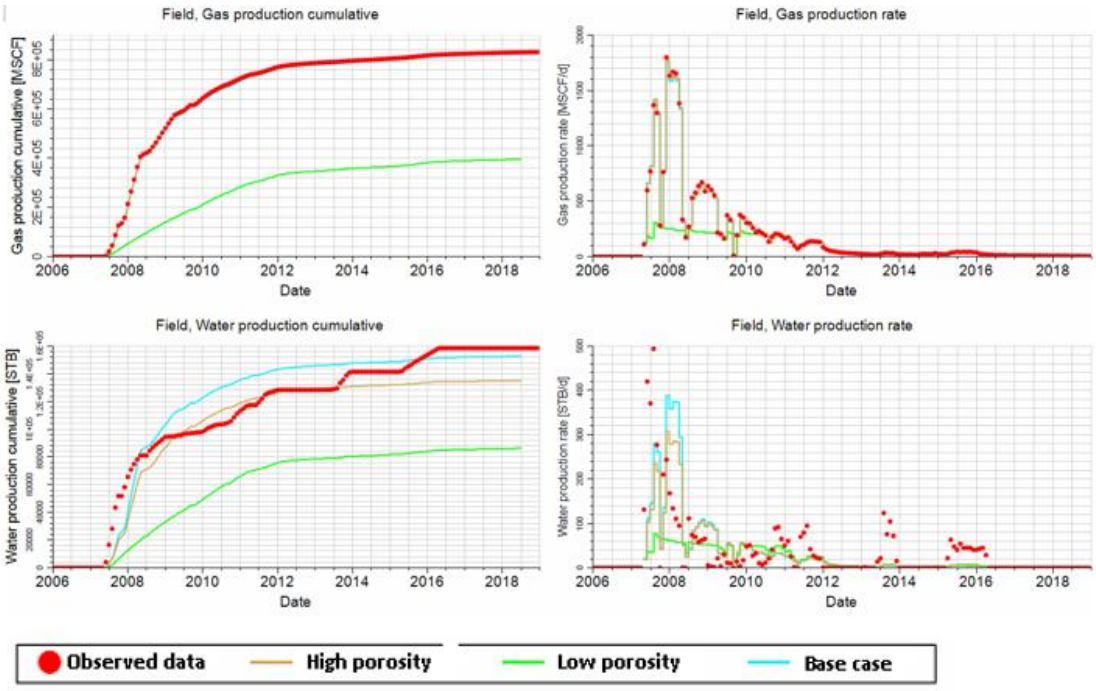

Figure 4.22 Porosity sensitivity analysis results.

4.2.3 Gas-diffusion Coefficient Sensitivity Analysis

The Anisotropic-homogeneous model was used to carry out a diffusion coefficient sensitivity analysis with the reservoir actual permeabilities which are relatively low and then with relatively high permeabilities. The values that were used for diffusion coefficient and permeabilities are indicated in **Table 4.4**. Again, matrix permeabilities impact is ignored compared to the impact of the cleat permeabilities. Thus, matrix permeability was kept constant.

Table 4.4 The values of the gas-diffusion coefficient and permeabilities that were used for the diffusion coefficient sensitivity analysis.

Property	Actual conditions	Low diffusion with low/actual permeability	High diffusion with low/actual permeability	Low diffusion with high permeability	High diffusion with high permeability
Diffusion coefficient, ft2/ ft	0.000093	0.00000093	0.0093	0.00000093	0.0093
Face cleat horizontal permeability (K_x), md	24	24	24	250	250
Face cleat vertical permeability (K_y)	7	7	7	100	100
Butt cleat permeability (K_z)	7	7	7	100	100
Matrix permeability (K)	0.37	0.37	0.37	0.37	0.37

Figure 4.23 illustrates the impact of changing the value of the diffusion coefficient with low permeabilities. one can see that the differences in gas and water production data are insignificant. This could be attributed to the fact that the simulator assumes that the flow is permeability-controlled and that the gas-diffusion coefficient is not a controlling parameter. This assumption may be accepted for such relatively low permeabilities.

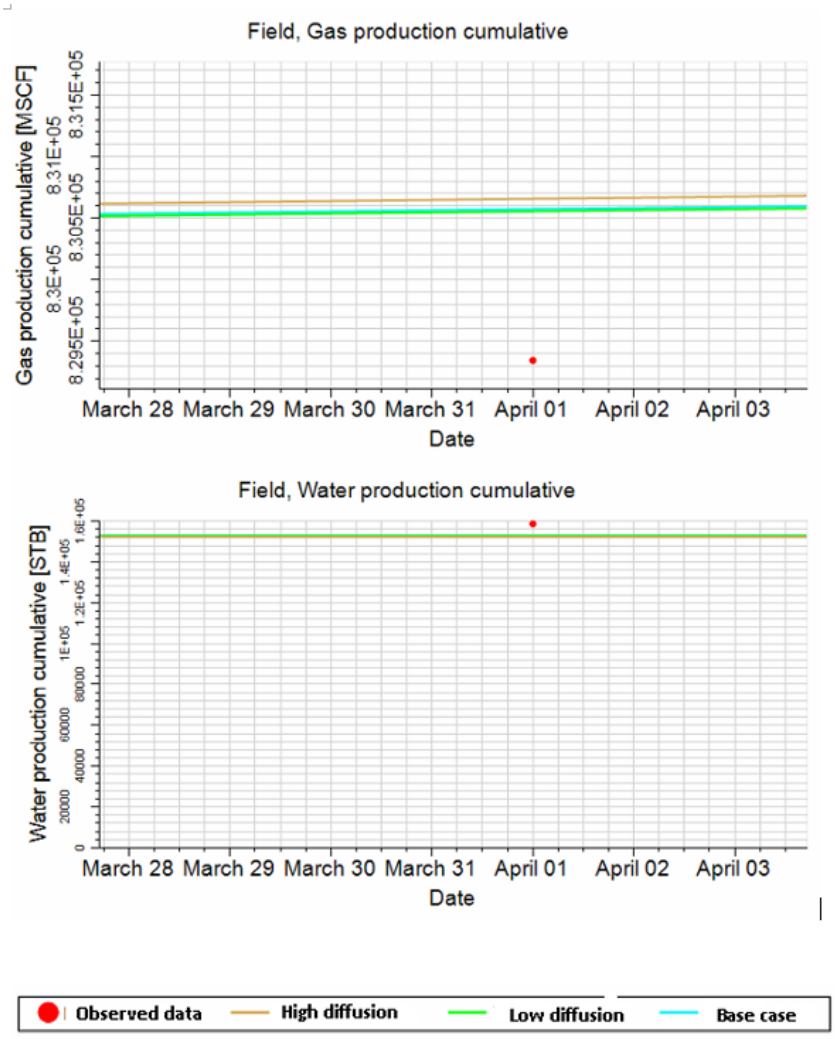

Figure 4.23 The impact of changing the value of the diffusion coefficient with low permeabilities. Illustrated the production during March and April 2018.

Figure 4.24 illustrates that when the permeabilities are high, the differences in the production rates are significant when one compares the resulted values obtained from implementing the low value of the gas-diffusion coefficient with the values obtained from implementing high gas-diffusion coefficient value. Additionally, it is very interesting that the trend is not the same over the production time as one can see that the low diffusion coefficient gave the more accurate values at later times (2018) **Figure 4.24**, while the high diffusion coefficient gave more accurate values at earlier times (December 2011 and January 2012) **Figure 4.25**. This

confirms that the gas-diffusion coefficient in CBM reservoirs is not constant and that the impact of its variability is more critical when dealing with high permeabilities. While the assumption that the flow is only permeability-controlled may be accepted at low permeabilities, it should not be accepted at high permeabilities. Diffusion coefficient should also be a controlling parameter alongside the permeability. It is important to note that the simulator assumes that the flow is permeability-controlled and that the diffusion coefficient is a constant, and yet there are significant production differences with changing that constant values. That is, if the diffusion coefficient was a controlling parameter and a variable, the production differences might have become higher. This is very critical to consider particularly when dealing with high-permeability CBM reservoirs or when utilizing the hydraulic fracturing techniques to enhance CBM reservoir permeabilities.

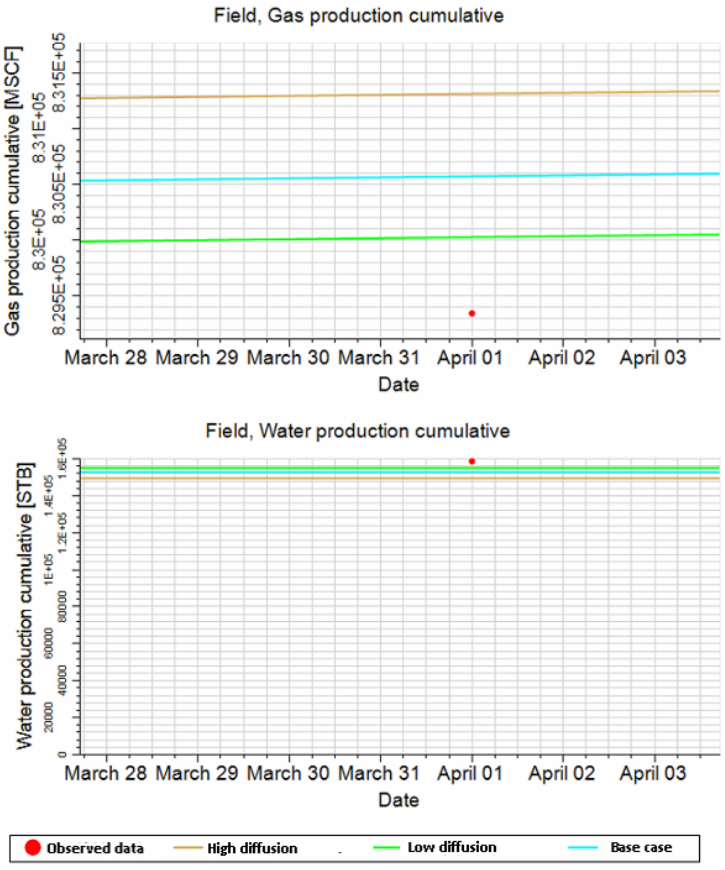

Figure 4.24 The impact of changing the value of the diffusion coefficient with high permeabilities. Illustrated the production during March and April 2018.

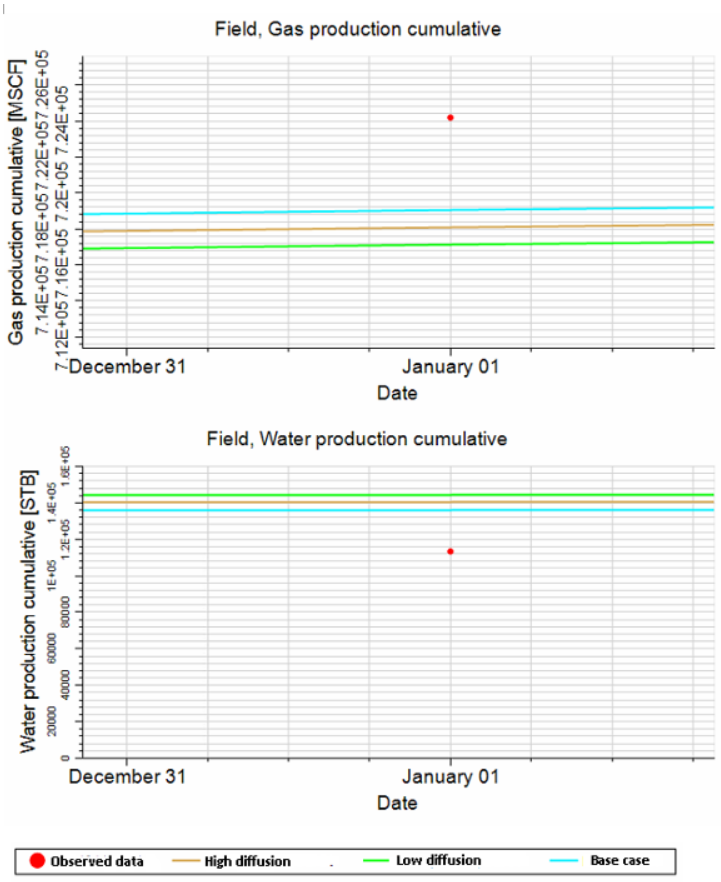

Figure 4.25 The impact of changing the value of the diffusion coefficient with high permeabilities. Illustrated the production during December 2011 and January 2012.

4.2.4 Initial Reservoir Pressure Sensitivity Analysis

Using Anisotropic-homogeneous model, a sensitivity analysis of the initial reservoir pressure was conducted. As previously mentioned, the gas adsorption capacity increases with increasing pressure for a given temperature. Thus, if a CBM reservoir has more adsorbed gas in place, the gas production will also be higher. **Figure 4.26** confirms the theory as gas cumulative production increases with increasing pressure from 200 psi to 600 psi and from 600 psi to 1500 psi. The cumulative gas production increase becomes less at higher pressure which is expected given the shape of the used adsorption isotherm where the slope decreases at higher pressures and the increases in adsorption capacity with increasing pressures become less. Also, it is noticed from

Figure 4.26 that when the initial pressure and gas production increase, cumulative water production decreases. This is expected because the reservoir volume is constant. Hence, the total volume of fluids is constant meaning that when the volume of one fluid increases, the volume of the other fluid decreases.

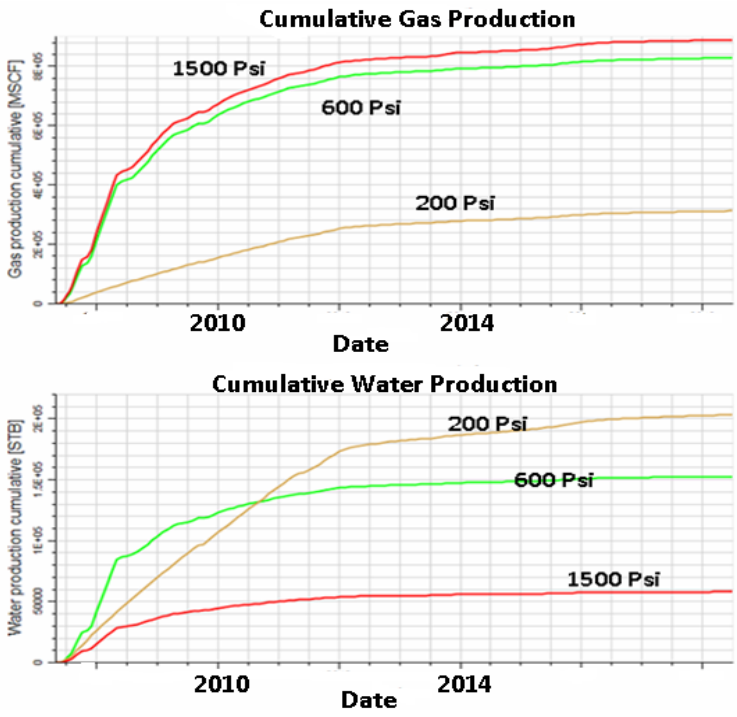

Figure 4.26 Initial pressure sensitivity analysis.

4.2.5 Reservoir Temperature Pressure Sensitivity Analysis

Using the Anisotropic-homogeneous model, a sensitivity analysis of the reservoir temperature was conducted. The theory suggests that the gases adsorption capacity decreases with increasing temperatures which means that gas production would also decrease. **Figure 4.27** that is derived from the model confirms this theory where the cumulative gas production is lower for higher reservoir temperatures. Thus, water production is higher for higher reservoir temperatures. 400 f and 50 f temperatures were tested besides the case of the reservoir actual temperature which is 100 f.

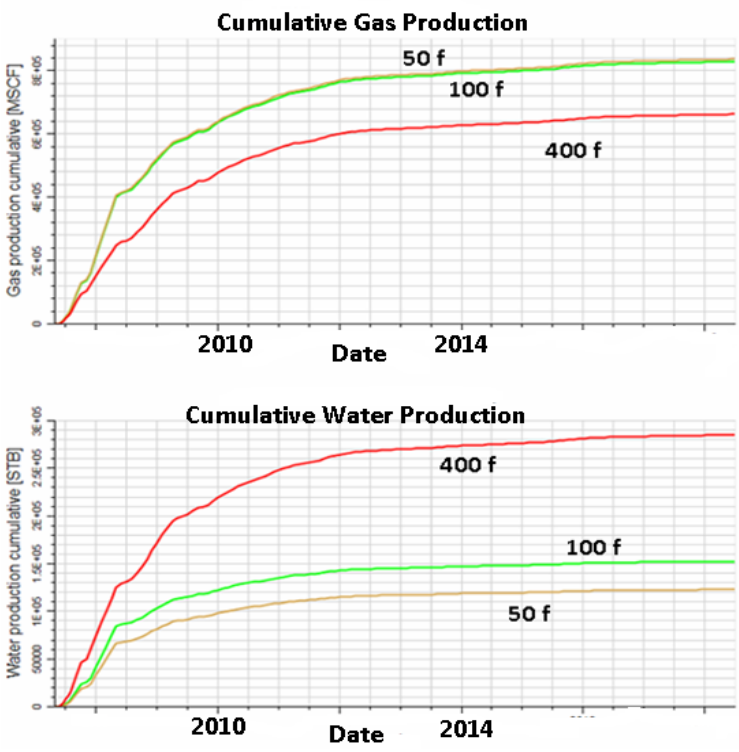

Figure 4.27 Reservoir temperature sensitivity analysis.

Chapter 5. Discussions and Limitations

5.1 Discussions

Through a comprehensive characterization of Big George Coal of Powder River Basin, this study investigated a comprehensive characterization approach of coalbed methane with focus on low-rank CBM reservoir characterization and modeling. I checked the different methods to characterize and model the different aspects of BGC such as the gas adsorption, gas diffusion, moisture content, gas contents, and permeability changes. To characterize the gas adsorption, Langmuir Isotherm for CH_4 and CO_2 adsorption that was derived from PRB coal samples was used. This Langmuir Isotherm accounted for moisture content impact on the CBM adsorption capacity. Langmuir Isotherm for dry coal could be used with using Langmuir scaling keywords to account for the reduction in the adsorption capacity due to the moisture. Extended Langmuir model was utilized to account for the gas mixture in BGC.

Dual-porosity model was used rather than a dual-permeability model since I did not need to account for the movement of the fluid from the cleat system to the matrix. In my future work, I shall utilize the dual-permeability model during enhanced coalbed methane recovery (ECBM) to account for the movement of the injected CO_2 or N_2 from the cleat system to the matrix. Time-dependent gas diffusion model was used rather than an instant diffusion model because the time-dependent diffusion approach is more representative of the actual case. However, ECLIPSE simulator requires the usage of the instant model when using the dual-permeability model. Hence, this was another reason for me to use the dual-porosity model at this stage.

5.2 Limitations

There are three main limitations that represent technical difficulties when characterizing a CBM reservoir using common commercial numerical simulators like ECLIPSE.

5.2.1 Free Gas Content Characterization

ECLIPSE simulator assumes that most of the gas stored in the coal matrix is stored as an adsorbed phase. This assumption may be acceptable for medium and high-rank coal formation where free gas content is negligible, but it is inaccurate for low-rank coal formations where free gas content is significant and should be considered for reserve calculations. Ignoring the free gas content in a low-rank CBM reservoir shall lead to underestimation of the gas in place and inaccurate forecasting for the gas future production. This aspect is particularly important for this study since Big George Coal is low-rank coal.

5.2.2 Moisture Content Characterization

It is a common practice that a numerical simulator does not allow the user to specify any water saturation inside the coal matrix meaning that it is only possible to have 100% gas saturation and 0% water saturation in the matrix. This represents an issue because the matrix water saturation for wet coal formations needs to be specified in order to account for the moisture content. Characterizing the moisture content is important since it has a significant impact on the coal adsorption capacity of the gases. Thus, ignoring the moisture content would cause an overestimation of the adsorbed gas in place and the forecasted gas production rates. ECLIPSE provides the option of Langmuir scaling that allows the user to scale down the adsorption capacities for a number of cells to account for the impact of the moisture on the adsorption capacity, but this is still not practical for two reasons: there is no way to model the cause itself which is the moisture content while ECLIPSE only allows modeling its impact on the adsorption capacity, and one cannot use ECLIPSE to predict the moisture content of the coal through history-matching if one had all the other parameters. That is, one must extract a coal sample of the basin to be able to determine how much moisture content that sample has, and the sample could be not representative

of the whole reservoir. Having the ability to input/predict moisture content through the simulator would save the money of developing the moist Langmuir Isotherm in the lab, give us a distribution of the moisture content in several regions of the reservoir, and allow for more testing of the moisture impact.

5.2.3 Gas-diffusion Characterization

It is a common practice that a numerical simulator assumes that the gas-diffusion coefficient is a constant input which is inaccurate for CBM reservoirs where it has been recently proven that the gas-diffusion coefficient in CBM reservoirs is a variable and should be handled as such. Additionally, the common practice of numerical simulators is to assume that the flow is only permeability-controlled which may be accepted for low-permeability CBM reservoirs. However, for high-permeability CBM reservoirs, the changing diffusion coefficient has a significant impact and should also be considered a controlling parameter. Thus, characterizing diffusion coefficient as a variable is particularly vital for high permeability CBM reservoirs or when considering enhancing the permeability of a CBM reservoir through hydraulic fracturing.

Chapter 6. Conclusions

This chapter encapsulates the major conclusions obtained from the studies conducted in this thesis. The highlights are as follows:

1. This thesis provides a comprehensive characterizing and modeling approach of Big George Coal of Powder River Basin of Wyoming.
2. In an integrated framework, gamma-ray logs and density logs were used to first determine the coal seam depths and thicknesses and characterize other litho-units. The final facies models included seven different facies: coal, shale, sandstone, shaly sand, sandy coal, shaly coal, and igneous intrusions.
3. The values of the petrophysical properties of the Big George Coal such as porosities and permeabilities were obtained from the literature and then populated in the 3D static models. Eventually, these values were further constrained through history-matching of 12.5 years of available production data.
4. The adsorption isotherms that Tang et al. (2005) developed through testing moist PRB coal sample were found suitable for adsorption characterization in the Powder River Basin CBM.
5. Palmer-Mansoori Model provided appropriate means to characterize the permeability changes as a function of pore volume reduction and matrix shrinkage/swelling in the study area.
6. The relative-permeability curves developed by Gash (1991) for San Juan Coal samples were used for BGC model. Mavor et al. (2003) also obtained a good production history-match of PRB simulations using the same relative permeability curves.

7. The static model was divided into five different models in order to address the huge size of the entire model and to compare the petrophysical properties that were obtained by history-matching from the different five models. I could tune the characterization and ensure the accuracy and reliability of the model knowing that all the models gave results that lie within the same plausible ranges.
8. A sensitivity analysis study was conducted to investigate the impact of anisotropy and heterogeneity on gas and water cumulative productions. The most accurate model was found to be the anisotropic-heterogeneous model, followed by the isotropic-heterogeneous model, the anisotropic-homogeneous model, and the isotropic homogenous model, respectively. This analysis confirms that coal formations are highly anisotropic and heterogeneous. It also suggests that the impact of the heterogeneity is potentially higher than the impact of anisotropy.
9. A sensitivity analysis was conducted to check the impact of cleat (fracture) porosities on the gas and water productions. The higher the cleat porosities, the greater the production. This confirms the cleat system provides major accommodation space for the gas in Powder River Basin.
10. The impact of changing the gas-diffusion coefficient was tested through a sensitivity analysis. The results support that variable gas-diffusion coefficient should be more appropriate in the CBM reservoirs than a single value. Additionally, variable gas-diffusion coefficients might be a controlling parameter for high-permeability CBM reservoirs.
11. Initial reservoir pressure and temperature sensitivity analyses were also carried out. The results confirm the theory that the gas adsorption capacity and production rate increase with increasing pressure and decrease with increasing temperature.

12. Moisture content impact on CBM adsorption capacity must be considered during CBM characterization and numerical modeling and simulation.
13. Free and soluble gas contents in low-rank CBM reservoirs are not insignificant and their amounts should be accounted for during CBM characterization and numerical modeling and simulation in order to avoid underestimation of the gas-in-place or forecasted gas production.

Chapter 7. Future Work

Based on the work performed in this thesis, investigating the following aspects can provide further insights into CBM reservoir dynamics and performance particularly in the Big George Coal of the Powder River Basin.

1. Production optimization should be conducted for the future gas-production rates in the Big George Coal.
2. Enhanced CBM (ECBM) recovery may be very promising in the Big George Coal. Investigating ECBM efficiency and the optimum well spacings considering turning the dead wells into injection wells could be viable field-development options. **Appendix A** provides a literature review on ECBM.
3. Hydraulic fracturing can be another suitable technology for CBM reservoirs. However, this will require extensive investigation to quantify the impact of HF on future gas-production rates.
4. A comparison of ECBM and hydraulic fracturing feasibility and efficiency may be conducted. This study should help decide which technique should be used to enhance CBM reservoir production or whether they both could be used simultaneously.
5. In the case of undersaturated coal and during ECBM, the injection of CO_2-rich gas leads to methane banking. The optimum well spacing from methane-banking perspective should be examined.
6. Depleted CBM reservoirs might become excellent candidates for carbon dioxide sequestration.
7. Further investigations on appropriate gas-diffusion coefficient variability in CBM reservoirs through numerical modeling and simulation could provide valuable insights.

8. More investigations on ways to account for free and soluble gas contents in CBM reservoirs could be insightful.

Nomenclature

a	Adsorbed gas content in Freundlich and Langmuir Isotherms
k, and n	Constants
a_m	The number of moles of the gas or adsorbate that cover the surface area of one gram of the adsorbent by forming a monolayer and it is also referred to as the adsorption capacity or the monolayer capacity
ω_m	The surface area that each molecule of the adsorbate occupies of the adsorbent
N	Avogadro's number
p_i	Gas partial pressure
θ_i	Fractional occupancy of the adsorption sites
a^s	Gas concentration on the surface of the adsorbent
a_m^s	Gas concentration where the surface is covered by the monolayer of the gas
M_t	Total mass of gas desorbed at time *t*, *g*
M_∞	Total desorbed mass after an infinite time, *g*
t	Diffusion time, *s*
R	Radius of the sphere, *mm*
D	Diffusion coefficient, mm^2/s
V_t	Volume of gas desorbed at time *t*, *ml*
V_∞	Final desorbed volume, *ml*
V_{it}	Volume of the adsorbed/desorbed gas in the micropores
R_i	Microsphere radius
$V_{i\infty}$	Final adsorbed/desorbed gas volume

D_i	Micropore diffusivity
V_{at}	Total volume of the adsorbed/desorbed gas in the macropores
R_a	Macrosphere radius
$V_{a\infty}$	Final adsorbed/desorbed gas volume
D_a	Macropore diffusivity
$V_{T,daf}$	Adsorbed gas content of the dry coal that has no ash at reservoir temperature, m^3/t
T_R	Reservoir temperature, c °
T_T	Experimental temperature, c °
$\Delta V'$	Adsorption decrement ratio
M_{ad}	Moisture content, *wt.%*
A_{ad}	Ash content on the air-dried basis, *wt.%*
V_g	Free gas content volume, m^3/t
Φ_r	Residual pore volume, m^3/t
p	Gas pressure, *MPa*
p_o	Standard pressure, *MPa*
T_o	Standard temperature, c °
T	Reservoir temperature, c °
Z	Gas compressibility factor
Φ	Measured total porosity, *%*
Φ_w	Water volume percentage of the porosity, *%*
Φ_p	Accumulative volume strain, *%*
ρ_{ca}	Coal apparent density, t/m^3

a and b	Constants
c	Methane concentration, *mol/kg*
n	Methane molar volume, *L/mol*
V_m	Soluble gas content, m^3/t
b_m	Methane solubility, m^3/m^3
ρ_w	CBM reservoir water density, *g/mL*
M_e	CBM reservoir moisture content, *%*
Φ_0	Initial porosity
$V(P_0)$	Pore volume at the initial pressure
K	Bulk modulus
M	Constrained axial modulus
β, ε_l	The parameters of the match between the change in a volumetric strain which results from matrix shrinkage, and the Langmuir Isotherm
g	Geometric factor (0-1)
f	fraction (0-1)
γ	Grain compressibility
c_f	Cleat volume compressibility caused by the effective horizontal stress perpendicular to the fractures/cleats
k_0	Initial permeability of the coal
α_{Sj}	Shrinkage/ swelling coefficient
V_j	j component specific adsorbed volume at current reservoir gas composition and pressure

V_{j0} j component specific adsorbed volume at initial reservoir gas composition and pressure

References

Boreck, D.L., and Weaver, J.N., 1984, Coalbed methane study of the Anderson coal deposit, Johnson County, Wyoming- A preliminary report: U.S. Geological Survey Open-File Report 84–831, 16 p.

Kapoor, A., Ritter, J. A., and Yang, R. T. (1990). An extended Langmuir model for adsorption of gas mixtures on heterogeneous surfaces. *Langmuir*, *6*(3), 660-664.

Arri, L. E., Yee, D., Morgan, W. D., and Jeansonne, M. W. (1992, January). Modeling coalbed methane production with binary gas sorption. In *SPE rocky mountain regional meeting*. Society of Petroleum Engineers.

Harpalani, S., and Chen, G. (1997). Influence of gas production induced volumetric strain on permeability of coal. *Geotechnical & Geological Engineering*, *15*(4), 303-325.

Pillalamarry, M., Harpalani, S., and Liu, S. (2011). Gas diffusion behavior of coal and its impact on production from coalbed methane reservoirs. *International Journal of Coal Geology*, *86*(4), 342-348.

King, G. (1985). *Numerical simulation of the simultaneous flow of methane and water through dual porosity coal seams during the degasification process*. Pennsylvania State Univ., University Park (USA).

Collins, R. E. (1991, May). New theory for gas adsorption and transport in coal. In *Proceedings of the 1991 Coalbed Methane Symposium, Tuscaloosa, USA* (pp. 425-431).

Zhao, X. (1991). An experimental study of methane diffusion in coal using transient approach.

Shi, J. Q., and Durucan, S. (2003). A bidisperse pore diffusion model for methane displacement desorption in coal by CO2 injection☆. *Fuel*, *82*(10), 1219-1229.

Thorstenson, D. C., and Pollock, D. W. (1989). Gas transport in unsaturated porous media: The adequacy of Fick's law. *Reviews of Geophysics*, *27*(1), 61-78.

Crank, J., 1975. Mathematics of Diffusion. Oxford University Press, London.

Clarkson, C. R., and Bustin, R. M. (1999). The effect of pore structure and gas pressure upon the transport properties of coal: a laboratory and modeling study. 2. Adsorption rate modeling. *Fuel*, *78*(11), 1345-1362.

Ruckenstein, E., Vaidyanathan, A. S., and Youngquist, G. R. (1971). Sorption by solids with bidisperse pore structures. *Chemical Engineering Science*, *26*(9), 1305-1318.

Cheng-Wu, L., Hong-Lai, X., Cheng, G., and Wen-biao, L. (2018). Modeling and experiments for the time-dependent diffusion coefficient during methane desorption from coal. *Journal of Geophysics and Engineering*, *15*(2), 315-329.

Pan, Z., Connell, L. D., Camilleri, M., and Connelly, L. (2010). Effects of matrix moisture on gas diffusion and flow in coal. *Fuel*, *89*(11), 3207-3217.

Wang, K., Zang, J., Feng, Y., and Wu, Y. (2014). Effects of moisture on diffusion kinetics in Chinese coals during methane desorption. *Journal of Natural Gas Science and Engineering*, *21*, 1005-1014.

Cui, X., Bustin, R. M., and Dipple, G. (2004). Selective transport of CO2, CH4, and N2 in coals: insights from modeling of experimental gas adsorption data. *Fuel*, *83*(3), 293-303.

Chen, Y. D., and Yang, R. T. (1991). Concentration dependence of surface diffusion and zeolitic diffusion. *AIChE Journal*, *37*(10), 1579-1582.

Staib, G., Sakurovs, R., and Gray, E. M. A. (2015). Dispersive diffusion of gases in coals. Part I: Model development. *Fuel*, *143*, 612-619.

Zheng, Q., Yu, B., Wang, S., and Luo, L. (2012). A diffusivity model for gas diffusion through fractal porous media. *Chemical Engineering Science*, *68*(1), 650-655.

Lesne, A., and Laguës, M. (2011). *Scale invariance: From phase transitions to turbulence*. Springer Science & Business Media.

Chen, Y., Wang, X., and He, R. (2011). Modeling changes of fractal pore structures in coal pyrolysis. *Fuel*, *90*(2), 499-504.

Keshavarz, A., Sakurovs, R., Grigore, M., and Sayyafzadeh, M. (2017). Effect of maceral composition and coal rank on gas diffusion in Australian coals. *International Journal of Coal Geology*, *173*, 65-75.

Hunt, J. W., and Botz, R. W. (1986). Outbursts in Australian coal mines: A petrographic factor. In *Bull. Proc. Australas. Inst. Min. Metall.* (Vol. 29, pp. 59-63).

Beamish, B. B., and Crosdale, P. J. (1995, March). The influence of maceral content on the sorption of gases by coal and the association with outbursting. In *International symposium-cum-workshop on management and control of high gas emissions and outbursts in underground coal mines: Wollongong, Australia, National Organising Committee of the Symposium* (pp. 353-361).

Crosdale, P. J., and Beamish, B. B. (1993, November). Maceral effects on methane sorption by coal. In *New Developments in Coal Geology, A Symposium, Brisbane* (pp. 95-98).

Laxminarayana, C., and Crosdale, P. J. (1999). Role of coal type and rank on methane sorption characteristics of Bowen Basin, Australia coals. *International Journal of Coal Geology*, *40*(4), 309-325.

Faiz, M. M., and Cook, A. C. (1991). Influence of coal type, rank and depth on the gas retention capacity of coals in the southern coalfield, NSW. In *Gas in Australian Coals. Symp. Proc* (Vol. 2, pp. 19-29). Geol. Soc. of Aust.

Faiz, M. M., Aziz, N. I., Hutton, A. C., and Jones, B. G. (1992, November). Porosity and gas sorption capacity of some eastern Australian coals in relation to coal rank and composition. In *Coalbed Methane Symposium, Townsville* (Vol. 19, p. 21).

Crosdale, P. J., and Beamish, B. B. (1994, December). Methane sorption studies at South Bulli (NSW) and Central (QLD) collieries using a high-pressure microbalance. In *Proceeding 28th Newcastle Symposium on Advances in the Study of the Sydney Basin Department Geology* (pp. 118-125).

Laxminarayana, C., and Crosdale, P. J. (1999). Role of coal type and rank on methane sorption characteristics of Bowen Basin, Australia coals. *International Journal of Coal Geology*, *40*(4), 309-325.

Xu, H., Tang, D., Zhao, J., Li, S., and Tao, S. (2015). A new laboratory method for accurate measurement of the methane diffusion coefficient and its influencing factors in the coal matrix. *Fuel*, *158*, 239-247.

Gan, H., Nandi, S. P., and Walker Jr, P. L. (1972). Nature of the porosity in American coals. *Fuel*, *51*(4), 272-277.

Smith, D. M., and Williams, F. L. (1984). Diffusional effects in the recovery of methane from coalbeds. *Society of Petroleum Engineers Journal*, *24*(05), 529-535.

Van Bergen, F., Spiers, C., Floor, G., and Bots, P. (2009). Strain development in unconfined coals exposed to CO2, CH4 and Ar: effect of moisture. *International Journal of Coal Geology*, *77*(1-2), 43-53.

Palmer, I., and Mansoori, J. (1998). *How permeability depends on stress and pore pressure in coalbeds: a new model. SPEREE 1 (6): 539–544.* SPE-52607-PA.

Fu, B., Liu, G., Liu, Y., Cheng, S., Qi, C., and Sun, R. (2016). Coal quality characterization and its relationship with geological process of the Early Permian Huainan coal deposits, southern North China. *Journal of Geochemical Exploration*, *166*, 33-44.

Tan, Y., Pan, Z., Liu, J., Kang, J., Zhou, F., Connell, L. D., and Yang, Y. (2018). Experimental study of impact of anisotropy and heterogeneity on gas flow in coal. Part I: Diffusion and adsorption. *Fuel*, *232*, 444-453.

Busch, A., Gensterblum, Y., Krooss, B. M., and Littke, R. (2004). Methane and carbon dioxide adsorption–diffusion experiments on coal: upscaling and modeling. *International Journal of Coal Geology*, *60*(2-4), 151-168.

Heriawan, M. N., and Koike, K. (2008). Identifying spatial heterogeneity of coal resource quality in a multilayer coal deposit by multivariate geostatistics. *International Journal of Coal Geology*, *73*(3-4), 307-330.

Tan, Y., Pan, Z., Liu, J., Zhou, F., Connell, L. D., Sun, W., and Haque, A. (2018). Experimental study of the impact of anisotropy and heterogeneity on gas flow in coal. Part II: Permeability. *Fuel*, *230*, 397-409.

Cai, Y., Liu, D., Pan, Z., Yao, Y., and Li, C. (2015). Mineral occurrence and its impact on fracture generation in selected Qinshui Basin coals: an experimental perspective. *International Journal of Coal Geology*, *150*, 35-50.

Koenig, R. A., and Stubbs, P. B. (1986, January). Interference testing of a coalbed methane reservoir. In *SPE Unconventional Gas Technology Symposium*. Society of Petroleum Engineers.

Liu, A., Fu, X., Wang, K., An, H., and Wang, G. (2013). Investigation of coalbed methane potential in low-rank coal reservoirs–Free and soluble gas contents. *Fuel*, *112*, 14-22.

Zhang, Q., Li, J., Zhang, X., Song, S., Yun, Z., and Zhang, P. (2001). CBM development potential of high-rank coal with reference to Qinshui coal field. *Shanxi: Coal Geology and Exploration*, *29*(6), 26-30.

Fu, X. H., Qin, Y., Quan, B., Fan, B. H., and Wang, K. X. (2008). Study of physical and numerical simulations of adsorption methane content on middle-rank coal. *Acta Geol Sinica*, *82*(10), 1368-1371.

Alexeev, A. D., Feldman, E. P., and Vasilenko, T. A. (2007). Methane desorption from a coal-bed. *Fuel*, *86*(16), 2574-2580.

Yongjun, C., Qun, Z., Hong, Z., and Qingling, Z. (2005). Adsorption of different rank coals to single component gases. *Natural Gas Industry*, *25*(1), 61-65.

Mares, T. E., Moore, T. A., and Moore, C. R. (2009). Uncertainty of gas saturation estimates in a subbituminous coal seam. *International Journal of Coal Geology*, *77*(3-4), 320-327.

ZHANG, X. M., HAN, B. S., and LI, J. W. (2006). CBM storage character of lignite and gas content estimate method [J]. *Coal Geology & Exploration*, *3*.

Chen, H., Wang, W., Wang, R., and Zhou, Y. (2004). Study on low-rank coal-bed gas exploration in Tuha Basin. *Tuha Oil & Gas*.

Yongjun, C., Qun, Z., Hong, Z., and Qingling, Z. (2005). Adsorption of different rank coals to single component gases. *Natural Gas Industry*, *25*(1), 61-65.

Clarkson, C. R., and Bustin, R. M. (1996). Variation in micropore capacity and size distribution with composition in bituminous coal of the Western Canadian Sedimentary Basin: implications for coalbed methane potential. *Fuel*, *75*(13), 1483-1498.

Levy, J. H., Day, S. J., and Killingley, J. S. (1997). Methane capacities of Bowen Basin coals related to coal properties. *Fuel*, *76*(9), 813-819.

Chen P (2001). Properties types and utilize of coal in China. Beijing: Chemical Industry Press.

Berbesi, L. A., Márquez, G., Martínez, M., and Requena, A. (2009). Evaluating the gas content of coals and isolated maceral concentrates from the Paleocene Guasare Coalfield, Venezuela. *Applied Geochemistry*, *24*(10), 1817-1824.

Clarkson, C. R., and Bustin, R. M. (1996). Variation in micropore capacity and size distribution with composition in bituminous coal of the Western Canadian Sedimentary Basin: implications for coalbed methane potential. *Fuel*, *75*(13), 1483-1498.

Yongjun, C., Qun, Z., Hong, Z., and Qingling, Z. (2005). Adsorption of different rank coals to single component gases. *Natural Gas Industry*, *25*(1), 61-65.

Fu, X. H., Qin, Y., and Wang, W. G. (2005). Study of gas-dissolving in coalbed water and prediction of gas content of lignite reservoir. *Natural Gas Geoscience*, *16*(2), 153-156.

ZHANG, X. M., HAN, B. S., and LI, J. W. (2006). CBM storage character of lignite and gas content estimate method [J]. *Coal Geology & Exploration*, *3*.

Fu XT, Wang ZP, Lu XF (1996). Gas soluble mechanism and solubility formula. Sci China 24(2):124–30.

Yang SB, Wang XJ, Zhang XL (1997). Water-soluble gas exploration and

development. Beijing: China University of Petroleum Press.

Chapoy, A., Mohammadi, A. H., Richon, D., and Tohidi, B. (2004). Gas solubility measurement and modeling for methane–water and methane-ethane–n-butane–water systems at low-temperature conditions. *Fluid phase equilibria*, *220*(1), 111-119.

Folas, G. K., Froyna, E. W., Lovland, J., Kontogeorgis, G. M., and Solbraa, E. (2007). Data and prediction of water content of high-pressure nitrogen, methane, and natural gas. *Fluid Phase Equilibria*, *252*(1-2), 162-174.

Sachs, W. (1998). The diffusional transport of methane in liquid water: method and result of experimental investigation at elevated pressure. *Journal of Petroleum Science and Engineering*, *21*(3-4), 153-164.

FU, X. H., QIN, Y., YANG, Y. G., and PENG, J. N. (2004). EXPERIMENTAL STUDY OF THE SOLUBILITY OF METHANE IN COALBED WATER [J]. *Natural Gas Geoscience*, *4*.

Wang JS, Wang L, Liu YM (200). Experimental study on characteristics and regulation of water dissolving coal gas. J Liaoning Tech Univ 25(1):14–6.

Shi, J. Q., and Durucan, S. (2005). CO2 storage in deep unminable coal seams. *Oil & gas science and technology*, *60*(3), 547-558.

Marsh, H. (1987). Adsorption methods to study microporosity in coals and carbons—a critique. *Carbon*, *25*(1), 49-58.

Stanton, R., Flores, R. M., Warwick, P. D., Gluskoter, H. J., and Stricker, G. D. (2001). Coal bed sequestration of carbon dioxide. In *First National Conference on Carbon Sequestration*.

Ceglarska-Stefańska, G., and Zarębska, K. (2002). The competitive sorption of CO2 and CH4 with regard to the release of methane from coal. *Fuel Processing Technology*, *77*, 423-429.

Cui, X., Bustin, R. M., and Dipple, G. (2004). Selective transport of CO2, CH4, and N2 in coals: insights from modeling of experimental gas adsorption data. *Fuel*, *83*(3), 293-303.

Busch, A., Gensterblum, Y., Siemons, N., Krooss, B. M., Van Bergen, F., Pagnier, H. J. M., and David, P. (2003, May). Investigation of preferential sorption behaviour of CO2 and CH4 on coals by high-pressure adsorption/desorption experiments with gas mixtures. In *Proceedings of the 2003 International CMB Symposium* (Vol. 5, No. 9).

McGovern, M. (2004). Allison unit CO2 flood. *SPE ATW Enhanced CBM Recovery and CO2 Sequestration, Denver, CO*, 28-29.

Seidle, J. P. (2000, January). Reservoir engineering aspects of CO2 sequestration in coals. In *SPE/CERI Gas Technology Symposium*. Society of Petroleum Engineers.

Harpalani, S., and Chen, G. (1995). Estimation of changes in fracture porosity of coal with gas emission. *Fuel*, *74*(10), 1491-1498.

Seidle, J. R., and Huitt, L. G. (1995, January). Experimental measurement of coal matrix shrinkage due to gas desorption and implications for cleat permeability increases. In *International meeting on petroleum Engineering*. Society of Petroleum Engineers.

Durucan, S., Shi, J. Q., and Syahrial, E. (2003). An Investigation into the Effects of Matrix Swelling on Coal Permeability for ECBM and CO2 Sequestration Assessment. *Final report on EPSRC Grant No GR N, 24148*.

Ziqiu, X., and Takashi, O. (2003). Laboratory measurements on swelling in coals caused by adsorption of carbon dioxide and its impact on permeability. In *2nd International workshop on research relevant to CO2 sequestration in coal seam* (pp. 57-66).

Reeves, S. R. (2002). The Coal-Seq Project: Field studies of ECBM and CO2 sequestration in coal. In *Coal Seq Forum, March* (pp. 14-15).

Pekot, L. J., and Reeves, S. R. (2003). Modeling the effects of matrix shrinkage and differential swelling on coalbed methane recovery and carbon sequestration. In *Paper 0328, proc. 2003 International Coalbed Methane Symposium. University of Alabama*.

Shi, J.Q., Durucan, s., Sinka, I.C. and Daltaban, T.S. (1997) A Numerical Investigation into the Laboratory and Field Behaviour of cavitated Coalbed Methane Wells, *Proc. 1st Southern*

African Rock Engineering Symposium (SARES'97), Johannesburg, 15-17 September, 131-142.

Smith, L. K., and Reeves, S. R. (2002). Scoping equilibrium geochemical modeling to evaluate the potential for precipitate formation when sequestering CO2 in San Juan basin Coals. *Topical Report, DOE Contract No. DE-FC26-00NT40924*.

Shi, J. Q., and Durucan, S. (2003). Modelling of enhanced methane recovery and CO2 sequestration in deep coal seams: The impact of coal matrix shrinkage/swelling on cleat permeability. In *Proc. 2003 Coalbed Methane Symposium, Alabama, May* (pp. 5-9).

Mavor, M. J., Gunter, W. D., and Robinson, J. R. (2004, January). Alberta multiwell micro-pilot testing for CBM properties, enhanced methane recovery and CO2 storage potential. In *SPE Annual Technical Conference and Exhibition*. Society of Petroleum Engineers.

Shi, J. Q., and Durucan, S. (2005). A numerical simulation study of the Allison unit CO2-ECBM pilot: the impact of matrix shrinkage and swelling on ECBM production and CO2 injectivity. In *Greenhouse Gas Control Technologies 7* (pp. 431-439). Elsevier Science Ltd.

Levine, J. R. (1996). Model study of the influence of matrix shrinkage on absolute permeability of coal bed reservoirs. *Geological Society, London, Special Publications*, *109*(1), 197-212.

Cui, X. (2004) Sequestration by sorption on organic matter, Presented at *the third International Forum on Geologic Sequestration of CO2 in Deep, Unminable Coalseams (Coal-Seq III)* Baltimore MD, March 25-26.

Stevens, S. H., Spector, D., and Riemer, P. (1998, January). Enhanced coalbed methane recovery using CO2 injection: worldwide resource and CO2 sequestration potential. In *SPE International Oil and Gas Conference and Exhibition in China*. Society of Petroleum Engineers.

Law, D. H. S., Van der Meer, L. G. H., and Gunter, W. D. (2002, January). Numerical simulator comparison study for enhanced coalbed methane recovery processes, Part I: Pure carbon dioxide injection. In *SPE gas technology symposium*. Society of Petroleum Engineers.

Law, D. H. S., Van der Meer, L. G. H., Mavor, M. J., and Gunter, W. D. (2000, August). Modelling of carbon dioxide sequestration in coalbeds: a numerical challenge. In *the International Conference on Greenhouse Gas Control Technologies (GHGT-5), Cairns, Australia, August* (pp. 13-16).

Law, D. H. S., van der Meer, L. B., and Gunter, W. B. (2003, January). Comparison of numerical simulators for greenhouse gas storage in coal beds, Part II: Flue gas injection. In *Greenhouse Gas Control Technologies-6th International Conference* (pp. 563-568). Pergamon.

Law, D.H.-S, L.H.G. van der Meer, and W.D. Gunter (2003) Comparison of numerical simulators for greenhouse gas storage in coalbeds, Part III: More Complex Problems, Paper presented at the *2nd annual conference on carbon sequestration,* Alexandria, VA, May 5-8, 2003.

Li, X., and Fang, Z. M. (2014). Current status and technical challenges of CO 2 storage in coal seams and enhanced coalbed methane recovery: an overview. *International Journal of Coal Science & Technology*, *1*(1), 93-102.

Parakh, S. (2007). Experimental investigation of enhanced coal bed methane recovery. *Report, Department of Petroleum Engineering of Stanford University*.

Gentzis, T., and Bolen, D. (2008). The use of numerical simulation in predicting coalbed methane producibility from the Gates coals, Alberta Inner Foothills, Canada: Comparison with Mannville coal CBM production in the Alberta Syncline. *International Journal of Coal Geology*, *74*(3-4), 215-236.

Ozdemir, E. (2009). Modeling of coal bed methane (CBM) production and CO2 sequestration in coal seams. *International Journal of Coal Geology*, *77*(1-2), 145-152.

Zheng, G., Pan, Z., Chen, Z., Tang, S., Connell, L. D., Zhang, S., and Wang, B. (2012). Laboratory study of gas permeability and cleat compressibility for CBM/ECBM in Chinese coals. *Energy Exploration & Exploitation*, *30*(3), 451-476.

Massarotto, P., Iyer, R. S., Elma, M., and Nicholson, T. (2014). An experimental study on characterizing coal bed methane (CBM) fines production and migration of mineral matter in coal beds. *Energy & Fuels*, *28*(2), 766-773.

Yan, F., Lin, B., Zhu, C., Shen, C., Zou, Q., Guo, C., and Liu, T. (2015). A novel ECBM extraction technology based on the integration of hydraulic slotting and hydraulic fracturing. *Journal of Natural Gas Science and Engineering*, *22*, 571-579.

Wright, C. A., Tanigawa, J. J., Shixin, M., and Li, Z. (1995, January). Enhanced hydraulic fracture technology for a coal seam reservoir in Central China. In *International meeting on petroleum engineering*. Society of Petroleum Engineers.

Li, L. C., Tang, C. A., Li, G., Wang, S. Y., Liang, Z. Z., and Zhang, Y. B. (2012). Numerical simulation of 3D hydraulic fracturing based on an improved flow-stress-damage model and a parallel FEM technique. *Rock Mechanics and rock engineering*, *45*(5), 801-818.

Pandey, V. J., Flottmann, T., and Zwarich, N. R. (2017). Applications of Geomechanics to Hydraulic Fracturing: Case Studies from Coal Stimulations. *SPE Production & Operations*, *32*(04), 404-422.

Johnson, R. L., Scott, M. P., Jeffrey, R. G., Chen, Z., Bennett, L., Vandenborn, C. B., and Tcherkashnev, S. (2010, January). Evaluating hydraulic fracture effectiveness in a coal seam gas reservoir from surface tiltmeter and microseismic monitoring. In *SPE Annual Technical Conference and Exhibition*. Society of Petroleum Engineers.

Ross, H. E. (2007). *Carbon dioxide sequestration and enhanced coalbed methane recovery in unmineable coalbeds of the Powder River Basin, Wyoming*.

Ross, H. E., Hagin, P., and Zoback, M. D. (2009). CO2 storage and enhanced coalbed methane recovery: reservoir characterization and fluid flow simulations of the Big George coal, Powder River Basin, Wyoming, USA. *International Journal of Greenhouse Gas Control*, *3*(6), 773-786.

Colmenares, L. B., and Zoback, M. D. (2007). Hydraulic fracturing and wellbore completion of coalbed methane wells in the Powder River Basin, Wyoming: Implications for water and gas production. *AAPG bulletin*, *91*(1), 51-67.

Flores, R. M., and Bader, L. R. (1999). Fort Union coal in the Powder River basin, Wyoming and Montana: A synthesis. *US Geological Survey Professional Paper*, *1625*, 49.

DOE, U. (2002). Powder River Basin coalbed methane development and produced water management study. *US Department of Energy. Office of Fossil Energy and National Energy Technology Laboratory Strategic Center for Natural Gas*.

Flores, R. M. (2004). Coalbed methane in the Powder River Basin, Wyoming and Montana: An assessment of the Tertiary-Upper Cretaceous coalbed methane total petroleum system. *US Geological survey digital data series dds-69-c*, *2*, 56.

Chatterjee, R., and Paul, S. (2012). Application of cross-plotting techniques for delineation of coal and non-coal litho-units from well logs in Jharia Coalfield, India. *Geomaterials*, 2, 94-104.

Journel, A. G., 1994, Geostatistics and reservoir geology: *in* J. M., Yarus and R. L. Chambers, eds., Computer Applications 3: Modeling and Geostatistics, AAPG, 19-20.

Deutsch, C. (2002).Geostatistical reservoir modeling: Oxford Univ. *Press, New York, New York*.

Twombly, G., Stepanek, S. H., and Moore, T. A. (2004, March). Coalbed methane potential in the Waikato Coalfield of New Zealand: A comparison with developed basins in the United States. In *2004 New Zealand Petroleum Conference Proceedings* (pp. 1-6). Ministry of Economic Development Auckland, New Zealand.

Mavor, M. J., Russell, B., and Pratt, T. J. (2003, January). Powder River Basin Ft. Union coal reservoir properties and production decline analysis. In *SPE Annual Technical Conference and Exhibition*. Society of Petroleum Engineers.

Ayers, W. B. (2002). Coalbed gas systems, resources, and production and a review of contrasting cases from the San Juan and Powder River basins. *AAPG bulletin*, *86*(11), 1853-1890.

Methane, C. B. (2000). Potential and Concerns, US Department of the Interior. *US Geological Survey, USGS Fact Sheet FS-123-00*.

Laubach, S. E., Marrett, R. A., Olson, J. E., and Scott, A. R. (1998). Characteristics and origins of coal cleat: a review. *International Journal of Coal Geology*, *35*(1-4), 175-207.

Wyoming Oil and Gas Conservation Commission (WOGCC), <http://wogcc.state.wy.us/>, accessed between 2017 and 2019

Kovscek, A. R., Tang, G. Q., and Jessen, K. (2005, January). Laboratory and simulation investigation of enhanced coalbed methane recovery by gas injection. In *SPE Annual Technical Conference and Exhibition*. Society of Petroleum Engineers.

Ellis, M. S. (2002). *Quality of economically extractable coal beds in the Gillette coal field as compared with other Tertiary coal beds in the Powder River basin, Wyoming and Montana* (No. 2002-174). US Geological Survey.

Kovscek, A. R., and F. M Orr, 2004, Rapid prediction of CO2 movement in aquifers, coal beds, and oil and gas reservoirs: Stanford University Global Climate and Energy Project (GCEP) Technical Report 2003-2004, 115-147, <http://gcep.stanford.edu/research/technical_report/2004.html>.

Clarkson, C. R., Pan, Z., Palmer, I. D., and Harpalani, S. (2010). Predicting sorption-induced strain and permeability increase with depletion for coalbed-methane reservoirs. *Spe Journal*, *15*(01), 152-159.

Orr, F. M., Jessen, K., and Kovscek, A. (2003, December). Rapid prediction of CO2 movement in aquifers, coal beds, and oil and gas reservoirs. In *AGU Fall Meeting Abstracts*.

Gash, B. W. (1991, January). Measurement of" Rock Properties" in Coal for Coalbed Methane Production. In *SPE Annual Technical Conference and Exhibition*. Society of Petroleum Engineers.

Mehana, M. (2016). On the Fate of the Fracturing Fluid and Its Impact on Load Recovery and Well Performance.

ECLIPSE Industry-Reference Reservoir Simulator, Reference Manual, Version 2018.1

ECLIPSE Industry-Reference Reservoir Simulator, Technical Description, Version 2018.1

Appendix A: Enhanced Coalbed Methane Recovery (ECBM) and Hydraulic Fracturing in CBM

1. Introduction

At least a high percentage of the gas stored in CBM reservoirs exists as an adsorbed gas. For the adsorbed gas to be produced, it must desorb off the coal matrix surface and diffuse through the matrix to the cleats where it flows easily towards the production wellbore. At reservoir pressures, only a small portion of the adsorbed gas desorbs. That is, to get a high methane recovery naturally, the reservoir pressure needs to reduce significantly. Additionally, most of coalbed methane reservoirs have very low permeabilities which makes it harder for the adsorbed gas to desorb and diffuse to be produced.

Hence, Improving the CBM reservoirs recovery should be either by stimulating the desorption of the adsorbed methane without having to have very low reservoir pressures or by increasing the CBM reservoir permeability.

Improving the methane recovery by stimulating the desorption of the adsorbed methane could be done through a technology named Enhanced Coalbed Methane Recovery (ECBM) where a gas- CO_2, N_2, or a mixture- is injected into the CBM reservoir to increase the desorbed methane amount through specific mechanisms. The process of injecting CO_2 into the CBM reservoirs is also named CO_2 sequestration where CBM reservoirs are considered very attractive formations to sequester CO_2 to fight global warming and the cost of CO_2 injection could be offset by the profit resulting from the additional methane recovery. On the other hand, CBM reservoirs permeabilities could be improved by utilizing the hydraulic fracturing technique.

In this chapter, I discuss the process, mechanisms, and issues of CO_2 sequestration/ECBM. I also address the hydraulic fracturing application in CBM reservoirs and whether both ECBM/gas injection and hydraulic fracturing could be applied simultaneously.

2. Enhanced Coalbed Recovery (ECBM) and CO_2 Sequestration

Gas storage mechanism in coal formations is entirely different than the gas storage in conventional reservoirs as the gas in coal formation is mainly stored as an adsorbed phase on the coal matrices surfaces while the gas in the conventional oil and gas reservoirs occupy the pore space as a distinct phase or presents as a soluble phase in the oil or water. Thus, enhancing gas recovery in CBM reservoirs by injecting CO_2 into the reservoir follows a different mechanism than when CO_2 is injected into conventional oil or gas reservoirs to enhance the hydrocarbon recovery. Carbon dioxide injection is being used in the conventional oil and gas reservoirs to enhance the recovery where it acts as a separate phase that gives more energy/pressure to the oil or gas phases so they could move further and be produced. However, using gas injection- CO_2 or N_2- in coal formations does not aim at enhancing the pressure, but it aims to interfere in the sorption processes to enhance the gas recovery. Through CO_2 injection into coal formations, one may try to encourage the CO_2 adsorption on the coal surfaces that originally have adsorbed methane. For that to occur, methane must desorb and be released and then diffuses to the cleat system and become mobile or recoverable. In other words, the CO_2 injection causes a displacement of gases where adsorbed methane is exchanged for adsorbed CO_2 (Shi and Durucan, 2005).

Additionally, coal formations are attractive formations for CO_2 sequestration which would help mitigate the greenhouse gases emissions and fight global warming. The CO_2 injection costs would also be offset by the excess methane production resulting from the enhanced coalbed methane process.

A. Comparison Between Carbon Dioxide Adsorption and Methane Adsorption

Like methane adsorption in coal formations, carbon dioxide adsorption is normally described using Langmuir Isotherm. That is, adsorption for both gases is governed by micropore-filling processes (Shi and Durucan, 2005). It is known that the surface area that is available for methane adsorption in coal formation is very large (20-200 m2/g) which gives the coalbed methane reservoirs the ability to contain five times more methane than the conventional gas reservoirs of comparable sizes (Marsh, 1987). This makes coal formations even more attractive for CO_2 sequestration knowing that carbon dioxide has greater affinity than methane meaning that coal formations can adsorb more carbon dioxide than methane. Coalbed methane reservoirs can adsorb at least twice the amount of methane as carbon dioxide and for BGC, it can store even more. This ratio increases with decreasing the coal rank resulting in having a 10:1 ratio of the carbon dioxide to methane adsorption capacities in some low-rank coal (Stanton et al., 2001). This gives a great advantage to Powder River Basin coal and makes it a great candidate for CO_2 sequestration since it is mainly composed of low-rank coal.

B. Competitive Sorption

CO_2 adsorption capacity ranges from 2 to 10 times greater than the methane adsorption capacity depending mainly on the pressure and coal rank. Thus, one might predict that when there is a binary mixture of CO_2-Methane in coal, it is more likely for the carbon dioxide to adsorb and for the methane to desorb. However, Ceglarska-Stefanska and Zarebsks (2002) concluded that some coal properties such as maceral composition and capillarity may cause that adsorption trend to become reversed where CO_2 desorbs, and Methane adsorbs. More research is needed to clarify the exact process directions.

Gas adsorption occurs mainly in the micropores and since the coal pore sizes are very heterogeneous, there might be a vital role for the relative size of the gas molecule to the pore structure in selecting which gas to adsorb/desorb (Shi and Durucan, 2005). Cui et al. (2003) Found that the apparent micropore diffusivities of methane, carbon dioxide and nitrogen in coal correlate with the kinetic diameter of each gas. That is, the smaller the gas kinetic diameter is, the larger the micropore diffusivity is, which explains the highest diffusivity of CO_2 in comparison to N_2 and CH_4 knowing that CO_2 has the smallest kinetic diameter compared to the other two gases (CO_2: 0.33 nm, CH_4:0.38 nm, N_2:0.364 nm) (Shi and Durucan, 2005). Also, Busch et al. (2003a) found that CO_2 desorbs fastest from coal compared to CH_4 and N_2.

C. CO_2 Injection Implications on Coalbed Permeability

As it was previously mentioned, the coal permeability reacts to the methane production and pore pressure reduction in two opposite ways. Thus, the pore pressure reduction results in the cleats compression and permeability reduction. However, pressure reduction initiates the gas desorption off the coal matrices which results in the matrix shrinkage and permeability increase. The interplay between the two effects, alongside the matrix expansion due to the pressure reduction, has been previously discussed. The permeability rebound might take place at later times and after dewatering because of these opposite effects. **Figure A.1** indicates the absolute coal permeability response due to pressure reduction after dewatering in the San Juan Basin (McGovern, 2004). One can see how the absolute permeability increased by 7 times as the pressure decreases from 5.5 to 0.07 MPa (Shi and Durucan, 2005). However, predicting the way of absolute permeability change at high pressure is complex because of the relative permeability effects (Shi and Durucan, 2005).

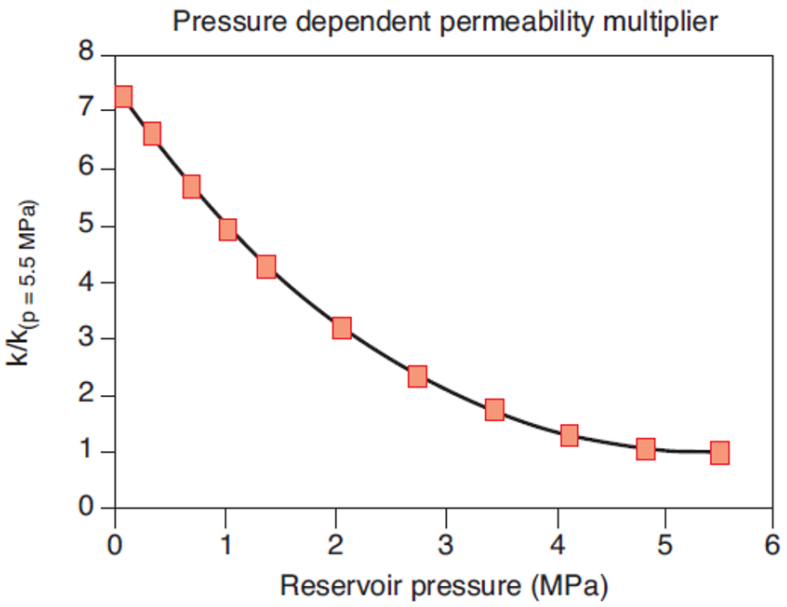

Figure A.1 The absolute coal permeability response due to pressure reduction after dewatering in the San Juan Basin (McGovern, 2004).

Enhanced recovery by injecting CO_2 makes the absolute permeability changes in coal more complicated. Injecting CO_2 adds another process to the number of processes that impact the permeability changes. In that case, one does not only deal with the matrix shrinkage due to gas desorption but also deals with its swelling due to CO_2 adsorption. Also, the existence of different gases would cause the coal matrix to have different shrinkage/swelling behaviors for each different gas. The coal swelling causes absolute permeability reduction. Thus, these two effects cause the permeability reduction: matrix swelling and cleats compression, and one effect that causes the permeability increase: matrix shrinkage. These effects need to be studied and quantified to be able to predict their overall impact on the coal absolute permeability.

CO_2 adsorption causes the swelling of the matrix which in turn reduces the cleats width and absolute permeability (Seidle, 2000). To quantify the matrix shrinkage/ swelling due to gas desorption/adsorption, Harpalani and Chen (1995) and Seidle and Huitt (1995) suggested that it is proportional to the gas volumes that are desorbed/adsorbed. Permeability reduction was reported

in other studies as well (Durucan et al., 2003; Xue and Ohsumi, 2003). However, coalbeds are normally laterally bounded, and this condition is not exactly simulated in the laboratory settings (Shi and Durucan, 2005).

Field investigation of the impact of CO_2 injection on the coal absolute permeability is limited. Reeves (2002) reported a significant reduction in the injection rates of CO_2 by up to 40% at Allison pilot in San Juan Basin during the early injection of carbon dioxide. Pekot and Reeves (2003) concluded that the reduction in CO_2 injectivity is caused by a two-order permeability reduction that resulted from the matrix swelling after the CO_2 adsorption on the coal matrix.

D. The Factors Affecting the CO_2 Injectivity in CBM Reservoirs

i. Temperature Difference

The injected CO_2 temperature might be different than the reservoir temperature. Thus, the CO_2 injectivity could be affected by the non-isothermal effects of the gas flow (Shi and Durucan, 2005).

ii. Wellbore Effects

The CO_2 injection affects the stress around the wellbore (Shi et al., 1997) which -besides pore pressure change effect- might mechanically alter the permeability around the wellbore (Shi and Durucan, 2005).

iii. Precipitate Formation

There is a potential precipitate formation due to the geomechanical reactions between injected CO_2 and the reservoir rock, and formation water. These reactions might affect the CO_2 injectivity and more laboratory studies are needed. The precipitate formation would reduce the coal permeability which would reduce the CO_2 injectivity (Smith and Revees, 2002).

Some techniques were proposed to reduce the impact of the matrix swelling due to CO_2 adsorption on the CO_2 injectivity. Two of these techniques are:

- Using horizontal wellbores to enhance reservoir connectivity.
- Injection of flue CO_2 gas instead of pure CO_2 (Shi and Durucan, 2005).

E. Permeability Models for ECBM

Pekot and Reeves (2003), Shi and Durucan (2003b), and Mavor et al. (2004) developed a permeability model to include the impact of matrix shrinkage/swelling and pore pressure changes on absolute permeability. The model that was introduced by Shi and Durucan (2004) has been successful at history matching the Allison ECBM pilot. The CBM absolute permeability is correlated with effective horizontal stress through **Equation A.1** (Shi and Durucan, 2005).

$$k = k_0 e^{-3c_f(\sigma-\sigma_0)} \quad \text{(A.1)}$$

Where,

c_f : The cleat volume compressibility caused by the effective horizontal stress perpendicular to the fractures/cleats, and

k_0 : The initial permeability of the coal (Shi and Durucan, 2005).

Pore volume compressibility for conventional reservoirs could be exchanged for the cleat volume compressibility in CBM reservoirs. Effective stress changes could be expressed through **Equation A.2** (Shi and Durucan, 2005).

$$\sigma - \sigma_0 = -\frac{\nu}{1-\nu}(p - p_0) + \frac{E}{3(1-\nu)}\sum_{j=1}^{n} \alpha_{Sj}(V_j - V_{j0}) \quad \text{(A.2)}$$

Where,

α_{Sj} : Shrinkage/ swelling coefficient,

V_j : j component specific adsorbed volume at current reservoir gas composition and pressure, and

V_{j0} : j component specific adsorbed volume at initial reservoir gas composition and pressure (Shi and Durucan, 2005).

Levine (1995) and Chui (2004) concluded that the matrix swelling is more adsorbate specific. That is, the gases with higher adsorption capacities exhibit higher swelling impact which is very important to consider when one models CO_2 injection in CBM reservoirs and its impact on coal permeability (Shi and Durucan, 2005). **Figure A.2a** shows that the reduction that occurs to the absolute coal permeability due to coal swelling is strongly affected by a ratio called the swelling coefficient (CO_2/ CH_4) and it was found that a match with the bottom-hole pressures would be achieved if the value of that ratio was 1.276. However, this ratio would result in significantly reducing the permeability around injection wellbore where all the gas is CO_2 around the wellbore. **Figure A.2b** shows the history matching of the bottom-hole pressures for an injection well at the Allison Unit CO_2 injection/ECBM pilot (Shi and Durucan, 2004).

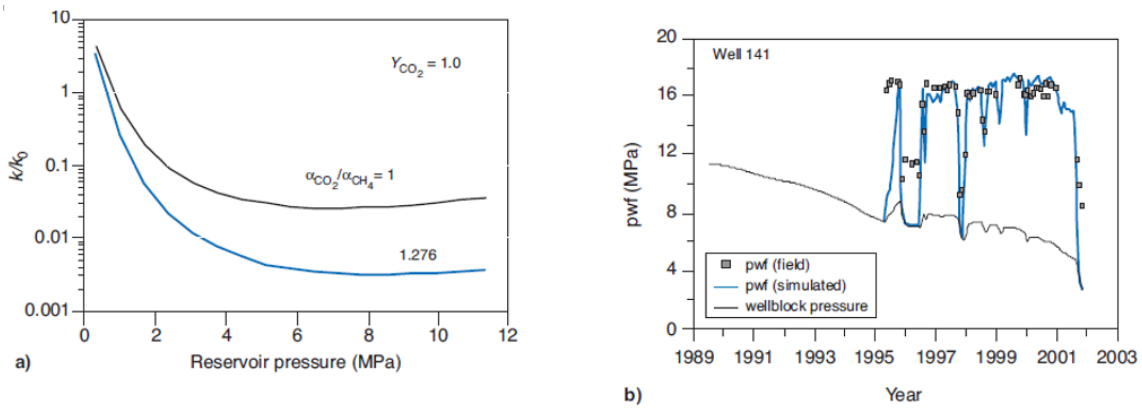

Figure A.2 a) shows that the reduction that occurs to the absolute coal permeability due to coal swelling is strongly affected by a ratio called the swelling coefficient (CO_2/CH_4). b) shows the history matching of the bottom-hole pressures for an injection well at the Allison Unit CO_2 injection/ECBM pilot (Shi and Durucan, 2004).

F. The Need for ECBM

Most of the CBM production nowadays occurs through only the primary depletion without applying the ECBM technique. The main production mechanism is driving the methane to desorb off the coal matrices by reducing the pore pressure after dewatering. Methane incrementally desorbs according to the sorption isotherm (Shi and Durucan, 2005). Such production technique might not be very efficient at most of the times and this inefficiency could be explained by looking at the sorption isotherms which are nonlinear isotherms and they are also skewed towards the low pressures (Shi and Durucan, 2005). The implication of that skewness is that the greater part of the methane in place could only be recovered at very low pressures. This was the motive behind introducing ECBM which could be performed by injecting either N_2 or CO_2. Utilizing ECBM would mean that the greater part of the gas in place could be recovered at reasonable pressure rather than very low pressures.

The mechanisms that are followed to enhance the methane recovery using gas injection are different for different gasses. Injected N_2 does not take the adsorption sites of the methane because

the N_2 affinity to coal is lower that CH_4 which means it has a lower ability to adsorb on the coal matrix than methane. N_2 injection aims at using the nitrogen to reduce the partial pressure of the methane and then initiates its desorption (Shi and Durucan, 2005). It is important to notice that the nitrogen only impacts the methane partial pressure, not the reservoir total pressure. Alternatively, CO_2 injection follows another mechanism that is usually referred to as competitive sorption and the reason for using CO_2 is that it has a higher adsorption capacity than methane in coal. CO_2 injection is usually preferred over N_2 injection because it has another benefit of reducing greenhouse gas emissions and combating climate change.

G. ECBM Geological Factors

Some important geological factors should be carefully investigated during evaluating the potential of a CBM reservoir for CO_2 sequestration or enhanced coal bed methane (ECBM) production (Shi and Durucan, 2005). These factors are:

- Rank: The higher the coal rank is, the higher the gas content becomes.
- Reservoir Pressure: The higher the pressure is, the higher the gas content becomes.
- Depth: The deepest the CBM reservoir, the higher the gas content becomes.
- Moisture content: The higher the moisture content is, the lower the adsorption capacities and gas content become.
- Local hydrology: Since CBM reservoirs are usually undersaturated with gas and thus need the dewatering to take place first for the gas to start being produced, hydrology and its constraint is an important factor for CO_2 sequestration (Shi and Durucan, 2005).
- Permeability: While the deeper CBM reservoirs tend to have higher pressure and gas content, they also tend to have lower permeabilities due to the overburden weight. The experience in the US CBM reservoirs indicated that the absolute permeability should not

be less than one millidarcy for the CBM reservoir production to be commercially feasible. Coal bed methane reservoirs that are deeper than 1500m (4920 ft) are not considered commercially feasible (Shi and Durucan, 2005).

- Structural setting: An excellent candidate for ECBM is a CBM reservoir that has coal formation that is vertically isolated from other strata and laterally continues (Stevens et al., 1998). Vertical isolation would help prevent CO_2 leakage into the overlying formations while the continuous coal would help achieve more efficient sweep. It is favorable also to have fewer faults to reduce any CO_2 channeling (Shi and Durucan, 2005).

H. ECBM Numerical Modeling

CO_2 injection/ECBM is still not very well understood and one needs to fully understand the CO_2 sequestration processes in order to have a reliable numerical simulator that can be used to accurately evaluate this process (Shi and Durucan, 2005). During a study by Albert Research Council to compare the performance of six current different numerical simulators that could be used to simulate ECBM, Law et al. (2000, 2002a, 2002b, and 2003) recommended that a successful simulator should have the ability to handle the following– besides the basic capabilities needed to simulate the Methane production during primary CBM production:

- Matrix shrinkage/swelling
- Binary/mixed gas diffusion
- Binary/mixed gas desorption/adsorption
- The non-isothermal effect when CO_2 temperature is different than the reservoir temperature.
- Binary/multi-component gas mixtures (Shi and Durucan, 2005).

I. ECBM Technical Challenges

Great progress has been made regarding the ECBM technique and more understanding is still needed. Major technical challenges include the CO_2 injectivity problems such as the low injectivity of come coal formations and the injectivity loss with time due to matrix swelling and other factors. Some studies are also being done to improve the efficiency of ECBM which would promote the application of this technique. Among these studies, there are using gas mixture instead of CO_2 and investigating the performance differences and utilizing hydraulic fracturing with ECBM and assessing the overall performance (Li and Fang, 2014). Another technical challenge that is associated with undersaturated CBM reservoirs when applying ECBM is methane banking.

i.1 Methane Banking

Saturated CBM reservoirs are the ones with significant amounts of methane stored in the coal seams (over 30% of the mixture) while undersaturated CBM reservoirs are the ones that have less recoverable amounts of methane- 0.05% of the mixture (Parakh, 2007).

Parakh (2007) performed analytical and experimental studies that suggested that methane banking would occur in the methane profile when injecting CO_2 in undersaturated CBM reservoirs.

Figure A.3a shows methane banking through the red curve of the methane profile for both studies. Also, **Figure A.3b** shows through the experimental study a leading shock in CO_2 (Parakh, 2007). Thus, through the results of the beforementioned analytical and experimental studies, methane banking in methane and small leading shock in CO_2 in undersaturated CBM reservoirs are illustrated.

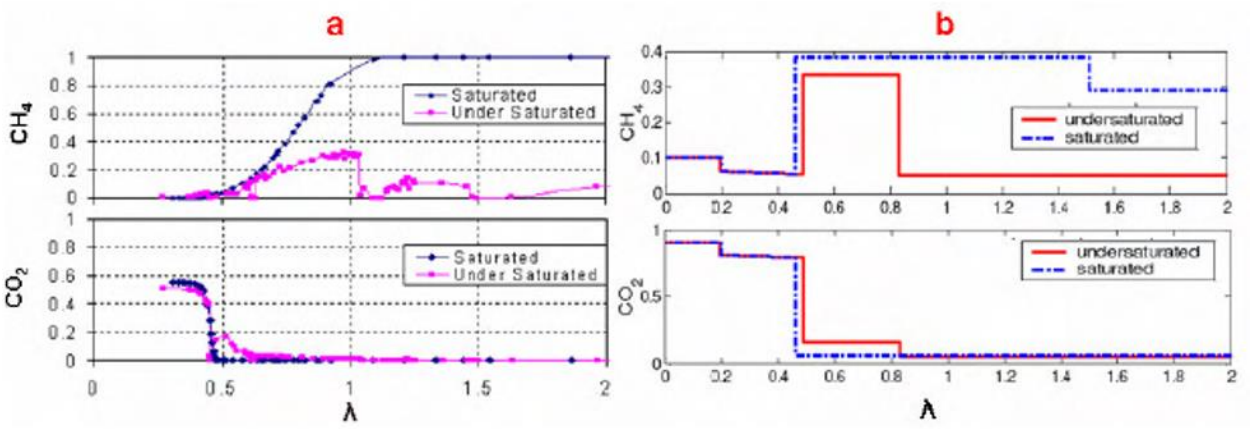

Figure A.3 a) shows methane banking through the red curve of the methane profile for both studies. b) shows through the experimental study a leading shock in CO_2 (Parakh, 2007).

3. Hydraulic Fracturing in CBM reservoirs

Many CBM reservoirs have very low permeability. Thus, hydraulic fracturing could be utilized in some CBM reservoirs to enhance the coal permeability. Hydraulic fracturing has proven to be effective in enhancing the permeability for the low-permeability reservoirs. However, CBM reservoirs cleat systems should be investigated first to avoid any leakage of the methane. Also, in the case of CO_2 sequestration, hydraulic fracturing might not be practical as it might cause the leakage of CO_2 to overburden formations and not benefitting from its existence to stimulate the methane desorption. Additionally, the coal formations are highly stress-sensitive and anisotropic, which makes it important to evaluate the hydraulic fracturing practicality before adopting it. Zhang et al. (2018) found that hydraulic fracturing could have a significant impact on increasing methane production from CBM reservoirs up to ten times the rates produced from low permeability CBM reservoirs. Enhancing CBM production through enhancing the coal permeability has been studied by many researchers (Gentzis and Bolen, 2008; Ozdemir, 2009; Zheng et al., 2012; Massarotto et al., 2014; Yan et al., 2015). Several other technologies that can enhance the permeability of coal

seams were also studied (Gentzis and Bolen, 2008; Ozdemir, 2009; Zheng et al., 2012; Massarotto et al., 2014; Yan et al., 2015).

Wright et al. (1995) Concluded that hydraulic fracturing in CBM reservoirs is influenced by several factors such as the mechanical complexity and stress sensitivity. Li et al. (2012) introduced a finite element 3D model to evaluate the hydraulic fracturing in CBM reservoirs. It was found that the coal heterogeneity might cause the fracture to turn and twist (Zhang et al., 2018).

Hydraulic fracturing in CBM reservoir is affected by the natural cleats that also increase the mechanical complexity of the reservoir (Zhang et al., 2018). The influence area of the hydraulic fracturing and the formation of effective fractures could be prevented by the interactions between the natural cleats and hydraulic fractures (Pandey et al., 2017; Johnson et al., 2010). That is, one must consider the cleat systems complexity and the coal heterogeneity before utilizing the hydraulic fracturing (Zhang et al., 2018). The burial depth of the coal formation should also be considered (Zhang et al., 2018). The impact of the salinity of the injected water on the hydrocarbon recovery when implementing the hydraulic fracturing should also be considered (Mehana, 2016).

Hydraulic fracturing could be very useful to enhance the CBM reservoirs recovery before CO_2 injection and to also improve the CO_2 injectivity during ECBM. However, it might cause CO_2 leakage into the surrounding strata (Shi and Durucan, 2005). Therefore, the decision should be made if hydraulic fracturing would be useful with CO_2 injection or not and if not whether it is more useful to apply hydraulic fracture or the ECBM through CO_2 injection, but then again CO_2 sequestration has another positive impact on the greenhouse gases emissions and climate change.